Structural/functional analysis of synaptotagmin 1 in synaptic transmission using hippocampal autapses

PhD Thesis

In partial fulfillment of the requirements
for the degree "Doctor of Philosophy (PhD)"
in the Molecular Biology Program
at the Georg August University Göttingen,
Faculty of Biology

Submitted by

Liyi Li

Born in

Jiangxi Province, P.R. China

Affidavit

The PhD thesis presented here is written independently and the content in the thesis is contributed by my own work with no other sources and aids than quoted.

PhD candidate : Liyi Li

Date of submission : 04-15-2005

List of publication

Two manuscripts are in submission:

1. Li, L.Y., Shin, O.H., Rhee, J.S,. Araç, D., Rizo, J., Sudhof, T.C., Rosenmund, C. Asymmetric regulation of neurotransmitter release probability by basic residues from the two C_2-domains of synaptotagmin 1.

2. Rhee, J.S.*, Li, L.Y.,* Shin, O.H., Rizo, J., Sudhof, T.C., Rosenmund, C. Synaptotagmin 1 gain-of-function mutants that increase the Ca^{2+} sensitivity of neurotransmitter release. (* equal contribution to this work)

Contents

Acknowledgments

Since September 2000, that I was fortunately accepted by Molecular Biology MSc/PhD international Program, Goettingen University and International Max-Planck Research School as a graduate student, more than four years has passed. In these years of my pursuing for the exciting moments in scientific research, I received numerous help and encouragement from my parents, advisors and colleagues and friends.

First of all, I am most grateful to my advisor Prof. Christian Rosenmund for supporting me on this project and for his constant encouragements and discussions over the last years. His sharp discernment in resolving problems, patience for the experimental progress, strictness of data acquisition and analysis and open mind has always served as a nice example for me.

I would like to thank Prof. Erwin Neher for his agreement to let me work and study in his department. Abteilung 140 is always a great place for scientific research and discussion. The three years' staying in his department, I had a precious opportunity to attend so many interesting seminars and experience the trends in neuroscience. Furthermore, I would like to thank him for taking time to review my PhD thesis manuscript and giving substantial detailed and constructive comments.

My PhD committee gave me quite a few directions during these years and I thank Prof. Reinhard Jahn, Prof. Willhart Knepel for their suggestions. Our molecular biology program provided countless assistance to make my study and life convenient in a foreign country. Especially, I wish to thank Dr. Steffen Burkhardt for his help to arrange the routine process related to my study.

I have learned a lot from the collaboration with Dr. Jeong Seop Rhee. Dr. Ok-Ho Shin and Prof. Thomas C. Sudhof. During the pursuit of my PhD work, their rich

knowledge in neuroscience and useful suggestions in experimental designs and close collaboration enlightened me quite a lot.

It is not an exaggeration for me to say that Albrecht Sigler smoothes my life in Goettingen and sometime I even felt that I abused his warm helps. In my PhD study, he helped me resolve many imaging problems in immunocytochemistry. During our more than three years' friendship, he guided me into classical music, which became one of my favorite hobbies.

I also want to thank Dr. Ralf Nehring for his typical "German working style": being precise and correct in working. Also I want to thank Dirk Reuter, not only for his help to produce viruses but also for his generosity to provide homemade beer.

My colleagues Dr. Jong Cheol Rah, Dr. Shutaro Katsurabayashi, Mingshan Xue, Jayeeta Basu, Dr. Hui Deng and Dr. Lidao Ke also aided me extensively in the last years, of which I am greatly appreciated. Also I would like to thank my friends, Martin Wienisch and Christian Rochford, with them I had enjoyed many wonderful trips and parties—I will always remember that pleasant and hot summer we had in Fuengirola.

During I wrote my thesis, generous help came from many people. Specifically I want to thank Hsiao Tuan Chao, Jayeeta Basu, Cindy Vi Ly for English grammar correction and proof reading.

I am really lucky to have some long-term close friends, Chong Li and Yuhui Li. I learned many wise life experiences from them and we exchanged different opinions of life, work and future.

At last I want to thank my parents, Hongfen Luo and Xun Li for their loving support and endless care—no matter where I was, where I am and where I will be.

List of figures and tables

Abstract

Synaptotagmin 1 is a presynaptic vesicular protein, which has been implicated as a putative Ca^{2+} sensor for fast neurotransmitter release in central nervous system. Structurally, it possesses two Ca^{2+} binding C_2 domains in its cytosolic C-terminal. The biochemical interaction of synaptotagmin 1 with other molecules has been extensively addressed in recent studies, while the exact physiological roles of the two C_2 domains and the mechanism of action of synaptotagmin 1 in exocytosis are still poorly understood.

To answer these questions better, a systematic study combining electrophysiological and molecular biological approaches was performed. The synaptic transmission of the cultured synaptotagmin 1 null murine hippocampal neurons transfected with the mutated synaptotagmin 1 was evaluated with standard whole-cell patch clamp electrophysiology. To take a closer look at how the structure of the C_2 domains is important for the function of synaptotagmin 1, we made a series of the C_2 domain mutations. Truncation of either C_2 domain, neutralization of the Ca^{2+} binding aspartate sites (namely, $D_{172, 230, 232}A$; $D_{303, 363, 365}A$) in either C_2 domain and replacement of either C_2 domains with the C_2 domain from other synaptotagmin isoform (i.e. synaptotagmin 7) all suggested that the two C_2 domains are non redundant in synaptic transmission. Specifically, the C_2A domain is related to readily releasable pool control and the regulation of fast release, whereas the C_2B domain is essential for fast release.

Synaptotagmin 1 has a set of hydrophobic residues (M_{173}, $F_{231, 234}$; V_{304}, Y_{364}, I_{367}) in the C_2 domains, which have been biochemically shown to interact with the phospholipid plasma membrane. We replaced these residues with Tryptophans with the idea of introducing greater hydrophobicity into the domains so as to correlate its physiological consequences on its phospholipid binding. These mutations result in enhancement in the release probability and apparent Ca^{2+} sensitivity. Furthermore, the polybasic residues in the C_2B domain of

synaptotagmin 1 have been shown to have multiple interactions (i. e. with another copy of synaptotagmin, PIP_2 in plasma membrane, AP-2 and Ca^{2+} channels, etc). These interactions can be abolished by neutralizing these residues (K_{326}, $_{327}A$). The physiological analysis of the phenotype of synaptotagmin 1 with K_{326}, $_{327}A$ mutation shows that the neurotransmitter release does not get abolished, rather it is reduced, which correlates with a corresponding decrease in *in vitro* Ca^{2+} dependent synaptotagmin 1-phospholipid binding. Interestingly, this K_{326}, $_{327}A$ phenotype bears striking similarity to the previously described synaptotagmin 1 C_2A domain $R_{233}Q$ mutation. To further investigate this phenomenon, the corresponding site of the $R_{233}Q$ mutation in the C_2B domain was mutated ($K_{366}Q$), however, the latter one showed a wild type like behavior both *in vitro* and *in vivo*. Taken together, the asymmetrical distribution of these basic residues for vesicle release control in the two C_2 domains indicates that the two C_2 domains interact with plasma membrane upon coming Ca^{2+} in different orientation.

Overall, these C_2 domain mutation studies suggest that the Ca^{2+} dependent synaptotagmin 1-phospholipid interaction is critical for the efficiency of synaptic transmission, which ultimately supports the general notion that synaptotagmin 1 must essentially interact with the plasma membrane so as to enable vesicle fusion.

1. Introduction

The human brain functioning as the information processing and storage center consists of more than a hundred billion basic units- neurons. A neuron is a specially polarized cell with three morphological parts: dendrites for receiving electric signals from other neurons; soma for information integration and axon for passing over regenerated signals to other recipients. The specialized terminal contacts for signal transmission from one neuron to another are termed as synapses by Sir Charles Sherrington (1897), which originally comes from the Greek "to fasten together". The high fidelity and fast speed of signal transmission through the synapses are mainly dependent on neurotransmitter release to transform the electrical signals to chemical signals. Especially the step of triggering of neurotransmitter release is the focus of this study.

This introduction will firstly address the structure and functions of synapses and then proceed on with the detail description of the vesicle cycle in the presynaptic terminals, emphasizing on the critical step of vesicular fusion culminating in release of neurotransmitters. The main focus of this thesis project being synaptotagmin, this section will include a brief insight into the family of synaptotagmins and the current overview of the mechanism of action of synaptotagmin in exocytosis.

1.1 The general structure and functions of synapses

Synapses are usually classified into two types, electrical or chemical synapses upon whether the transmission occurs in neuronal terminals via direct electrical pulses propagation or via chemical intermediates. Usually, the signal transmission in electrical synapses is bi-directional, while in chemical synapses it propagates in single direction (although retrograde signal transmissions generally

exist in these synapses). Here all descriptions are of chemical synapses unless mentioned.

Synapses under electron microscopy (EM) are easily recognized by their morphological characters and are distinguished from other organelle structures with two hallmarks: a cluster of small, round and electron-lucent vesicles with uniform size apposite or docking to a layer of plasma membrane/ protein matrix (named as active zone) and a thickened electron-dense scaffold/ membrane opposite to it (named as postsynaptic density, PSD)(Fig 1.1). A typical synapse compromises of three parts, presynaptic terminal accommodating numerous vesicles, postsynaptic terminal holding receptors to bind with neurotransmitters and synaptic cleft separating them. According to the synaptic functions, central nervous system (CNS) synapses have two major groups, excitatory (primarily glutamatergic) and inhibitory (primarily γ-aminobutyric acid (GABA) or glycinergic) synapses.

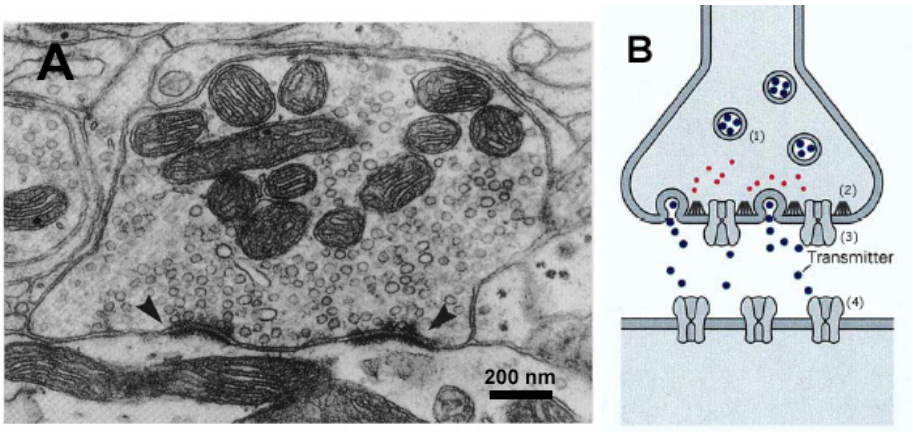

Figure 1.1 Structure of a synapse. A. Electron micrograph of a neuronal synapse, the arrows indicate the active zones in the presynaptic terminal (image from Prof. Kristen M. Harris's lab); B. a schematic illustration of the synapse. (1) synaptic vesicles, (2) active zone matrix, (3) voltage-gated Ca^{2+} channels; (4) postsynaptic receptors. Red dots represent the Ca^{2+} ions and black dots represent neurotransmitters (diagram adapted from "Principles of Neural Science", 4th edition, by Eric R. Kandel et al.).

Synapses can keep the synaptic transmission in high spatial precision and speed through neurotransmitters (chemical intermediates) released from presynaptic vesicles. The general scheme of synaptic transmission is as follows: In resting state, a neuron keeps a certain potential difference across the membrane, which is called the membrane potential (ranging from -60 to -90 mV, the intracellular potential lower than the extra cellular one). Depolarization of the neuronal membrane potential above a certain threshold leads to Na^+ ions influx and firing action potentials (APs), which propagate along the axon to presynaptic terminals. Coupled to the invasion of APs, the voltage-dependent calcium channels (mostly P/Q- and N- type) present on the presynaptic membrane open and external Ca^{2+} ions (milimolar range) flux into the presynaptic terminals where a low Ca^{2+} concentration is maintained in resting condition (about 100 nM, Zucker RS and Regehr WG, 2002). A transient elevation of presynaptic terminals Ca^{2+} concentration (tens of micromolar or higher, Bollmann JH, et al., 2000; Schneggenburger R and Neher E, 2000) facilitates Ca^{2+} binding to Ca^{2+} sensors, which activate a not completely defined molecular machinery. This can induce the fusion of the vesicular membrane with the plasma membrane to release vesicular neurotransmitters. After crossing the synaptic cleft by diffusion, neurotransmitters bind ionotropic receptors on postsynaptic membrane and open ligand-gated ion channels on postsynaptic neuron for ions influx/efflux (Na^+, K^+, Cl^- and Ca^{2+}, etc.). The change of the intra/extra cellular ion concentration ratio in the postsynaptic terminals will depolarize or hyperpolarize the neuron, thus the chemical signal converts back to an electric signal. If the signal recipient neuron is held in whole-cell voltage clamp mode, excitatory/ inhibitory postsynaptic currents (EPSCs/ IPSCs) can be recorded. In the absence of stimulations in presynaptic terminals, synaptic activities with small amplitudes (about 20 pA) can be observed, which is believed to be due to spontaneous vesicle fusion (called as miniature response). As the vesicles deplete their contents, their membrane is internalized and the vesicles are refilled with neurotransmitters for next round of release.

The important property of synapses is not only that they can convey information between neurons, but also that they can regulate the synaptic strength. The change in synaptic strength has a short-term effect (Short-term plasticity. for review, Zucker RS and Regehr WG, 2002), which lasts for at most a few minutes and a long-term effect (Long-term plasticity. for review, Malenka RC, 2003; Collingridge GL, et al., 2004) that can last more than a few hours, even to weeks. Both forms of synaptic plasticity can be an enhancement or attenuation of synaptic strength, but the origins of these two forms of synaptic plasticity are quite different.

Short-term synaptic enhancement, such as facilitation or augmentation, is proposed to be mainly due to the elevation of residual Ca^{2+} concentration in presynaptic terminals (Katz B and Miledi R, 1968; Delaney KR and Tank DW, 1994; Regehr WG, et al., 1994); and the short-term synaptic depression is originated from many aspects, such as depletion of vesicles ready for release, presynaptic terminals regulation by release of modulatory substances (Miller RJ, 1998; Wu LG and Saggau P, 1997) and desensitization of postsynaptic receptors (receptors become less sensitive to neurotransmitters, MacDermott AB, et al., 1999). As far as the long-term synaptic plasticity is concerned, besides the presynaptic mechanism, the membrane trafficking of postsynaptic ionotropic receptors, especially the glutamate receptors, such as NMDAR (N-methyl-D-aspartate receptor) and AMPAR (α-amino-3-hydroxy-5-methyl-4-isoxazole-propionic acid receptor), have been suggested to be pivotal for the initiation of long-term synaptic plasticity (for review, Collingridge GL, et al., 2004).

1.2 Synaptic vesicle recycling

The postulation that neurotransmitters are released in quantal mode (Del Castillo J and Katz B, 1954a-d) and the EM observation of small vesicular organelles (with the size ranging from 20 to 150 nm) in presynaptic terminals (Palay SL and Palade G, 1955) greatly absorbed people's interests in understanding their

correlation. Physiological study suggests that three different vesicle pools exist in the presynaptic terminal: the readily releasable pool which is immediately releasable upon stimulations; the recycling pool which maintains releasing vesicles under moderate stimulations and the reserve pool whose vesicles will not release unless intense stimulations occur (for review, Rizzoli SO and Betz WJ, 2005). Although there are distinct physiological properties of vesicles in the synaptic vesicle pool, under EM these vesicles do not have morphological differences and there is no convincing evidence to show that their distribution in presynaptic terminal is different.

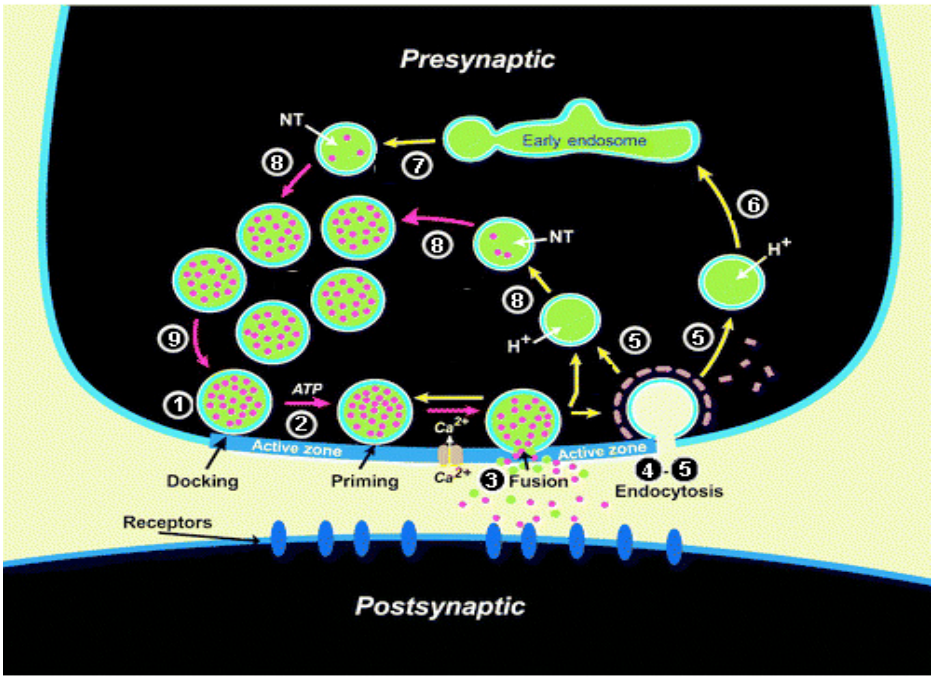

Figure 1.2 The schematic illustration of the synaptic vesicle recycle (Detailed description is in text. Figure is adapted from the review, Sudhof TC, 2004.)

To understand synaptic vesicles better, their activities in presynaptic terminals are worth investigating, especially their recycling pathway. The classical model of vesicle cycle conceptually contains nine steps, as described in the following: vesicles dock on the presynaptic active zone (step 1, docking); after that, an ATP-dependent prefusion occurs between vesicles and plasma membrane (step 2, priming); then presynaptic Ca^{2+} influx triggers a rapid reaction completing

membrane fusion and neurotransmitters are released (step 3, fusion); after exocytosis, the vesicles undergo clathrin-mediated retrieval (step 4, endocytosis); later on, these recovered vesicles leave the active zone and fuse with the endosome (step 5, 6); simultaneously, some new formed vesicles bud off the endosome (step 7) and are filled with neurotransmitters consuming the energy provided by the electrochemical gradient that vacuolar proton pumps build up (step 8); matured vesicles translocate and approach the active zone ready for a next round of release (step9) (Heuser JE and Reese TS, 1973; Sudhof TC, 1995). Although this model has been accepted generally, an alternative pathway of vesicle recycling, namely "kiss-and-run", has been found both at neuromuscular junction (Ceccarelli B, et al., 1973) and in central synapses (Stevens CF and Williams JH, 2000; Gandhi SP and Stevens CF, 2003). The main difference between these two modes of vesicle recycling lies in whether vesicles keep their identities during recycling. 'Kiss-and-run' mode vesicles are retrieved from the membrane quickly and keep their identities for the next round fusion, while in classical mode, the vesicles after releasing the neurotransmitters will remix with the endosome before the next turn occurs.

Synaptic vesicle recycling is a complex process (for review, Sudhof TC, 2004), and even a single step involves many protein interactions. Taking the step most relevant to this study, vesicular exocytosis, as an example, numerous works have been done and quite a few proteins participating in this step have been identified. Essentially, there are two molecular level questions existing in vesicular exocytosis: how can the vesicular membrane fuse to the plasma membrane and how can vesicles sense the Ca^{2+} influx signal?

To fuse the vesicular membrane with the plasma membrane, firstly the membranes need to overcome their own electrostatic counteracting forces to be in close proximity; secondly the close membranes will be destabilized and a non-bilayer transition state is generated leading to later fusion pore forming (for review, Jahn R, et al., 2003). The vesicular **s**oluble **N**-ethylmaleimide-sensitive

factor **a**ttachment protein **re**ceptor (SNARE) proteins present on both membranes have been suggested to form extraordinarily stable coiled coils (named as core complex or SNARE complex), which contribute the energy needed for membranes to overcome the counteracting force barrier (Fasshauer D, et al., 2002). There are three different SNARE proteins (one copy each) in the SNARE complex: synaptobrevin on vesicular membrane (also referred as v-SNARE), syntaxin and SNAP-25 (**s**y**n**aptosomal-**a**ssosicated **p**rotein of **25** k Da) on plasma membrane (referred as t-SNAREs). T- /v-SNAREs share a common motif consisting of about 60 amino acids, which form four parallel α helixes in the SNARE complex (two helixes from SNAP-25 and each of the others contributes one, Poirier MA, et al., 1998). Crystal structure of this α-helix bundle revealed several layers of interior hydrophobic residues and some polar residues (one/two glutamines from syntaxin/SNAP-25 and one arginine from synaptobrevin) in the centre of the complex (Sutton RB, et al., 1998).

Reconstitution experiments showed that synaptobrevin and SNAP-25/syntaxin incorporating into separate liposomes could cause membrane fusion, which strongly argues for the SNARE complex as the minimal machinery for fusion process (Weber T, et al., 1998). The slow Ca^{2+} dependent fusion rate observed in these experiments together with other in vitro studies (Hu K, et al., 2002) has been questioned of their physiological relevance. The possible explanations can be the instability of the SNARE complex and/or that the shortage of some protein(s) sensing Ca^{2+} slows down this fusion process.

Complexin, a cytoplasmic protein interacting with SNARE via its C-terminal α helix in high affinity (dissociation constant about 10nM, Pabst S, et al., 2002) is thought to tighten the interface between synaptobrevin and syntaxin so as to stabilize the SNARE complex (Chen X, et al., 2002; Rizo J and Sudhof TC, 2002). Knocking out complexin 1 and 2 can reduce the evoked synchronous release (reflecting those vesicles with full tightened SNARE complex) but no change in the asynchronous release (reflecting vesicles with incomplete

tightened SNARE complex) in hippocampal neuronal terminals (Reim K, et al., 2001). Parallelly, it has been suggested that the degree of tightness of the SNARE complex can affect the vesicle release from the heterogeneous readily releasable pool in adrenal chromaffin cells (vesicles with fully zippered SNARE complex form rapidly releasable pool, while vesicles with insufficient assembling of the SNARE complex form slowly releasable pool, Rettig J and Neher E, 2002). Whether the hypothesis is applicable to synaptic terminals is not completely sure, since the unresolved issue is whether synchronous release and asynchronous release originates from rapid and slow readily releasable pool respectively, although the existence of heterogeneous readily releasable pool has been reported both in the calyx of Held (a giant synapse in the auditory pathway, Sakaba T and Neher E, 2001a-b; Trommershauser J, et al., 2003) and in hippocampal neurons (Murthy VN, et al., 1997; Rosenmund C, et al., 2002).

Besides complexin, there are other proteins that have been shown to interact with the SNARE complex. Synaptotagmin 1, a presynaptic protein, has been shown to regulate SNARE complex assembling *in vivo* (Littleton JT, et al., 2001) and the Ca^{2+} dependent binding of synaptotagmin 1 to the C-terminal SNAP-25 in the SNARE complex is essential for Ca^{2+} triggered exocytosis in PC12 cells (Gerona RR, et al., 2000; Zhang X, et al., 2002).

The function of synaptotagmin 1 is thought to be more than just interaction with the SNARE complex. That the murine neurons lack of synaptotagmin 1 only exhibited the asynchronous release (Geppert M, et al., 1994) led to a proposition of synaptotagmin 1 as the Ca^{2+} sensor for fast synaptic transmission. This notion was further supported by the observation that the addition of synaptotagmin 1 greatly accelerated the SNARE complex mediated membrane fusion *in vitro* (Tucker WC, et al. 2004). Additionally, the SNARE complex has been suggested to be directly involved in Ca^{2+} sensing, since if neutralizing two residues in SNAP25 (E_{170}, Q_{177}), which are postulated to be involved in Ca^{2+} cooperation for vesicle release, the fast Ca^{2+} triggered exocytosis was abolished (Sorensen JB,

et al., 2002). While a recent study showed different opinion by screening the surface of the SNARE complex for appropriate Ca^{2+} affinity binding sites (Chen X, et al., 2005). The results excluded the SNARE complex as the Ca^{2+} sensor due to its rather low Ca^{2+} affinity. Furthermore, the neutralization of those two residues (E_{170}, Q_{177}) in SNAP25 was found to have no effect on the SNAP-25/ synaptotagmin 1 interaction but to destabilize the SNARE complex. These findings taken together suggest that the SNARE complex does not act directly as Ca^{2+} receptors but its assembly is tightly coupled to Ca^{2+}-sensing, and the lack of Ca^{2+} sensing molecule(s) (i.e. synaptotagmin 1) may lead to the slow fusion rate observed in the previous reconstitution experiments (Weber T, et al., 1998).

The dual role of synaptotagmin 1 (interaction with SNARE complex and Ca^{2+} sensor) makes the molecular level explanation of exocytosis very complicated, so it is necessary to understand the function of synaptotagmin 1 in exocytosis better.

1.3 The family of synaptotagmins

Since synaptotagmin 1 was found in an antibody screening for synaptic proteins (Matthew WD, et al., 1981), 16 different synaptotagmin isoforms have been subsequently identified (for review, Sudhof TC, 2002; Fukuda M, 2003a-b). Most of them are poorly characterized with the exception of synaptotagmin 1, 2, 3, 4 and 7. The family members are classified by a common structural building: an N-terminal transmembrane region (TMR), a central linker and two C-terminal C_2 domains.

Most synaptotagmin proteins mainly express in the brain, while in some tissues out of the central nerve system, some of these proteins have also been detected. For example, synaptotagmin 1 and 2 were found in adrenal chromaffin cells; synaptotagmin 7 was detected in heart, lung and spleen (Li C, et al., 1995) and synaptotagmin 13 has been found in sperm heads (Hutt DM, et al., 2002) and in

the kidney (Kishore BK, et al., 1998). These ubiquitously expressed synaptotagmins also show different localization in presynaptic terminals. Synaptotagmin 1, 2, 9 are vesicular proteins; while the localization of synaptotagmin 3 and 7 is controversial, since some studies suggested they are vesicular proteins (Ullrich B, et al., 1994; Martinez I, et al., 2000), and other studies defined them as plasma membrane proteins (Xu T and Bajjalieh SM, 2001; Sugita S, et al., 2001; Sugita S, et al., 2002).

Synaptotagmins contain two C_2 domains, referred as the C_2A and the C_2B domain, accounting for most functions of synaptotagmin. Each C_2 domain has a similar eight-strand β barrel tertiary structure with three top loops (Fig. 1.3). It has been reported that three and two Ca^{2+} ions can bind to the C_2A domain (Ubach J, et al., 1998) and C_2B domain (Fernandez I, et al., 2001) respectively in synaptotagmin 1 (a recent study showed that the third Ca^{2+} coordination site in C_2B domain can be generated by D_{309} and N_{333} in higher Ca^{2+} concentration (600mM $CaCl_2$), Cheng Y, et al., 2004). The Ca^{2+} binding sites in each domain specifically contain five aspartates that exist in the two out of three top loops (Loop 1 and 3, Shao X, et al., 1996). The number of bound Ca^{2+} ions in the C_2 domains is the same for synaptotagmin 1-3, 5-7 and 9-10. For synaptotagmin 8, 12, 13, they lack Ca^{2+} binding residues in two C_2 domains and for synaptotagmin 4 and 11, their C_2A domain can only bind one or two Ca^{2+} ions. The intrinsic Ca^{2+} affinity in each C_2 domain is low (K_d>1mM and >0.3mM for the C_2A domain and C_2B domain of synaptotagmin 1 respectively), but in the presence of phospholipid, it can be increased more than 100 folds (1-20 μM, Fernandez-Chacon R, et al., 2001; Fernandez I, et al., 2001). Since the Ca^{2+} affinity of the C_2 domains (in the presence of phospholipid) falls in the range of microscopic Ca^{2+} concentration upon Ca^{2+} influx in presynaptic terminal (10-25 μM, Bollman JH, et al., 2000; Schneggenburger R and Neher E, 2000), this leads to the speculation of synaptotagmins functioning as Ca^{2+} sensors for exocytosis. The structure and function of synaptotagmin 1 are by far the most well studied protein in this family and also it is the central molecule investigated in this thesis.

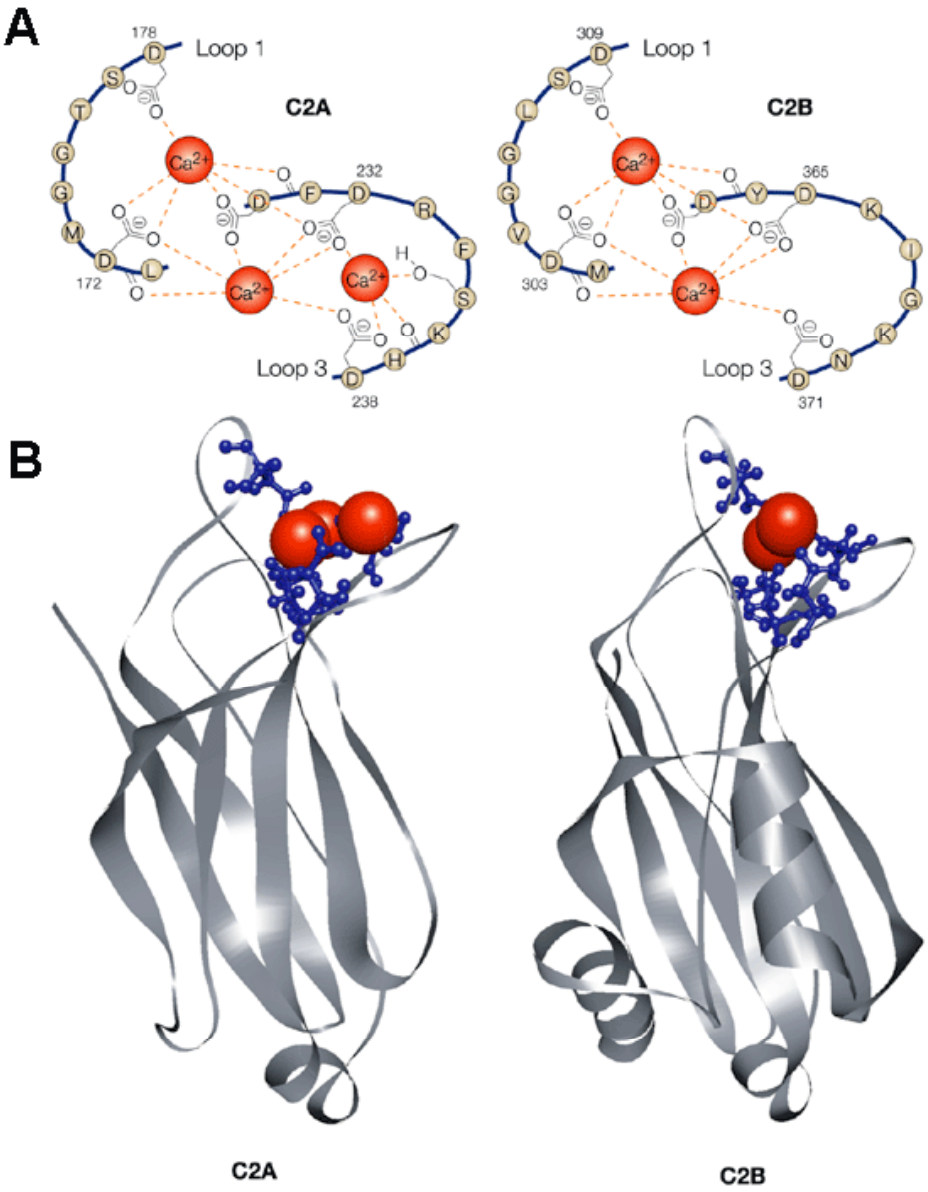

Figure 1.3 The structure of the C_2 domains of synaptotagmin 1. A. Schematic drawing shows the interaction between the Ca^{2+} ions and amino acids in the C_2A and C_2B domains. B. Three dimensional structure of the C_2A and C_2B domains in Ca^{2+} binding state. Red balls represent Ca^{2+} ions. (From the review, Chapman ER, 2002)

1.4 The mechanism of action of synaptotagmin for exocytosis

In respect to Ca^{2+} influx, evoked neurotransmitter release can be separated into a fast (synchronous) form and a slow (asynchronous) form. This biphasic release form leads to the speculation that it is differentially regulated by two distinct Ca^{2+} sensors (Goda Y and Stevens CF, 1994). A low affinity Ca^{2+} sensor can trigger a fast release and the higher affinity Ca^{2+} sensor mainly senses the tail of Ca^{2+} transient to induce a slow but long lasting vesicle fusion. This 'two Ca^{2+} sensor model' was supported by some genetic studies of synaptotagmin 1 knock out models (Nonet ML, et al., 1993; Littleton JT, et al., 1993; Geppert M, et al., 1994), where the total release decreased, or synchronous release was eliminated. Thus, synaptotagmin 1 appear to be as the most likely Ca^{2+} sensor candidate for synchronous release. (In the following part, without other mentioning, synaptotagmin refers to synaptotagmin 1)

1.4.1 Multiple functions of synaptotagmin in vesicle recycling

In addition to a role in Ca^{2+} sensing, synaptotagmin has been postulated to have multiple functions in vesicle recycling, such as vesicle docking, fusion pore regulation, and vesicle endocytosis.

The quantitative morphological finding that the number of docked synaptic vesicles in synaptotagmin null *Drosophila* larvae was significantly reduced led to the hypothesis that synaptotagmin facilitates vesicle docking (Reist NE, et al., 1998). While a long lasting (>1 hr) high K^+ induced vesicle fusion was observed in synaptotagmin null *Drosophila* (Yoshihara M and Littleton JT, 2002) and similar quanta release by hypertonic solution application was found between wild type and synaptotagmin null mutants (from review, Tucker WC and Chapman

ER, 2002), it strongly questioned the previous hypothesis that synaptotagmin affects the vesicle docking process.

After the close proximity of vesicle membrane and plasma membrane, a fusion pore forms to connect the vesicle lumen with the extra cellular environment. The amperometry study can directly monitor the fusion pore kinetics: the neurotransmitters (catecholamine, a class of hormone stored in large dense core vesicles of PC12 cells) dilation of the fusion pore result in a spike of amperometric current, which is proceeded by a steady level of current (PSF, pre-spike foot) reflecting the limited flux of neurotransmitters through the fusion pore before its dilation. It has been observed that overexpression of synaptotagmin in PC12 cells increased the duration of PSF signals, indicating that synaptotagmin can stabilize the fusion pore to regulate the last step of membrane fusion (Wang CT, et al., 2001); a further study even suggested that the C_2A domain favors a full vesicle fusion while the C_2B domain regulates “kiss-and-run” mode fusion (Wang CT, et al., 2003). The fusion pore dynamics is not solely controlled by synaptotagmin, since disrupting the synaptotagmin/t-SNARE interaction has been showed graded reductions in the duration of PSF signals (Bai J, et al., 2004b).

Vesicle retrieval from plasma membrane is AP-2 dependent (a class of adaptor protein, binding to synaptic vesicle to trigger assembly of clathrin for endocytosis). The biochemical study revealed a high affinity interaction between AP-2 and synaptotagmin (Zhang JZ, et al., 1994), which in general agrees to the findings that a marked depletion of synaptic vesicles was seen at nerve terminals of synaptotagmin null *C. elegans* (Jorgensen EM et al., 1995) and a kinetic deficiency of endocytosis in synaptotagmin null mice hippocampal neurons (Nicholson-Tomishima K and Ryan TA, 2004). To determine the AP-2 binding sites in synaptotagmin, a screening study was performed and localized the position to the C_2B domain ($K_{326,\ 327}$, Chapman ER, et al., 1998), which was confirmed by the findings that the fly mutant with the deletion of the C_2B domain

had a dysfunctional vesicle recycling (Littleton JT, et al., 2001). Another study argued that this AP-2 binding site in synaptotagmin is a regulator of endocytosis instead of an internalization signal (Jarousse N, et al., 2001) and a new internalization site in synaptotagmin was reported to be a tryptophan residue in the last β strand of the C_2B domain (Jarousse N, et al., 2003). The polybasic site ($K_{326, 327}$) in the C_2B domain is very interesting, because it has been identified to bind multiple molecules besides AP-2, for example, inositol polyphosphates (Fukuda M, et al., 1994), another copy of synaptotagmin (oligomerization, Chapman ER, et al., 1996; Sugita S, et al., 1996; Desai RC, et al., 2000), Ca^{2+} channels (Sheng ZH, et al., 1997; Kim DK and Catterall WA, 1997), etc. So it is necessary to clarify the sequence of these interactions and their relationship with endocytosis (if it exists). A recent finding shed some light in this direction, which showed that the C_2B domain oligomerization is a prerequisite for AP-2 binding (Grass I, et al., 2004). Since synaptotagmin oligomerization is thought to be involved in the vesicular exocytosis process (Littleton JT, et al., 2001), then the oligomerization step preceding the AP-2 binding step depicts a regulatory transition of vesicles from exocytosis to endocytosis by synaptotagmin.

1.4.2 The mechanism of action of synaptotagmin for vesicle fusion

So far the multiple roles of synaptotagmin in vesicle recycling has been described except for exocytosis, which actually is by far the most well-studied and controversial topic about synaptotagmin (for review, Koh TW and Bellen HJ, 2003; Bai J and Chapman ER, 2004; Sudhof TC, 2004).

During vesicle exocytosis, several interactions of synaptotagmin are important for understanding the mechanism of action of synaptotagmin: 1) Phospholipid interaction; 2) the SNARE complex interaction; 3) homo-/hetero-synaptotagmins interaction. An important issue is whether these interactions are Ca^{2+} dependent.

Initially, only the C_2A domain of synaptotagmin was found to bind phospholipid in a Ca^{2+} dependent manner and this interaction has been showed to be in an electrostatic way instead of by the phospholipid head group (Zhang X, et al., 1998; Davletov B, et al., 1998). This notion was later partially corrected after the observation that Ca^{2+} triggers direct insertion of Ca^{2+} binding loop 3 into lipid bilayers by a quenching experiment (Chapman ER and Davis AF, 1998). This study showed that lipid-embedded quencher can decrease tryptophanyl fluorescence of the C2A residues ($F_{231,234}W$) substitution. So it is now believed that the C_2A domain interacts with phospholipid through electrostatic interaction, which can be further stabilized by the hydrophobic interaction between the C_2A domain and the plasma membrane (Gerber SH, et al., 2001). The early study of immobilized GST-isolated C_2B domain did not show its Ca^{2+} dependent interaction with phospholipid (Schiavo G, et al., 1995; Bai J, et al., 2000), because the initial synaptotagmin cDNA encoded a point mutation that leads to a defective C_2B domain (Perin MS, et al., 1990; Ubach J, et al., 2001). A properly purified C_2B domain indeed can bind phospholipid in Ca^{2+} dependent manner (Ubach J, et al., 2001; Fernandez I, et al., 2001) and further more, the C_2B domain was found to be able to insert into lipid bilayers if it is linked to the C_2A domain (Bai J, et al., 2002). Therefore both C_2 domains can interact with phospholipid cooperatively, there should be a certain mechanism for the domains to distinguish plasma membrane from vesicular membrane. The interaction between synaptotagmin and inositol polyphosphates, which are exclusively present on the plasma membrane has been carefully studied (Bai J, et al., 2000; Bai J, et al., 2004a). Indeed, PIP_2 (phosphotidyl inositol 4,5-bisphosphate, a type of inositol polyphosphates) was shown to steer the reconstituted synaptotagmin to penetrate into PIP_2 –harboring bilayers in presence of Ca^{2+} *in vitro*. The polybasic region in the C_2B domain of synaptotagmin was found responsible for the interaction with PIP_2 (Bai j, et al., 2004a).

Synaptotagmin-phospholipid interaction was proven by biochemical experiments *in vitro*. Their consequential effect on physiological synaptic transmission has

been started now. A study of the C_2A domain of synaptotagmin showed that neutralizing a single positive residue in the C_2A domain ($R_{233}Q$) leads to a two-fold decrease in Ca^{2+} dependent phospholipid binding affinity, parallel with a half reduction of synaptic transmission efficiency in hippocampal neurons (Fernandez-Chacon R, et al., 2001). Similar correlation was found in two other strains of knock-in mice ($D_{232}N$ and $D_{238}N$), where no change in Ca^{2+} dependent phospholipid binding was observed along with normal synaptic transmission (Fernandez-Chacon R, et al., 2002). These elegant studies suggest that synaptotagmin-phospholipid interaction is quite essential for vesicle release.

That both C_2 domains with the similar 3D structure show the redundant phsopholipid binding activity *in vitro* leads to a question: are they redundant in physiological condition for synaptic transmission as well? Several studies tried to resolve this question. For example, the neutralization of some Asp residues in Ca^{2+} binding sites of the C_2B domain severely diminished fast neurotransmitter release (Robinson IM, et al., 2002; Nishiki T and Augustine GJ, 2004b), while mutation studies carried out in the C_2A domain showed a shift in Ca^{2+} sensitivity of synaptotagmin without changing fast synaptic transmission (Stevens CF and Sullivan JM, 2003; Mackler JM, et al., 2002). Similarly, a study using the C_2B domain truncated synaptotagmin mutant in Drosophila found a reduced but not eliminated synchronous release together with completely abolished the Ca^{2+} cooperativity (Yoshihara M and Littleton TJ, 2002). These results taken together, suggest that the physiological functions of the C_2 domains of synaptotagmin clearly are unequal and non-redundant.

The Ca^{2+} dependent binding of synaptotagmin to syntaxin (Li C, et al., 1995; Kee Y and Scheller RH, 1996) was discovered to occur at the sequences of the C_2A domain that surround the Ca^{2+} binding sites (Shao X, et al, 1997). The disruption of a single Ca^{2+} binding site abolished this binding and it was found that positively charged residues near Ca^{2+} binding sites are required for syntaxin binding (Ubach J, et al., 1998). The binding site in syntaxin is thought to map to

the transmembrane domain and H3 domain (corresponding to the region of syntaxin that assembles into SNARE complex; Chapman ER, et al., 1995; Kee Y and Scheller RH, 1996). Since it was also found that synaptotagmin can facilitate the SNARE complex formation *in vitro* and a mutation ($Y_{364}N$) in synaptotagmin disrupting the conformation change required for synaptotagmin oligomerization results in a decrease but not loss of the SNARE assembly *in vivo* (Littleton JT, et al., 2001). Therefore, it was speculated that synaptotagmin regulates SNARE assembling upon Ca^{2+} influx and pulls the membranes closer simultaneously (Davis AF, et al., 1999). The finding that synaptotagmin can bind to the C-terminal of SNAP-25 in presence of Ca^{2+} and influence secretion in PC12 cells reinforced this speculation (Zhang X, et al., 2002).

However, recently it has been reported that the SNARE complex can be copurified with synaptotagmin from brain material in the absence of Ca^{2+}. The Ca^{2+} independent binding site of synaptotagmin to the t-SNARE heterodimer is localized to the polybasic region of the C_2B domain (Shin OH, et al., 2003; Rickman C and Davletov B, 2003; Rickman C, et al, 2004). The fusion of reconstituted v-/t-SNARE proteoliposomes *in vitro* by synaptotagmin facilitating SNARE complex formation in the absence of Ca^{2+} was also reported (Mahal LK, et al., 2002). Alternatively, another study showed the analogue of Ca^{2+} ion, Sr^{2+}, binding to the Ca^{2+} binding sites in the C_2B domain of synaptotagmin can trigger vesicle release, which occurs through the Sr^{2+} dependent synaptotagmin-phospholipid interaction while bypassing the synaptotagmin-SNARE complex interaction (Shin OH, et al., 2003). This observation is an indirect evidence to support the notion that synaptotagmin-SNARE interaction is not essential for vesicular release.

The Ca^{2+}-promoted self-association of synaptotagmin has gained great attention since its first report (Wendland B and Scheller RH, 1994). First of all, it is necessary to determine the locus of the self-association site(s). By using yeast two-hybrid interaction screen assay, the C_2B domain of synaptotagmin was

identified as the regulator of Ca^{2+} dependent oligomerization (Sugita S, et al., 1996). Later on, a further screening of the C_2B domain of synaptotagmin unveiled the polybasic region ($K_{326, 327}$) as the oligomerization site (Chapman ER, et al., 1998). By neutralizing this site, Ca^{2+} dependent oligomerization but not membrane binding was disrupted (Wu Y, et al., 2002) and inhibition of secretion from PC12 cells was observed (Desai RC, et al., 2000). Together with these findings, a synaptotagmin mutant ($Y_{364}N$) in *Drosophila*, which showed disruption of the conformation change required for synaptotagmin oligomerization, resulted in a post-docking defect in exocytosis (Littleton JT, et al., 2001) and a drastic reduction of release (Yoshihara M and Littleton JT, 2002).

Based on the above description, there are now two proposed models to explain the mechanism of action of synaptotagmin in vesicle fusion. One is described as the following (Bai J and Chapman ER, 2004): 1) Before Ca^{2+} influx, synaptotagmin targets on plasma membrane through the interaction with PIP_2; 2) In the presence of Ca^{2+}, PIP_2 steers the Ca^{2+} binding pockets of both C_2 domains of synaptotagmin to insert into the plasma membrane; simultaneously, synaptotagmin interacts with t-SNAREs to help the SNARE complex assemble through self-oligomerization; 3) The tightened SNARE complex together with the oligomerized synaptotagmins pulls the vesicular membrane into close proximity to the plasma membrane and overcome the energy barrier for membrane fusion; 4) Fusion pore forms and neurotransmitters release. The second model is as the following (Rettig J and Neher E, 2002; Sudhof TC, 2004): 1) Before Ca^{2+} influx, complexin is bound to fully assembled SNARE complex (regulated by Sec1/Munc-18 like proteins) and synaptotagmin constitutively associates with the SNARE complex. The synaptic vesicle membrane and plasma membrane are forced into close proximity by SNARE complex assembly, which shows an unstable intermediate state (hemi-fuse state); 2) Ca^{2+} influx triggers the Ca^{2+} binding loops of synaptotagmin to insert into plasma membrane, which further destabilizes the fusion intermediate and mechanically perturbs to open the fusion pore. 3) Neurotransmitters release from vesicles through the fusion pore. The

prominent difference between these two models is whether the SNARE complex forms before or after Ca^{2+} influx, and whether it is synaptotagmin dependent or relies more on other molecules.

1.5 The aim of this study and work overview

The aim of this study is to understand the mechanism of action of synaptotagmin for exocytosis better. As described above, there are until now three main contributors of synaptotagmin known: phsopholipid, SNARE complex and synaptotagmin itself. In this study, the Ca^{2+} dependent phospholipid interaction is the central question. Especially, until the project was started, only a few electrophysiological investigations of synaptotagmin in murine neurons had been started (Geppert M, et al., 1994; Fernandez-Chacon R, et al., 2001). The main approach is to rescue synaptotagmin null neurons with synaptotagmin carrying various mutations and postulate the functions of the mutated residues by comparing mutants and wild type synaptotagmin rescued neurons. In this way, I try to uncover the possible interactions between synaptotagmin and phospholipid or synaptotagmin itself and subsequently deduce the mechanism of action of synaptotagmin in exocytosis.

There are several studies in this thesis: A) a basic characterization of synaptotagmin knock out (sytKO) neurons with comparison to WT neurons; B) truncation of either C_2 domains of synaptotagmin to evaluate their importance in synaptic transmission; C) neutralization of the Ca^{2+} binding sites of each domain to better understand the role of the Ca^{2+} dependent synaptotagmin-phospholipid interaction in vesicle release; D) replacing the hydrophobic residues in the Ca^{2+} binding sites with tryptophans to further clarify the importance of synaptotagmin-phospholipid interaction and the contribution of each C_2 domain for synaptic vesicle fusion; E) replacing each synaptotagmin C_2 domain with the corresponding C_2 domain from synaptotagmin isoform (synaptotagmin 7) to gain the insight of the importance of these C_2 domains in synaptic transmission.

2. Materials and methods

2.1 Experimental approach

The experimental design here is to investigate the physiological functions of a synaptic protein by overexpressing the exogenous protein or its mutants on the cultured murine hippocampal neurons (Ashery U, et al., 1999).

When a hippocampal neuron is grown on the isolated micro-island formed by astrocytes, the axon of the neuron is forced to grow within the dendritic region of the cell itself to form a large number of autaptic synapses. The parameters, such as kinetics, pharmacological properties, miniature currents, etc in both the excitatory and inhibitory autapses show little differences between cultured neurons and slices preparation (Bekkers JM and Stevens CF, 1991). In such a culture system, the total quantal size estimation is possible, since the origin of all synapses on the neuron is known.

The patch clamp technique initially developed for single ion channel current measurement (Neher E and Sakmann B, 1976) was adapted for whole cell recording, which is obtained by establishing a giga-seal and breaking a patch beneath the pipette tip with a strong pulse of suction (Hamill OP, et al., 1981). In the voltage clamp mode, the membrane potential is held constant (at about –70mV in resting condition) and the current flowing through the ion channels on the membrane is measured. With a brief depolarization at the soma in whole-cell voltage clamp mode, the basic scheme of synaptic transmission can be obtained as evoked postsynaptic currents by action potential induced neurotransmitter release. It is thought that usually one or no vesicle in the readily releasable pool (RRP) per synapse can be released by an action potential. To quantify the vesicular release probability (normalizing evoked release charge to total RRP charge), the RRP size is measured by hypertonic solution perfusion (i. e. 500 mM

sucrose for 4 seconds) through the fast flowing pipette. Although the exact mechanism of release mediated by hypertonic solution is not clear, it is believed that a Ca^{2+} independent mechanical stress on presynaptic cytoskeleton decreases the energy barrier for vesicle fusion (Stevens CF and Tsujimoto T, 1995; Rosenmund C and Stevens CF, 1996). Change in vesicular release probability is expected to alter synaptic strength (i. e. short term plasticity). In cultured hippocampal neurons, high frequency stimulation (i. e. 10 Hz) usually leads to a marked activity-dependent depression, which is mainly due to a depletion of RRP. Since the molecule studied here is synaptotagmin, a protein involved in Ca^{2+} sensing for vesicular release, another parameter worth considering is the Ca^{2+} sensitivity of the synapses. Technical difficulties (i. e. inaccessibility to the presynaptic terminal in this preparation, difficulty of monitoring the presynaptic Ca^{2+} transient, etc.) restrain the direct measurement of the synaptic Ca^{2+} sensitivity. The alternative way is to measure the apparent Ca^{2+} sensitivity by exogenous application of various Ca^{2+} concentrations (0.5 -12 mM).

The overexpression method based on the Semliki Forest virus (SFV) makes it possible to express exogenous proteins in the cultured hippocampal neurons. The gene of the interest can be ligated to a DNA cloning vector encoding nonstructural SFV gene for replicase, reverse transcriptase and helicase. After in vitro transcription, resultant RNA along with the helper vector is electroporated into a host cell line (i. e. BHK-21 cells, baby hamster kidney cells) for virus production. Enhanced yellow or green fluorescent protein is used here as a marker to detect the transfected neurons. The high viral expression efficiency of the protein makes the physiological measurement possible after 12 hours transfection on the cultured neurons.

2.2 Materials

2.2.1 Chemicals and solutions for neuronal culture

5-Fluro-2'-deoxyuridin
Albumin, bovine
Agarose Typ II-A
Cystein
Poly-D-Lysine
Trypsin Inhibitor
Uridine
-- from Sigma Co.

B27-Supplement
DMEM (Dulbecco's modified Eagle medium)
Glutamax-I Supplement
HBSS (Hanks Balanced Salt Solution)
N2-Supplement
NBA (Neurobasal A)
-- from Gibco BRL Co.

MITO
Collagen
-- from Collaborative Biomedical products Co.

Penicillin/Streptomycin
-- from Boehringer Mannheim Co.

Papain
-- from Worthington Biomedical Co.

Typsin/EDTA (Ethyldiaminetetraacetic acid)
-- from Biochrom Co.

FBS (Fetal Bovine Serum)
-- from Seromed Co.

Coating mixture

Acetic acid (17mM)	300 µl
Poly-D-Lysine (0.5mg/ml)	100 µl
Collagen (1mg/ml)	100 µl

Full medium (for astrocyte culture)

DMEM	180 ml
Fetal Calf Serum (FCS)	20 ml
Penicillin/Streptomycin	400 µl
MITO	200 µl

Store at 37°C, 5% CO_2 incubator

FUDR stock

5-fluoro-2'-deoxyuridine	25 mg
Uridine	62.5 mg
DMEM	12.5 ml

Neuron culture medium

NBA	100 ml
B27-supplement	2 ml
Glutamax	1 ml
Penicillin/streptomycin	200 µl

Enzyme digestion solution

Cystein	2 mg
DMEM	10 ml
$CaCl_2$ (100mM)	0.1 ml
EDTA (50mM)	0.1 ml
Papain	25 u/ml

Bubbling with carbogen (95% O_2 and 5% CO_2) for 15min before using.

Enzyme inhibition solution

Albumin	25 mg
Trypsin-Inhibitor	25 mg
Full Medium	10 ml

2.2.2 Materials for molecular biology

Those semliki forest virus (SFV) plasmids carrying synaptotagmin 1 (syt or syt1) wild type or mutant genes listed below were generated by Dr. Shin from Prof. Thomas C. Sudhof's lab. (pSFV1: the SFV plasmid; IRES, Internal Ribosome Entry Site; EGFP/EYFP: Enhanced Green/Yellow Fluorescence Protein)

SFV plasmids	syt inserts
pSFV1 – sytWT –IRES EYFP	Wild type syt;
pSFV1 – sytΔC_2A –IRES EYFP	Deletion of the C_2A domain (135-265), the C_2B domain (266-421) linked directly to Trans Membrane Region (1-134) of WT syt;
pSFV1 – sytΔC_2B –IRES EYFP	Deletion of the C_2B domain (266-421) from WT syt;
pSFV1 – sytC_2A3DA –IRES EYFP	Asps at 178, 230, 232 position of the C_2A domain replaced with Alas;
pSFV1 –sytC_2B3DA –IRES EYFP	Asps at 309, 363, 365 position of the C_2B domain replaced with Alas;
pSFV1 –sytC_2AB6DA –IRES EYFP	Asps at 178, 230, 232, 309, 363, 365 position replaced with Alas;
pSFV1 –sytC_2A3W –IRES EYFP	Met at 173, Phes at 231, 234 position of the C_2A domain replaced with Trps;

pSFV1 –sytC$_2$B3W –IRES EYFP	Val at 304, Tyr at 363, Ile at 367 position of the C$_2$B domain replaced with Trps;
pSFV1 –sytC$_2$AB6W –IRES EYFP	Met at 173, Phes at 231, 234, Val at 304, Tyr at 363, Ile at 367 position replaced with Trps.
pSFV1 –sytR$_{233}$Q –IRES EYFP	Arg at 233 position replaced with Gln;
pSFV1 –sytK$_{366}$Q –IRES EYFP	Lys at 366 position replaced with Gln;
pSFV1 –syt1(syt7 C$_2$B) –IRES EGFP	the C$_2$B domain (266-421) of syt1 replaced with the C$_2$B domain (260-403) of syt7;
pSFV1 –syt1(syt7 C$_2$A) –IRES EGFP	the C$_2$A domain (135-265) of syt1 replaced with the C$_2$A domain (135-258) of syt7;
pSFV1 –syt1(syt7 C$_2$AB) –IRES EGFP	Both C$_2$ domains (135-421) of syt1 replaced with the two C$_2$ domains (135-403) from syt7;

Besides these pSFV constructs, a few more SFV plasmids with syt mutants were made by myself:

SFV plasmids	syt inserts
pSFV1 –sytWT –IRES EGFP	
pSFV1 –sytΔC$_2$A –IRES EGFP	
pSFV1 –syt2KA –IRES EGFP	Lyses at 326, 327 position of the C$_2$B domain replaced with Alas;

Semlik forest virus plasmids

pSFV1 and its Helper-2
BHK-21 (Baby hamster kidney -21) cell line
-- from Gibco BRL Co.

Restriction enzymes

SpeI
BamHI
BssHII
Eco47III
-- from New England BioLabs Co.

Other chemicals

Taq DNA polymerase (pfu)
XL-1 Competent cells
-- from StrataGene Co.

DEPC (Diethylpyrocarbonate)
MOPS (4-Morpholinpropansulphonic acid)
Na-acetate
Glycerin
Phenol
Chloroform
--from Sigma Co.

dNTPs (Solution Mix of dATP, dGTP, dTTP and dCTP)

dATP (3. 2 -deoxyadenosine-5 Triphosphate)
dGTP (4. 2 -deoxyguanosine-5 Triphosphate)
dTTP (2. 2 -deoxythymidine-5 Triphosphate)
dCTP (1. 2 -deoxycytidine-5 Triphosphate)
-- from InvitroGene Co.

T4 DNA ligase
SOC medium
SP6 RNA polymerase
RNAse inhibitor
--from Gibco BRL Co.

MiniPrep box
MaxiPrep box
Gel purification box
PCR purification box
--from Qiagen Co.

Formaldehyd
Formamid
-- from BioRad Co.

PCR primers for mutagenesis

2KA For: 5'-AAGAAGGCAGCGACGACGATTAAGAAGAAC-3'

2KA Rev: 5'-CGTCGTCGCTGCTTCTTCAGCCTCTTACC-3'

-- for 2KA point mutation in C2B domain;

C_2B For: 5'-GAGAAACTGCAGAGCGCTGAGAAAGAAGAG-3'

C_2B Rev: 5'-AGCGCTCTGCAGTTTCTCCTCTTCCTTGGG-3'

-- for C2A domain deletion;

syt For: 5'-TATGGATCCGCCACCATGGTGAGTGCCAGTCATCC-3'

syt Rev: 5'-TATGCGCGCTTACTTCTTGACAGCCAGCAT-3'

-- for full length Syt.

-- from Ibc GmbH

2.2.3 Chemicals for electrophysiology

Internal solution (in mM)

KCl	136
$MgCl_2$	0.6
K_4EGTA	1
GTP-Na	0.3
ATP-Mg	4
HEPES	17.8
Phosphocreatin	12
Creatin-Phosphokinase	50 u/ml

---

pH 7.4, Osm 315;

External solution (in mM)

NaCl	140
KCl	2.4
$CaCl_2$	4
$MgCl_2$	4
Glucose	10
HEPES	10

---

pH 7.4, Osm 315.

EGTA (Ethylene glycol-bis(β-aminoethyl ether)
-N,N,N',N' tetra-acetic acid)
CsCl
$SrCl_2$
Sucrose
-- all from Sigma Co.
TTX (Tetrodotoxin)
NBQX (2,3-Dihydroxy-6-nitro-7-sulphamoylbenzo[f]quinoxaline)
-- from Tocris Co.

2.2.4 Electrophysiological hardware

Digitizer (Digidata 1322A)
Amplifier (Axopatch 200B, MultiClamp 700B)
-- from Axon Co.
Microscope (IX51)
-- from Olympus Co.
Drug Application System
-- from Warner Co.
Glass Pipette
($Ø_{inner}$x$Ø_{outer}$xLength, 0.86x1.5x80 mm)
-- from Science Products GmbH
Pipette Puller (P-97)
-- from Sutter Instrument Co.

2.2.5 Data analysis software

Clampex 9.0 (for data acquisition)	--from Axon Co.
Axograph 4.9 (for data analysis)	--from Axon Co.
Kaleidagraph 3.0 (for data analysis and graph presention)	--from Abelbeck Software
ClarisDraw (graph presentation)	--from Claris Co.

2.3 Methods

2.3.1 Mutagenesis of synaptotagmin (syt) mutants

Taking pSFV1-Syt 2KA-IRES EGFP Construction as an example:
The codons for Lysines (Lys, K) at the 326th, 327th position of amino acid sequence of Syt are replaced with two DNA codons for Alanine (Ala, A) in the two primers (2KA for and 2KA rev). Another two primers (Syt for and Syt rev) matching two terminals of Syt DNA sequence were also designed.
Two rounds of PCR programs were performed. The first round PCR procedure is listed as following:

PCR cocktail:			PCR program:	
Templet (pSFV-syt WT-IRES EGFP, 10ng/μl)	1	μl		
Primers (Syt for & 2KA rev, 20pmol/μl)	2.5	μl/each		
[or (Syt rev & 2KA for, 20pmol/μl)	2.5	μl/each]		
dNTP (2.5mM/μl)	4	μl		
10x PCR buffer	5	μl	94 °C	1 min
Taq Enzyme	0.5	μl	44 °C	1 min
H_2O	34.5	μl	72 °C	1 min
	---			---
	50	μl		x 25 runs

Following the above PCR procedure, two PCR products were generated, P1 and P2. Then the second PCR procedure was applied as following:

PCR cocktail:		PCR program:		
Templets (P1 & P2, 10ng/μl)	1 μl/each	A) 94 °C	1	min
Primers (Syt for & Syt rev, 20pmol/μl)***	2.5 μl/each	48 °C	1	min
dNTP (2.5mM/μl)	4 μl	72 °C	1.5	min
10x PCR buffer	5 μl	----------		
Taq Enzyme	0.5 μl		x 1	run
H_2O	33.5 μl			
	----------			
	50 μl	B) 94 °C	1	min
		44 °C	1	min
*** The primers were added after PCR program A		72 °C	3	min
		----------		
		x 25 runs		

Syt2KA PCR product and the plasmid vector (pSFV1-IRES-EGFP) were cut with restriction enzymes (BamH1 and BssHII separately) and then ligated in a ratio of 3:1, at 16 °C, overnight. On the second day, the ligation reaction was transformed to competent cells and plated on LB medium containing Ampicillin. Plates were kept at 37 °C, overnight. Bacterial colonies growing on the plates were selected and cultured in the LB medium, 37 °C overnight. Plasmid DNAs of colonies were extracted and characterized with restriction enzymes (BamHI and SpeI). Colonies with right inserts were maxipreped and later confirmed by DNA sequencing.

2.3.2 Semliki forest virus (SFV) replication

This work was done by technicians, Dirk Reuter and Hui Deng in our lab, just briefly described here:

2.3.2.1 mRNA *in vitro* preparation

4μg DNA (pSFV-1 plasmid containing synaptotagmin mutant) and 5μg helper DNA were linearized with SpeI to produce a 5' overhang. The linearized DNA

was purified by extraction with phenol-chloroform and ethanol precipitation. DNA restriction digest was vortexed with 150μl DEPC H_2O, 200 μl Phenol and 200μl chloroform. After centrifuge for 10 min at 14,000 rpm, the upper phase (containing DNA) was transferred to a fresh tube with 200 μl chloroform. After another centrifuge step (5min, 14,000 rpm), DNA was recovered from the upper phase by precipitation for 16 hours at –20 °C with 500 μl ethanol in the presence of 20 μl 3 M sodium acetate. The DNA was pelleted by centrifugation at 14,000 rpm for 15-30 mins, washed with 500 μl 70% ethanol and redissolved in 13 μl DEPC treated H_2O. For in vitro transcription, the DNA was mixed with RNA polymerase buffer (8 μl), SP6 RNA polymerase (2 μl), RNAse inhibitor (1 μl) and DEPC H_2O (16 μl) for 1hours at 37 °C. Afterwards, the DNA-RNA mix was added with 36 µl DEPC-treated H_2O and 4µl DNAse (50 u) and incubated at 37 °C for 20 min. The resulting RNA was purified from protein by extraction with phenol and chloroform as described above for DNA. The precipitated RNA was collected, desiccated and dissolved in 20 μl Rnase free water. 1 μl RNA was denatured at 65 °C for 10 min, and then checked on gel.

2.3.2.2 Electroporation of BHK-cells and harvest of viruses

The BHK-21 cells grown confluent up to 80-90% were split with trypsin (0.05%)-EDTA (0.02%) solution. Dissociated cells were spun down at low-speed centrifuge at 1,500 rpm for 5 min. After washing with ice-cold PBS, the cells were resuspended in the same buffer to the density of 10^7/ml. Then 10μg of each of the RNAs were mixed with 0.8ml of cell suspension in a tube. These cells were electroporated with 25ms 300V pulse once, then transferred into a tube with 9ml NBA medium and plated in cell culture flask. After incubation at 37 °C for 24 to 30 hours, the cells were centrifuged at 3,000 rpm for 10 min. The medium supernatant containing viruses was collected in 450μl tube and frozen at –80 °C before using.

2.3.3 Hippocampal neurons culture

The characteristic features of the syt -/- mice different from syt -/+ or WT new born mice are that the former have less milk in stomachs and the sizes are usually smaller comparing to the latter. Besides this, when the tail of syt -/- mouse was pinched, it will give a weaker and irregular sound. As to other parameters for distinguishing the syt-/- mice from the syt-/+ or WT ones, both genotyping and electrophysiology are applicable.

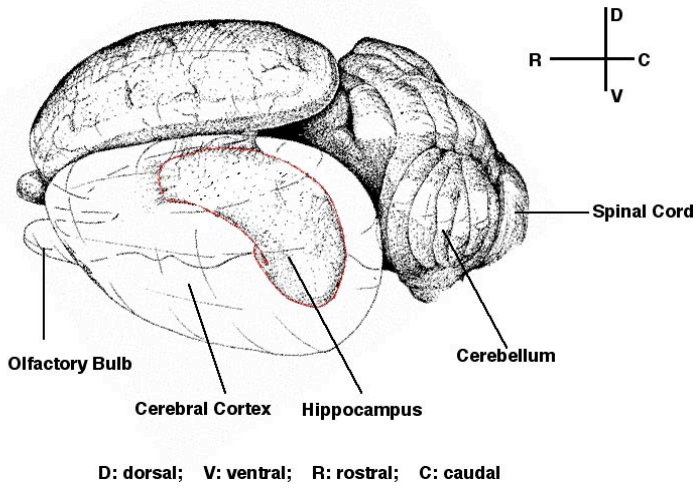

Figure 2.1 Stereo diagram of rat brain depicts the position of hippocampus. (Mouse brain is similar to it, picture is adapted from prof. John Jefferys' website, http://www.neuroscience.bham.ac.uk/neurophysiology/research/hippocampus.htm)

The procedure for hippocampus dissection out of mouse brain is quite simple. The mouse brain was cut down through the neck, then the skin and inner skull covering the brain were peeled off. The brain (fig. 2.1) was transferred quickly into cold HBSS medium. Under microscope, the two cortexes were pulled apart with slimmer forceps until the banana shaped hippocampus is visible. Then the hippocampus was taken out, put in enzyme digestion solution (500 μl) and kept shaking at 700 rpm, 37 °C for 1 hour. Afterward, digestion solution was replaced

with the same volume of enzyme inhibition solution and kept shaking at 37 ºC for 15 min. Well digested neurons were homogenously triturated and plated into 6 well plate containing confluent astrocyte microisland in low density (3-4 K/well). Cells were kept growing for 10 days before starting electrophysiological recording.

2.3.4 Astrocyte culture

The microisland autaptic neuron culture is the standard system in our lab for electrophysiological investigation. There are several steps to build up it: First of all, the sterilized glass coverslip was covered with a thin layer of agarose to prevent cell growing on it, then a regular collagen/PDL substrate dots were stamped on it, which are the microislands for astrocytes growing. Astrocytes were plated to form a confluent monolayer on the microislands, and later the neurons in low density were scattered individually on microislands to grow and form synapses between its own axon and dendrites.

The cleaned sterilized glass coverslips (∅ 30 mm) were coated with a thin layer of 0.15% agarose gel. After drying, coating mixture was stamped on the top of agarose gel with a rubber stamp with protruding pins of regularly spaced squares (200x200 μm) to form microislands. The plates were sterilized with UV light before plating astrocytes.

A half of the cortex from newborn wild type mouse was digested in 1 ml enzyme digestion solution at 37 °C for 1 hour (shaking at 700 rpm). After digestion, the cortex is transferred to a tube with 0.5 ml inhibition enzyme solution at 37 °C for 15 min (shaking at 700 rpm). After homogenizing the digested cortex, the cells were plated on 75 cm^2 flask in 10 ml full medium growing for 1 week until approaching confluence. Confluent astrocytes dissociated with trypsin (10 ml) were suspended and then centrifuged at 1,600 rpm for 5min. Astrocytes resuspended in 10 ml full medium were plated into glass coverslips in the density

of 30 K/well and kept growing. After approaching confluent microislands, astrocytes were controlled with FUDR (20 μl/well).

2.3.5 Electrophysiological characterization of syt mutants rescued neurons

2.3.5.1 Electrophysiology setup

The electrophysiology setup consists of two parts: a pharmacological manipulation part and data acquisition part. The pharmacological manipulation part consists of a microscope for localizing the neurons for patching, a manipulation system for positioning the electrode and fast solution flowing system (pipette shifting in 100 ms range) for drug application. The data acquisition part is composed of a digitizer for transforming the acquired analog data to digital data, an amplifier for amplifying the recording signals from patched neurons and a computer for data storage.

The open tip resistances of glass pipettes were about 2.0~3.5 MΩ in KCl based internal solution. Cells were whole-cell voltage clamped at -70 mV with the amplifier under control of the Clampex program. Currents were low-pass filtered at 2 or 5 kHz and stored at either 10 or 20 kHz. The series resistance was compensated to 70–80 %. Only cells with series resistances below 10 MΩ were analyzed.

2.3.5.2 Viral transfection on syt knock out neurons

After about 10 day's culture, neurons usually show prominent EPSC response. EPSC time course difference between WT and sytKO neurons helps distinguish the genotypes of plated neurons at this period.

The viruses were activated with 100 µl α-chymotrypsin for 30 min and then inactivated with addition of 100 µl Aprotinin to the mixture. Virus solution was added into culture plate 12~18 hours before starting electrophysiological recording. The fluorescence intensity of infected neurons (due to the expression of EG(Y)FP in virus constructs) indicated the infection efficiency and only those cells with bright fluorescence were recorded.

2.3.5.3 EPSC synchronous and asynchronous components analysis

The EPSC time course has two distinct components, which indicate the heterogeneous vesicular release modes: synchronous and asynchronous release. To quantify the amplitude of the components and their time constants, EPSC is integrated to show the charge accumulation. Double exponential curve fit was performed to acquire those parameters. The formula of double exponential is listed below:

$$A = A_{total} + A_0 * \exp(-t/\tau_s) + A_1 * \exp(-t/\tau_{as})$$

2.3.5.4 Readily releasable pool (RRP) size and vesicular release probability (Pvr) definition

RRP size of a neuron can be quantified by hypertonic solution stimulation, while the mechanism of it is not clear, maybe because high osmotic pressure decrease membrane fusion energy barrier (Rosenmund C and Stevens CF, 1996). As to the Pvr, it is defined as following:

$$Pvr = \text{EPSC charge} / \text{RRP charge}$$

The patched neuron was voltage clamped at –70 mV with a constant external solution flowing (~1 ml/min). A single evoked response preceded 4 s 500 mM sucrose application with an interval of 3 s. The charge of the single response and

the charge of transient invert current by sucrose are quantified as EPSC charge and RRP charge respectively (Fig. 2.2).

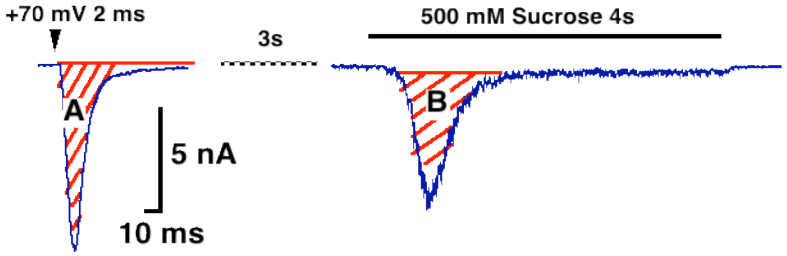

Figure 2.2 Definition of EPSC charge and readily releasable pool (RRP) size. As shown on the left, EPSC charge is calculated as the area A in red shadow; RRP size defined with 500 mM sucrose stimulation is calculated as the area B in red shadow (right side).

2.3.5.5 Evoked response recovery after RRP depletion

After hypertonic solution depleting the RRP, some reserve pool vesicles in the presynaptic terminal are thought to become fusion competent, refilling the RRP. During the RRP recovering period, action potential (AP) evoked response recovers gradually simultaneously.

To measure the EPSC recovery after RRP depletion, the experimental design was shown in Fig. 2.3. The first action potential (AP) evoked response preceded 4 s 500 mM sucrose application for RRP depletion. After that, various time intervals (ΔTs, 200 ms, 400 ms, 800 ms, 1 s, 2 s… etc.) were generated before the second action potential was initiated. The 2nd AP evoked EPSC charge was normalized to the 1st EPSC, representing the EPSC recovery.

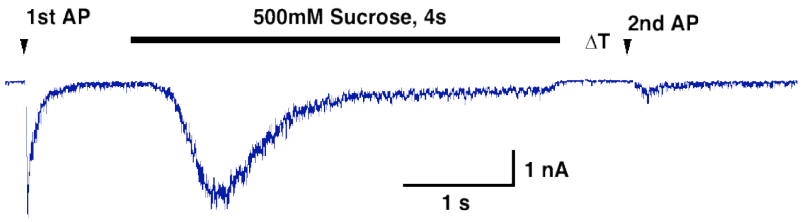

Figure 2.3 Experimental design for EPSC recovery measurement after RRP depletion in sytKO neurons.

2.3.5.6 Short term plasticity (STP) of neurons

A consecutive AP stimulation in high frequency usually will change the synaptic transmission efficiency, for instance, increasing or decreasing vesicular release probability, vesicular release becoming more asynchronous or more synchronous, etc. All these are called the short-term plasticity of neurons. An investigation of neuronal STP can provide information for the working efficiency of those molecules involved in this process (for review, Zucker R and Regehr WG, 2002).

Neuronal STP was generated with a 10 Hz AP trains for 5 s. The individual evoked EPSC amplitude was normalized to the first response during the train and the time course of the normalized EPSC amplitudes were plotted (Fig. 2.4).

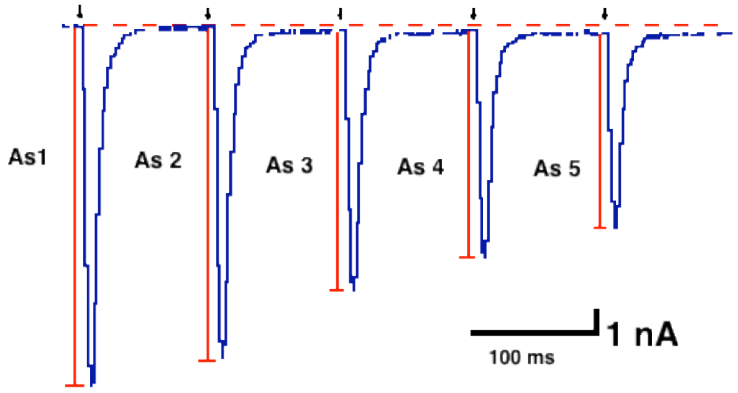

Figure 2.4 The EPSC amplitude measurement for quantifying STP. Arrow represents stimulation; Asi (i=1,2,3…) is the amplitude of the ith EPSC.

2.3.5.7 Spontaneous vesicular release analysis

In the presence of 300 nM TTX in external solution, the Na^{2+} channels required for firing APs were completely blocked. The recorded events represent the spontaneous vesicular release or miniature EPSC. To determine spontaneous vesicular release rate, 50 consecutive sweeps of 2 s recording were performed.

For data analysis, first of all, a standard mEPSC template with variable amplitude was defined. Its rise time (80% of the amplitude) was set as 0.5ms and exponential decay time constant as 3ms. The Detection criterion is calculated from the template scaling factor (Scale, peak amplitude of the event), and from the goodness-of-fit (SSE, the **s**um of **s**quares for **e**rror) between the scaled template and the data, which is defined as the following:

Detection=Scale/sqrt(SSE/ N-1)

Where, sqrt, square root function

Since sqrt(SSE/N-1) approximates the noise standard deviation, the dection criterion is related to the signal-to-noise ratio for the detected events. Usually, Detection is set as 3.5, a reasonable threshold for events with a significant deviation from the noise (Fig. 2.5 A). The mean EPSC was calculated by averaging all detected events (Fig. 2.5 B). The mini rate was the frequency of events occurring, which was calculated as the following:

$$F_{mepsc}$$= Number of events/ recording time scale (100s)

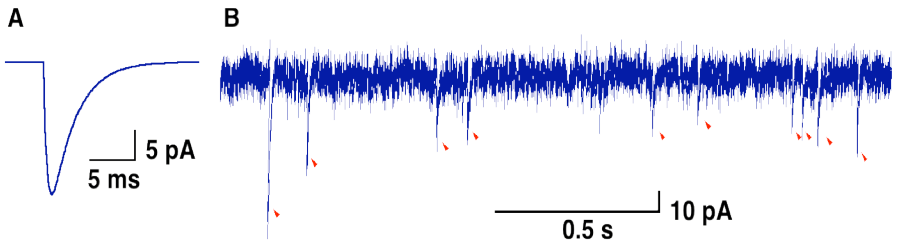

Figure 2.5 mEPSC analysis A. The template mEPSC given by exponential function; B Events detected with the mEPSC template in a sweep of 2s recording (Red arrows point out those detected events).

2.3.5.8 Apparent Ca^{2+} sensitivity measurement

Vesicle release efficiency upon Ca^{2+} influx is greatly affected by the Ca^{2+} sensitivity of the Ca^{2+} sensor(s). The direct method measuring presynaptic Ca^{2+} concentration at the release site is not available in hippocampal neurons.

However, apparent Ca^{2+} sensitivity can be detected using various external Ca^{2+} concentrations.

EPSCs under normal external solution (in mM, 4 Ca^{2+}, 4 Mg^{2+}) were recorded before and after certain Ca^{2+} concentration solution application; 6 to 9 traces were recorded in each condition (Fig. 2.6).

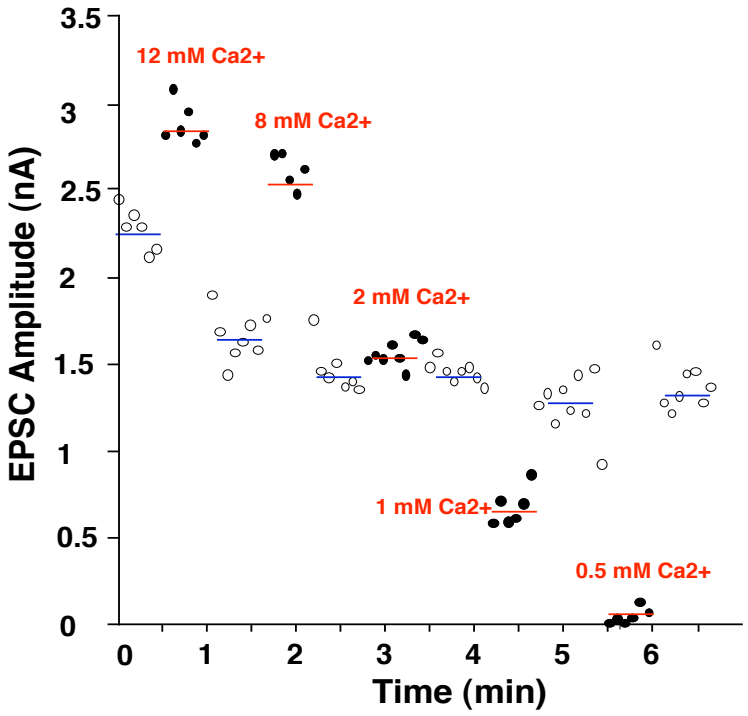

Figure 2.6 EPSC amplitudes in various external Ca^{2+} concentrations recorded from a single neuron. Circle dots represent EPSCs in control solution (4 mM Ca^{2+}, 4 mM Mg^{2+}) and filled dots represent external solution with various Ca^{2+} concentrations (0.5, 1, 2, 8, 12 mM Ca^{2+}, in presence of 1 mM Mg^{2+}). Blue dashed bars are mean control responses and red dashed bars are mean values of EPSC in different Ca^{2+} concentrations.

The mean value of blue dashed bars before and after EPSC amplitude in certain Ca^{2+} concentration is defined as the control EPSC amplitude. EPSC amplitude in certain Ca^{2+} concentration (red dashed bar value) is normalized to the control

amplitude, and is plotted against external Ca^{2+} concentrations. Data points are fitted with Hill equation:

$$Y=Y_{max}/(1+(K_d/[Ca^{2+}])^n)$$

Here K_d is the Ca^{2+} dissociated constant; $[Ca^{2+}]$ is the external Ca^{2+} concentration; n is the Ca^{2+} cooperativity.

2.3.6 Data analysis and experimental bias minimization

Cultured neurons show a relatively high variability in EPSC and RRP size measurement due to variable geometry of microdots and the number of synapses formed. Additionally, the value of these parameters will increase with neuronal culture days *in vitro* due to the increase in synapse number. To resolve this variability problem, I usually recorded more than 15 neurons for one parameter, and collected similar number of cells in the control and the test group per day. Neuronal recording is restricted in 10^{th} –16^{th} days' culture *in vitro*, unless it is noted in the text. For other parameters, such as vesicular release probability, I found that it is less sensitive to neuronal development (Fig. 3.3B).

For the comparison of two groups of data to determine whether they are likely to have come from the same underlying population that have the same mean value, unequal variance Student's t-test (two-tailed distribution) was performed. For comparison of more than two groups of data, Kruskal-Wallis (KW) nonparametric ANOVA test was performed to give a conservative estimation whether the difference in groups is significant. Based on the KW nonparametric test results, Dunn's multiple comparisons test specifies the pairs of groups with significant difference.

3. Results

The functional significance of synaptotagmin 1 (syt or syt1) for exocytosis has been depicted both in the *Drosophila* and Murine systems by knock out techniques. In *Drosophila* neuromuscular junctions, the vesicular neurotransmitter release was severely impaired by eliminating of syt (Littleton JT, et al., 1993). In the Murine central neuronal synapses, the lack of syt leads to much slower time course of evoked response (Geppert M, et al., 1994).

This study consists of two parts, namely: A) a detailed analysis of the phenotype of syt knock out (sytKO) hippocampal neurons by evaluating the effect of syt in Ca^{2+} evoked response. Furthermore, additional parameters were also examined, such as, the readily releasable vesicle pool (RRP), evoked response recovery after RRP depletion, apparent Ca^{2+} sensitivity and presynaptic Ca^{2+} buffering effect. B) an in depth structure/function study of syt using a viral rescue approach to overexpress exogenous syt carrying amino acid mutations in sytKO neurons.

3.1 Basic characterization of sytKO hippocampal neurons

3.1.1 Neonatal features of sytKO mice

The sytKO mouse strain was generated in Prof. Thomas C. Sudhof's lab. The behavior phenotype of these mice has been previously described (Geppert M, et al., 1994) and my observation of the mice is in full agreement with the description. The following is a brief characterization of the sytKO phenotype:

The sytKO mice delivered by syt +/- parents usually die on the first day of birth. As described in section 2.3.3, the newborn pups lacking syt were characterized by an absence of milk in stomach and a morphologically smaller size as

compared to their syt heterozygous or wild type littermates. No evident morphological dysfunction in neuronal development has been observed in cultured hippocampal neurons due to knocking out syt.

3.1.2 Postsynaptic response (PSC) time course of the excitatory and inhibitory sytKO hippocampal neurons

In order to examine the function of presynaptic proteins, such as syt, the initial test is to verify whether the evoked vesicular release in central neurons is affected by removal of this protein.

Using standard whole-cell patch clamping mode, parallelly cultured sytKO and wild type neurons were stimulated with a 2 ms, 70 mV membrane depolarization pulse at a frequency of 0.2 Hz and the subsequent somatic excitatory postsynaptic current (EPSC) was recorded (Fig. 3.1 Left). The delayed EPSC response in syt null neurons is consistent with the previous report (Geppert M, et al., 1994), but the characteristics of evoked response in inhibitory hippocampal neurons was not examined previously.

The same experiment was performed in inhibitory hippocampal neurons. Interestingly, the evoked inhibitory postsynaptic current was also slower (Fig. 3.1 right).

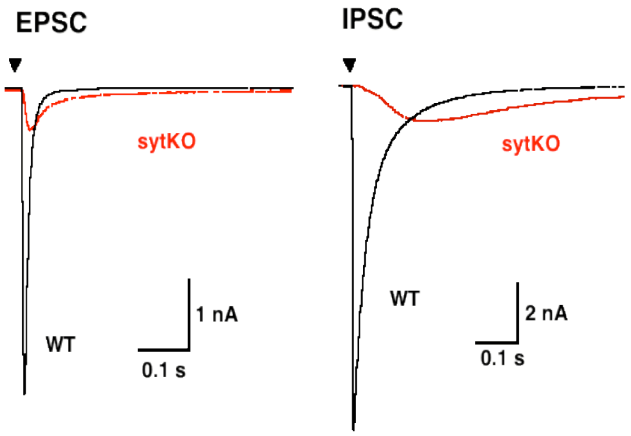

Figure 3.1 PSC traces recorded from excitatory and inhibitory neurons reveal slower time course by knocking out syt. (Black arrows indicate the depolarization pulse)

The one second PSCs cumulative charges were fitted with double exponential equation (section 2.3.5.3) and the time constants of two components in each type of hippocampal neurons are listed in the following table:

Table 3.1 Time constants of the components of PSCs

Hippocampal neurons	τ_{fast} (ms)	τ_{slow} (ms)
WT excitatory	~7	~170
sytKO excitatory	~38	~310
WT inhibitory	~36	~150
sytKO inhibitory	~69	~600

The slower evoked response of both types of hippocampal neurons by knocking out syt suggests that syt has a similar function in these neurons. Furthermore, these data show that both the fast and slow components of the evoked response are slowed down by knocking out syt in hippocampal neurons, indicating that syt may play a role not only in the synchronous release but also in the asynchronous release.In the following studies, most experiments were performed on excitatory hippocampal neurons unless otherwise indicated.

3.1.3 The evoked vesicular release and the readily releasable pool (RRP) in sytKO neurons

Evoked vesicular release efficiency is determined both by the vesicular release speed and the amount of released vesicles. Knocking out syt leads to slower vesicular release as shown in above section, whether the number of released vesicles is altered or not is not clear. In order to clarify this question, the charges of EPSC from parallel wild type and sytKO neuronal culture were compared.

The EPSC traces from both groups were integrated in a period of 1 s and the cumulative charges were calculated. Clearly there is a gradual increase in EPSC charge during neuronal development in both sytKO and WT neurons (Fig. 3.2 A) and the evoked response of sytKO neurons is smaller than that of WT ones throughout the days of measurement. The average EPSC charge for WT (from the 8^{th} to 14^{th} day) is 55.1± 4.1 pC (n=93) and for sytKO neurons is 19.7± 2.5 pC, (n=89) (t-test $p<0.001$, Fig. 3.2 B). By fitting the EPSC time course with the double exponential equation, the amplitude of each component for sytKO is Q_{fast}= 9.3± 1.1 pC and Q_{slow}= 11.3± 1.4 pC; while for the WT the values are Q_{fast}= 55.2± 3.9 pC and Q_{slow}= 5.7± 0.5 pC. This shows mainly a reduction in the fast component amplitude together with an increase of slow component amplitude in sytKO neurons. Additionally, no change in either amplitude or frequency of miniature EPSCs was found in sytKO neurons compared to WT neurons throughout the neuronal development (data not shown). This suggests that the reduction of evoked release is neither due to defects of postsynaptic receptors nor contents of vesicles ready for fusion in sytKO neurons.

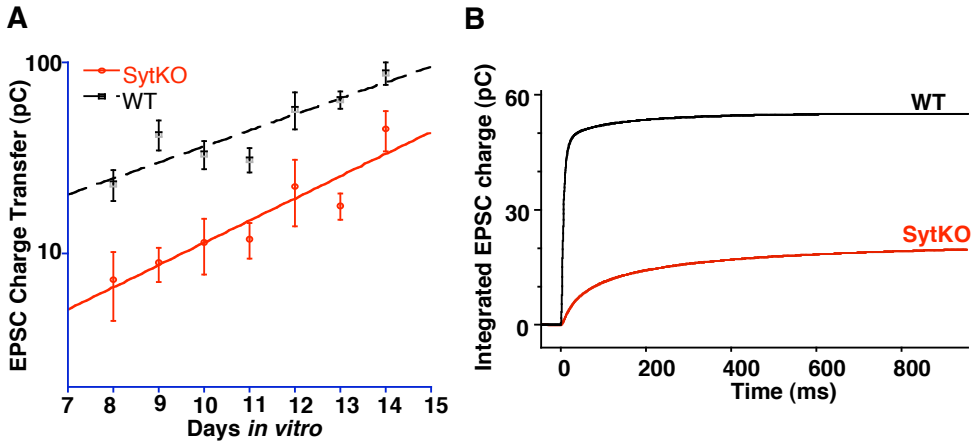

Figure 3.2 Parallel comparison of EPSC charge recorded from the sytKO and the WT hippocampal neurons. A, Developmental increase of EPSC charges of the sytKO and the WT neurons. Data were fitted with single exponential equation. Cells were recorded from the 8th to 14th days after neuronal culture and each data point is the mean value of 10-15 cells. (Student's t-test indicates that EPSC charge of sytKO neurons is significantly different from that of WT neurons in each day's comparison. For 8th, 9th, 10th, 11th and 13th day, $p<0.001$ and for 12th, 14th day, $p<0.05$) B, The average integration of EPSC charges of the sytKO and the WT neurons (WT n=93 and sytKO n=89, data from one batch of neuronal culture).

To rule out the possibility that the reduction of EPSC charge is due to a defect in other steps of vesicle recycling preceding exocytosis, such as vesicular priming, vesicular refilling, the RRP size was quantified by hypertonic solution application.

A 4s pulse of 500 mM sucrose was applied to the patched neuron and the transient inward current was measured. No difference in RRP size was found between sytKO neurons and WT neurons (Fig. 3.3 A). The mean RRP size of the sytKO neurons was 451± 46 pC, n=83, and the mean value for the WT neurons was 471± 39 pC, n=90. Student's t-test suggests no difference of RRP size between sytKO neurons and WT neurons in each day's comparison. The similar RRP sizes calculated from these two groups suggests that the EPSC charge reduction in sytKO neurons is not due to a shortage of fusion competent vesicles.

Since both EPSC charge and RRP size will increase along with the neuronal development (Fig. 3.2 A and 3.3 A), the variance of these values is relatively high, which makes the comparison between sytKO and WT neurons become less reliable with development. The vesicular release probability (Pvr) of each type of neurons was calculated by normalizing EPSC charge to RRP size to consolidate the above findings (Fig. 3.3 B). The relative constant Pvr in each individual day of measurement suggests that there is a reduction of release efficiency in sytKO neurons compared to WT neurons.

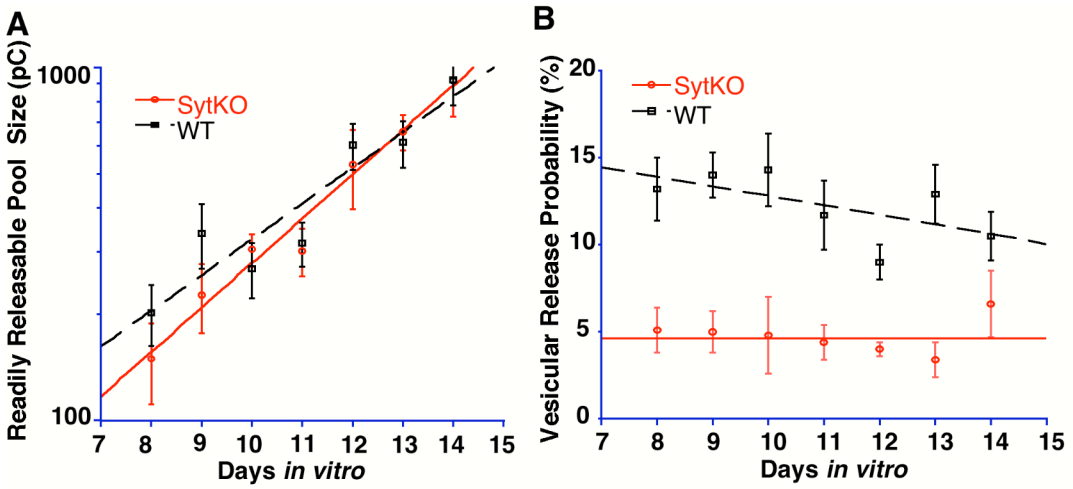

Figure 3.3 RRP size and Pvr comparison between sytKO and WT neurons. A) Unchanged RRP size in sytKO neurons compared to WT neurons (Data were fitted with single exponential equation.); B) Neuronal development independent Pvr in sytKO and WT neurons. Each data point represents the mean value of 10-15 cells (Student's t-test suggests that Pvr of sytKO neurons is significantly different from WT neurons in each day's comparison (except the 14th day), $p < 0.01$) Data were from one batch of neuronal culture and fitted with linear equation).

3.1.4 EPSC recovery following Ca^{2+} independent RRP depletion in sytKO neurons

Since knocking out syt mainly reduced the amount of evoked fast vesicular release without affecting the total number of the fusion competent vesicles in all synapses, sytKO neurons is a very good model to study the characteristics of the slower release (so called, asynchronous release). Different fusion competent vesicles release modes in sytKO and WT neurons may be based on different refilling kinetics. Based on this rationale, the EPSC recovery after vesicle pool depletion was measured as described in section 2.3.5.5.

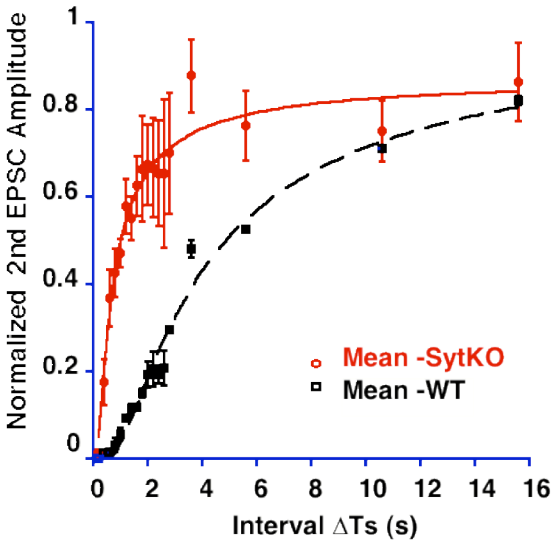

Figure 3.4 the recovery of EPSC after RRP depletion in sytKO neurons and WT neurons (sytKO n=10, WT n=3). (Data were collected from 16-day old sytKO neurons and 11-day old WT neurons respectively.)

As shown in Fig. 3.4, the EPSC recovery after RRP depletion developed faster in sytKO neurons than in WT neurons. By fitting these data with a single exponential equation, τ_{sytKO} was 0.57 s and τ_{WT} was 3.4 s. Since the evoked vesicle release in sytKO neurons is predominantly asynchronous, the faster recovery observed above may imply that the asynchronous vesicles have a faster refilling rate than the synchronous vesicles. However, the data were recorded from cultures with different day *in vitro* and the number of WT neuron is small, so this interesting finding needs further confirmation.

3.1.5 Different Ca^{2+} sensing properties of fusion competent vesicles between WT and sytKO neurons

3.1.5.1 Decreased apparent ca^{2+} sensitivity by knocking out syt in hippocampal neurons

The reduction of evoked responses in sytKO neurons (Fig. 3.2) may be due to decreased Ca^{2+} sensitivity of the vesicles in the absence of syt. To evaluate this possibility, the apparent Ca^{2+} sensitivity was measured in sytKO neurons. By varying the exogenous Ca^{2+} concentration and studying its effect on vesicular release efficiency, one can elucidate the possible role of syt in Ca^{2+} sensing for exocytosis.

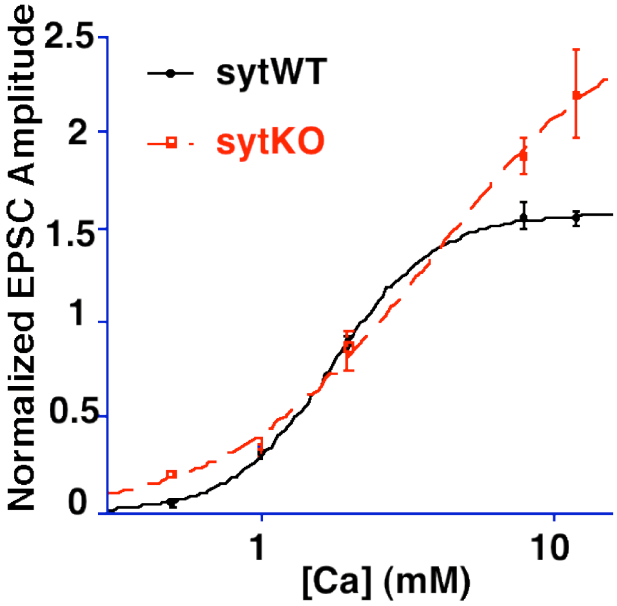

Figure 3.5 Apparent Ca^{2+} sensitivity of sytKO neurons and sytWT rescued neurons. (Data were fitted with Hill equation, Ca^{2+} cooperativity for sytKO, 1.3± 0.2, n=6; sytWT 2.5± 0.1, n=16)

As shown in Fig 3.5, by fitting the Ca^{2+} dose response data with the Hill equation, the K_d of Ca^{2+} for sytWT rescued neurons is 1.8± 0.04 mM (similar to a previous report in WT hippocampal neurons, K_d =1.9± 0.2 mM, Fernandez-Chacon R, et al., 2001) and for SytKO is 3.8± 1.2 mM. By knocking out syt, the apparent Ca^{2+} sensitivity was decreased about two fold, which explains the low release efficiency in sytKO neurons compared to WT cells.

It is important to take into consideration certain factors that may affect accuracy of the apparent Ca^{2+} sensitivity measurement. The first factor is that 12 mM Ca^{2+}

cannot saturate the EPSC response in sytKO neurons. Ideally it will be better to measure the EPSC response in a higher Ca^{2+} concentration (i. e. 16 mM Ca^{2+}) to generate a correct fit for these data. Since high Ca^{2+} concentration can cause the reduction of the excitability of the axon and thereby negatively affect the EPSC response due to poor action potential propagation. Therefore the recordings become more unreliable by increasing Ca^{2+} concentration. Second, the data set is from one culture of neurons, to consolidate the finding, another set of experiment would be desirable.

3.1.5.2 Inhibition of vesicular release with pipette injection of EGTA in sytKO neurons

Synchronous release and asynchronous release are thought to be regulated by different Ca^{2+} sensors (Goda Y and Stevens CF, 1994). It has also been suggested that these two components are dominated by the distance of vesicles from Ca^{2+} channels (Neher E, 1998). Vesicles located closer to Ca^{2+} channels experience a rapid Ca^{2+} transient rise, thus they will be released synchronously; The longer time for Ca^{2+} diffusion to reach those vesicles located further from Ca^{2+} channels helps explain the asynchronous release.

EGTA is a widely used Ca^{2+} binding buffer. When a high concentration of EGTA is applied to presynaptic terminals, it causes a narrower range of Ca^{2+} diffusion from the Ca^{2+} channels, together with a competition against Ca^{2+} sensor to bind to Ca^{2+} ions.

To understand the mechanism of synchronous and asynchronous release, the experiment of EGTA (1 mM or 50 mM) injection via patch pipette was performed. After patching a cell, EPSCs were recorded with 0.2 Hz stimulation for 10 min in both sytKO and WT neurons. Every five consecutive EPSC responses were averaged as one data point shown in the Fig 3.6.

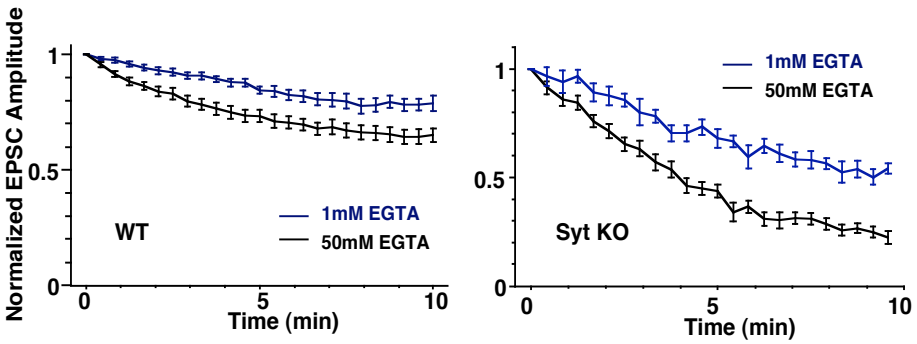

Figure 3.6 Pipette injected EGTA inhibits evoked neurotransmitter release. (For WT, 1 mM EGTA n=14, 50 mM EGTA n=19; For sytKO, 1 mM EGTA n=13, 50 mM EGTA n=15)

The inhibition of neurotransmitter release in the sytKO neurons is stronger than the WT neurons under 1 mM/ 50 mM EGTA condition, which indicates that asynchronous release is more easily inhibited by EGTA compared to synchronous release.

The reduction of EPSC by a high concentration of EGTA in the sytKO neurons may be due to either buffering the Ca^{2+} transient during its diffusion to releasable vesicles or shorter onset time for Ca^{2+} binding EGTA comparing to unknown Ca^{2+} sensor on vesicles. If we can find another Ca^{2+} buffer, which has similar Ca^{2+} onset time as EGTA but lower Ca^{2+} affinity, then perhaps the mechanism can be better explained.

An alternative explanation can be that asynchronous released vesicles have lower Ca^{2+} sensitivity compared to synchronous released vesicles (section 3.1.5.1). When high concentration of EGTA exists in the presynaptic terminals, the asynchronous released vesicles that need high concentration of Ca^{2+} to release will be affected more severely than the synchronous released vesicles that can detect lower Ca^{2+} concentration.

3.2 Functional/structural analysis of syt by over-expressing syt mutants in sytKO neurons

The transfection of the cultured sytKO hippocampal neurons with Semliki forest virus (SFV) carrying wild type syt construct can restore sytKO EPSC time course to wild type level (Han WP, et al., 2004). The physiological function of syt can be studied in detail by taking the advantage of the rescue approach.

The experimental design for this study was initiated in 2002, when there were few reports about the functions of syt using murine neurons as a model. The mechanism of action of syt in exocytosis was better illustrated with the progress of this project and the fast development of relevant studies in this field (Stevens CF and Sullivan JM, 2002; Nishiki T and Augustine GJ, 2004b). Although during my study period, other labs have reported some findings of syt by similar approach, the parameters that I have examined are not completely overlapped.

The experimental design for syt functional study is to try to reveal the residues crucial for the functions of syt by using site directed mutagenesis. (A) Since syt is a protein with two Ca^{2+} binding domains in the cytosolic part, truncation of either C_2 domain to evaluate the loss of function of syt can be the starting point to reveal the importance of the C_2 domain for the function of syt. (B) To gain deeper insight of the function of syt, those aspartates in either C_2 domain which have been shown to be important for Ca^{2+} dependent syt-phospholipid interaction in *in vitro* biochemical studies (Zhang X, et al., 1998; Davletov B, et al., 1998; Ubach J, et al., 2001; Fernandez I, et al., 2001) were neutralized. Additionally, this can be helpful to reveal the physiological importance of syt-phospholipid interaction. (C) The hydrophobic residues in the top Ca^{2+} binding loops (Loop 1 and 3) of the two C_2 domains, which have been reported to insert into phospholipid membrane in *in vitro* studies (Chapman ER and Davis AF, 1998; Bai J, et al., 2002) were investigated by mutating them to the bulky hydrophobic amino acid, tryptophan,

to test whether a gain of function mutant can be acquired. This study can give further implications on the physiological importance of syt-phospholipid interaction. (D) It has been shown that the polybasic region of the C_2B domain interacts with multiple molecules (Chapman ER, et al., 1998). Therefore by neutralizing these basic residues to abolish the interactions, one can evaluate whether these interactions, especially syt self-oligomerization, are essential for synaptic transmission. (E) Finally, a study of syt1/7 chimera constructs was performed, which not only shed some light on the physiological functions of the C_2 domains of syt7, but also gave hints on the physiological importance of the C_2 domains of syt1.

3.2.1 The importance of the two C_2 domain of syt

Semliki forest virus carrying full length syt or syt lacking either C_2 domain was transfected in cultured autaptic sytKO neurons. The direct evaluation of these constructs is via the EPSC amplitude and time course of release. The RRP size quantified by hypertonic solution application is also a good parameter for revealing their functions.

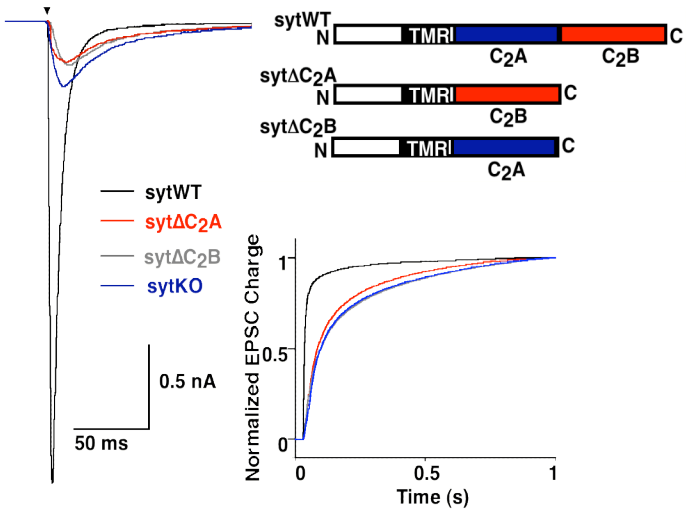

Figure 3.7 EPSC traces of sytKO neurons rescued with sytWT, syt C_2A fragment (sytΔC_2B) or syt C_2B fragment (sytΔC_2A). Insert shows the EPSC time course of different mutants. Black arrow represents the 2 ms, +70 mV depolarization of the neuron. (Subsequent figures will mainly use integrated EPSC curve to emphasize the time course of release, which is the major factor in revealing the function of syt.)

Constructs transfected in sytKO neurons with loss of either C_2 domain failed to rescue fast neurotransmitter release (Fig. 3.7). The total evoked EPSC charge of truncated constructs was reduced to about 50% of that in sytWT rescues (sytWT 22.7 ± 2.4 pC, n=49; sytΔC_2B 13.8 ±1.4 pC, n=57; sytΔC_2A 12.0 ± 2.4 pC, n=53; sytKO 19.6 ± 1.7 pC, n=52). These indicate that both C_2 domains are indispensable for syt fulfilling its function.

Hypertonic solution was used to quantify the RRP size of these mutants, as shown in Fig 3.8 A. Deletion of the C_2A domain leaves the RRP size unchanged (sytΔC_2A compared to sytKO), while any syt rescue constructs containing the C_2A domain reduced the RRP size to about 60% (sytΔC_2B 315 ± 38 pC; sytWT 260±25 pC; compared to sytKO 512 ± 48 pC). This suggests that overexpression of the C_2A domain of syt can reduce RRP size. In Fig 3.8 B, the vesicle release probability (Pvr), as calculated by normalizing EPSC charge to RRP size, is increased more than two fold if sytKO neurons are rescued with sytWT construct (sytKO 4.3 ± 0.4%; sytWT 9.5 ± 0.7%), but neurons transfected with truncated syt constructs have smaller Pvr than sytWT rescued neurons (sytΔC_2B 6.8 ± 0.7%; sytΔC_2A 3.1 ± 0.7%).

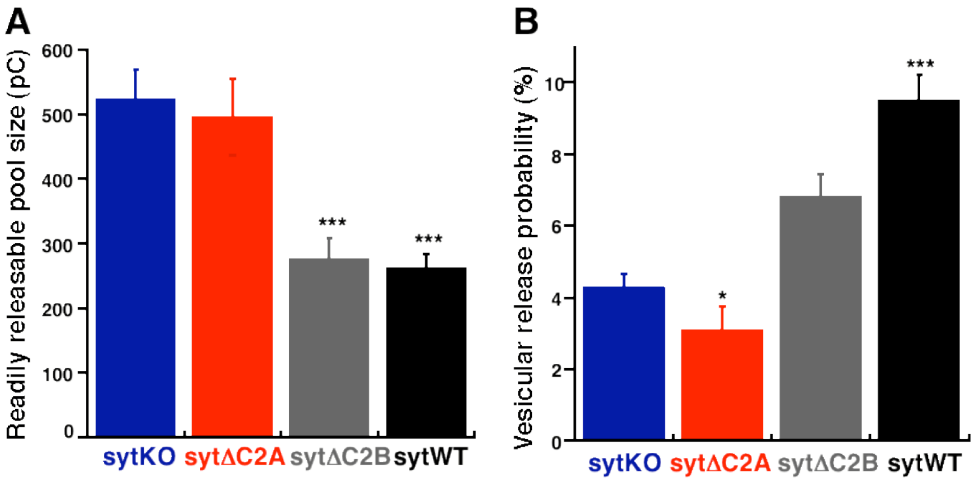

Figure 3.8 A. RRP size of the syt truncated mutants or sytWT rescued neurons and sytKO neurons (*** indicates KW nonparametric test and Dunn's multiple comparison test, $p<0.001$, each rescue compared to sytKO neurons; B. Vesicular release probability (Pvr) of three constructs rescued neurons compared to sytKO neurons (* and *** indicate KW nonparametric test and Dunn's multiple comparison test, $p<0.05$ and $p<0.001$ respectively; t-test shows that the Pvr of sytΔC_2B rescue is significantly different from that of sytWT rescue, $p<0.05$). sytKO n=52, sytΔC2A n=53, sytΔC2B n=55, sytWT n=49. Data are collected from three batches of neuronal cultures.

It is important to note that sytWT rescued neurons have similar EPSC charge as sytKO neurons (sytWT 22.7 ± 2.4 pC, n=49 and sytKO 19.6 ± 1.7 pC, n=52), which seems inconsistent with the finding in section 3.1.3, where the EPSC charge of sytKO neurons is much smaller than that of WT ones (Fig. 3.2). However, the reduction of RRP size in sytWT rescued neurons compared to sytKO neurons (Fig.3.8 A) explains this discrepancy, because in section 3.1.3, the RRP size of WT neurons is similar to that of sytKO neurons (Fig. 3.3). The viral overexpression of sytWT leads to reduced EPSC charge and RRP size, but has no significant effect on the vesicular release probability (sytKO 4.8 ± 0.5%, n=83 and WT 12.2 ± 0.6%, n=90 in section 3.1.3; sytKO 4.3 ± 0.4%, n=52 and sytWT 9.5 ± 0.7%, n=49, in this section).

3.2.2 Differential roles of the Ca^{2+} binding sites in two C_2 domains for fast vesicular release (partial contribution from Jeong Seop Rhee)

Each C_2 domain has five Asp residues in the top loop1 and 3 that contribute to the Ca^{2+} mediated phospholipid binding (Shao X, et al., 1996). Neutralizing the 2nd to 4th Asp residues in the C_2A domain ($D_{172,\ 230,\ 232}A$) or the corresponding Asp residues in the C_2B domain ($D_{303,\ 363,\ 365}A$) decreases the Ca^{2+} dependent syt-phospholipid interaction *in vitro* (Ok-Ho Shin, personal communication). To evaluate the consequence of these mutations in physiological conditions, the following experiments were performed.

3.2.2.1 Neutralizing the 2nd, 3rd and 4th Asp to Ala in the C_2A domain (Abr. sytC$_2$A3DA)

SytC$_2$A3DA rescued sytKO neurons produces fast synaptic response like sytWT, but the statistics showed about a 40% reduction in EPSC amplitude of this mutant (sytWT 1.64 ± 0.14 nA; sytC$_2$A3DA 1.05 ± 0.09 nA). By comparing the normalized cumulative EPSC charge of sytWT and sytC$_2$A3DA rescued neurons, the latter has a relatively higher asynchronous release component (Fig. 3.9).

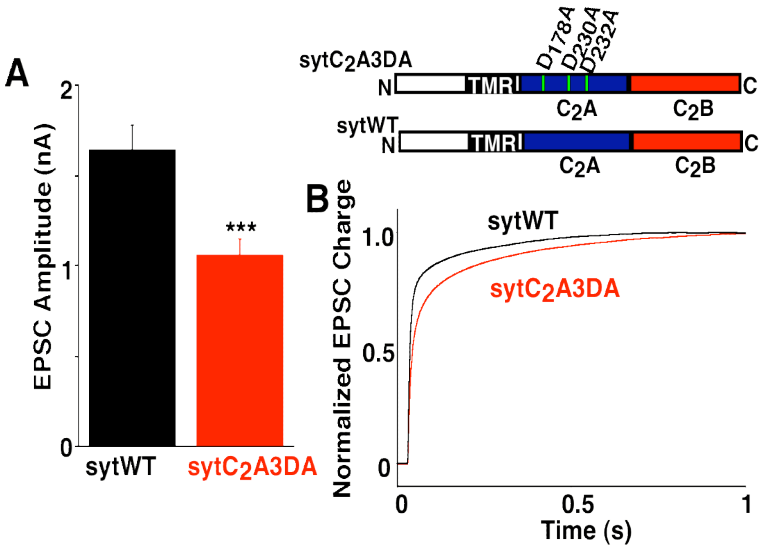

Figure 3.9 Basic EPSC characteristics of sytC$_2$A3DA mutant. A. EPSC amplitudes of sytWT and sytC$_2$A3DA rescued neurons (sytWT n=58; sytC$_2$A3DA n=82, data were collected from 5 batches of neuronal cultures and *** indicates t-test p<0.001). B. Normalized cumulative EPSC charge in a period of 1 s.

The RRP size and vesicular release probability of the rescued sytKO neurons were also quantified and Student's t-test showed no significant differences between sytC$_2$A3DA and sytWT rescued neurons in the tested parameters (data not shown). These results suggest that the Ca^{2+} binding sites in the C$_2$A domain regulate synchronous release efficiency. Neutralizing these binding sites leads to a smaller synchronous release but larger asynchronous release without affecting the total release.

3.2.2.2 Neutralizing the 2nd, 3rd and 4th Asp to Ala in the C$_2$B domain (Abr. sytC$_2$B3DA)

In contrast sytKO neurons transfected with sytC$_2$B3DA, a mutant that neutralizes three Asps in the C$_2$B domain, does not rescue the fast synaptic transmission. The EPSC charge is reduced to about 50% in this mutant in contrast to that of sytWT rescued neurons, while the RRP size was not changed. The sytC$_2$AB6DA construct, with the six Asps neutralized in both the C$_2$A and the C$_2$B domain, was tested simultaneously with the sytC$_2$B3DA. As expected, no rescue was found in the sytC$_2$AB6DA mutant and no change in either EPSC charge or RRP size compared to sytKO neurons (Fig 3.10).

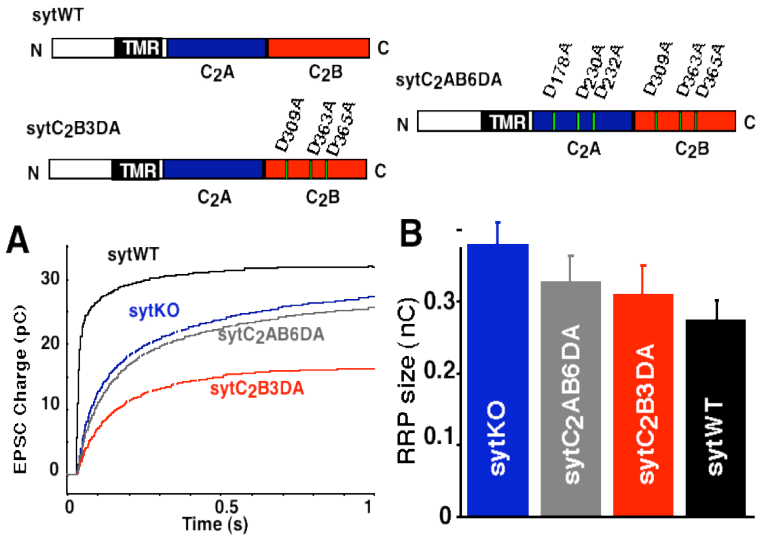

Figure 3.10 Basic characteristics of sytC$_2$B3DA and sytC$_2$AB6DA mutants A. cumulative EPSC charge of mutants, sytWT rescued neurons and sytKO neurons. B. RRP size of neurons rescued by the constructs and sytKO neurons (sytKO n=70, sytC$_2$AB6DA n=51, sytC$_2$B3DA n=42 and SytWT n=64. Data were collected from 3 batches of neuronal cultures).

Since neutralization of these sites completely eliminates the fast component of EPSC, from these data, it is clearly shown that the Ca^{2+} binding sites in the C_2B domain is essential for evoked synchronous release.

In summary, although both C_2 domains can bind Ca^{2+} ions, the physiological functions of the binding sites are not equivalent. The Ca^{2+} binding sites in the C_2A domain regulate the ratio of synchronous release component and asynchronous release component without affecting the total release efficiency, while the Ca^{2+} binding sites in the C_2B domain is essential for maintaining synchronous release.

3.2.3 The role of hydrophobic residues in Ca^{2+} binding loops of the two C_2 domains (partial contribution from Jeong Seop Rhee)

There are three hydrophobic residues in the Ca^{2+} binding loops (L1, L3) of each C_2 domain, Met_{173}, $Phe_{231,\ 234}$ in the C_2A domain and Val_{304}, Tyr_{364}, Ile_{367} in the C_2B domain. Ala replacement of Met_{173} residue, Trp replacement of $Phe_{231,\ 234}$ residues or Cys replacement of Ile_{367} residue in previous studies indicated that both domains can insert into the phospholipid membrane via Ca^{2+} binding loops (Gerber SH, et al., 2001; Chapman ER and Davis AF, 1998; Bai J, et al., 2002), although the physiological effect of this membrane insertion is unknown. To test whether syt-membrane insertion contributes to the overall function of syt in synaptic vesicular release, three constructs of syt mutants were generated (by Ok-Ho Shin): Tryptophan replacement of M_{173}, $P_{231,\ 234}$ in the C_2A domain ($sytC_2A3W$), Tryptophan replacement of V_{304}, Y_{364}, I_{367} in C_2B domain ($sytC_2B3W$) and Tryptophan replacement of all six hydrophobic residues in both C_2 domains ($sytC_2AB6W$). Biochemical evidence shows that all three W mutants can enhance syt-membrane interaction (Fig. 4.1).

3.2.3.1 SytC$_2$AB6W significantly enhances synaptic transmission

The initial analysis of evoked postsynaptic currents (EPSCs) showed that syt6W rescued fast neurotransmitter release was similar to the sytWT rescue construct. The mean EPSC amplitudes of sytWT and syt6W were comparable (sytWT 2.2 ± 0.2 nA, n=56; sytC$_2$AB6W 2.0 ± 0.2 nA, n=46; Fig. 3.11). This indicated that the 6W mutation did not change the overall function of syt.

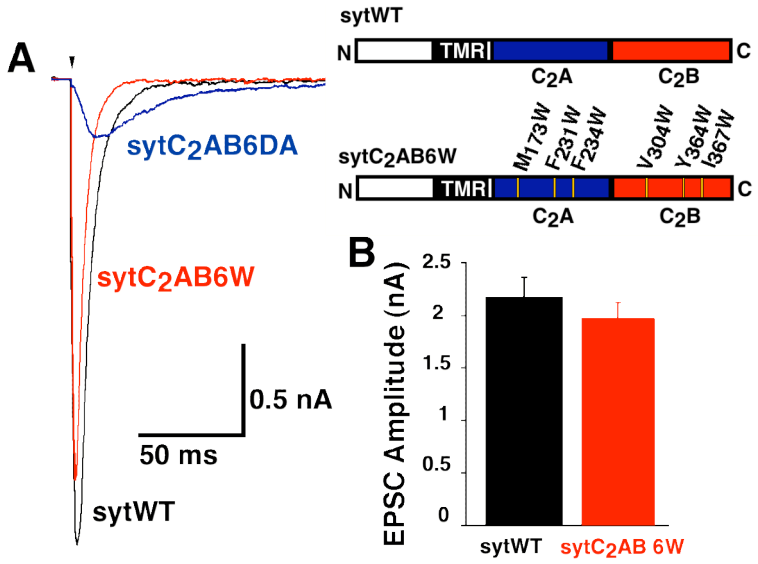

Figure 3.11 Exemplary EPSCs of sytWT and sytC$_2$AB6W mutant recorded in normal external solution. A. Raw EPSC traces of these two constructs and sytC$_2$AB6DA as a non-rescued negative control; B. Mean EPSC amplitudes of sytWT and sytC$_2$AB6W. Black arrow represents 2 ms, +70 mV depolarization of the neurons.

Next we specifically studied several release parameters by a side-by-side experiment comparing sytC$_2$AB6W and sytWT. First, we tried to answer the question of whether the sytC$_2$AB6W mutant could affect the synaptic transmission efficiency by varying external Ca^{2+} concentrations. As described in the section 2.3.5.8, EPSCs were recorded in 0.5-12 mM Ca^{2+} at a constant 1 mM Mg^{2+} condition and later normalized to the response amplitudes with control Ca^{2+} concentration (4 mM Ca^{2+}, 4 mM Mg^{2+}). A drastic left shift in the apparent Ca^{2+} sensitivity in contrast to sytWT was found. As the raw traces show in Fig. 3.12 A,

with lower external Ca^{2+} (0.5 mM), only about 50% reduction of the EPSC response in sytC$_2$AB6W mutant compared to the barely detectable EPSC in sytWT was observed. By fitting the dose response data with a standard Hill equation (Fig. 3.12 B), we observed a decrease in Ca^{2+} cooperativity (sytWT 2.5 ± 0.1 vs sytC$_2$AB6W 1.4 ± 0.2) as well as an approximate 3 fold increase in the apparent Ca^{2+} affinity (sytWT 1.80 ± 0.04 mM vs sytC$_2$AB6W 0.59 ± 0.04 mM). This clearly indicates that the increasing hydrophobicity at the top loop of the C_2 domains enhances the synaptic transmission, suggesting that Ca^{2+} dependent membrane penetration is key in syt function. The decreasing Ca^{2+} cooperativity suggests that the interaction of sytC$_2$AB6W with the membrane becomes less Ca^{2+}-dependent compared to sytWT.

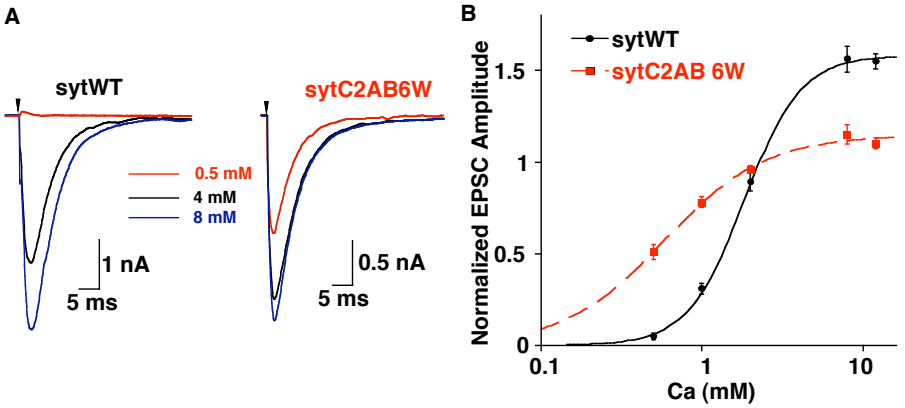

Figure 3.12 Excitatory synapses expressing sytC$_2$AB6W mutant showed an enhanced apparent Ca^{2+} sensitivity of release. A. Exemplary EPSCs from sytWT rescues (left) and sytC$_2$AB6W rescues (right), measured at 0.5 mM (green trace), 4 mM (black) and 8 mM external Ca^{2+}. Black arrows represent 2 ms, +70 mV depolarization of the neurons. B. External Ca^{2+} dependent EPSC responses in sytWT and sytC$_2$AB6W rescues. Hill Equation fit indicates a three-fold increase in apparent Ca^{2+} sensitivity of evoked release in the hydrophobic top loop mutant (sytC$_2$AB6W n=12, sytWT n=18).

An increase in Ca^{2+} sensitivity should lead to enhanced efficacy of Ca^{2+} triggered fusion and therefore to increased probability of release. To test this idea, a train of action potentials to estimate the efficiency of Ca^{2+} triggered release was performed in neurons rescued with the sytC$_2$AB6W construct. EPSC amplitudes

during 50 consecutive action potentials applied at a frequency of 10 Hz were recorded. In general, unreliable, low release probability synapses displays facilitation, while more efficient synapses show more depression (Zucker R and Regehr WG, 2002). The sytWT rescues showed regular moderate depression of EPSC amplitudes (depression at the end of train 29 ± 5%, n=46), and in contrast, the sytC$_2$AB6W mutant displayed very pronounced depression of the synaptic response (79 ± 2%, n=46, p<0.01; Fig. 3.13 A), indicating an enhanced release probability of synaptic transmission in the sytC$_2$AB6W mutant.

To prove that the enhanced short-term depression mutant correlates with the higher release probability in the sytC$_2$AB6W mutant, we measured release probability with an independent method. The vesicular release probability can be simply computed by normalizing the charge of EPSC to the charge of RRP. By comparing the sytC$_2$AB6W rescued neurons with those transfected with sytWT, a significant reduction of the RRP size was found (sytWT: 0.50 ± 0.07 nC, n=44; syC$_2$AB6W: 0.29 ± 0.04 nC, n=36) (Fig 3.13 B). The computed vesicular release probability in the sytC$_2$AB6W transfected neurons was strongly enhanced (sytWT 5.6 ± 0.7%, n=44; sytC$_2$AB6W: 14.1 ± 2.6%, n=36), therefore the increase of vesicular release probability is consistent with the enhanced depression of EPSC during trains of action potentials (Fig 3.13 A).

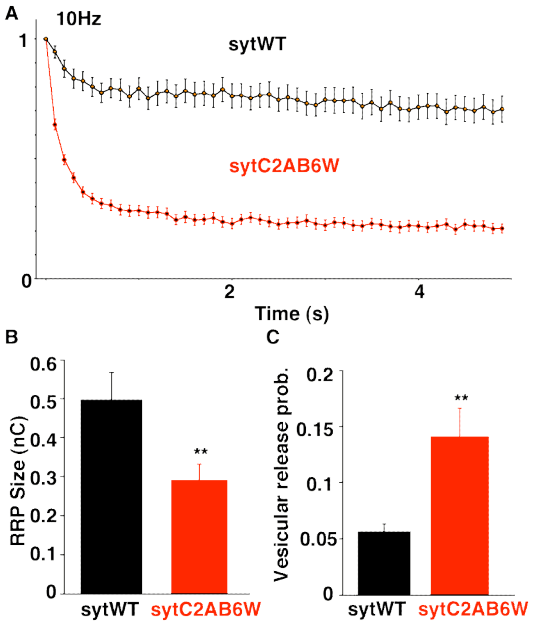

Figure 3.13 Lower release probability predicts heavier short-term depression in sytC$_2$AB6W mutant. A. Short-term depression of neurons rescued with sytC$_2$AB6W and sytWT. Each EPSC amplitude during the 10 Hz 5s stimulation train was normalized to the first EPSC response; B. Mean RRP sizes of the two constructs quantified with sucrose; C. Computed vesicular release probabilities of sytWT and sytC$_2$AB6W mutant. (** indicates t-test p<0.01)

Due to the reduction of the readily releasable vesicle pool size in the sytC$_2$AB6W mutant, which could affect Ca^{2+} independent spontaneous release, we measured mEPSC release activity in neurons rescued with sytWT and sytC$_2$AB6W. In our experiment, there was a higher mEPSC release rate in the sytC$_2$AB6W mutant than in sytWT (sytWT 3.2 ± 0.6 Hz, n=25; sytC$_2$AB6W 6.0 ± 0.6 Hz, n=21, Fig. 3.14 B). Although the increased mEPSC release rate may in principle contribute to depletion of the vesicle pool, the increase in spontaneous mEPSC rate is far too small to explain the 42% reduction of the RRP. Additionally, the normal amplitude and charge of mEPSCs in sytC$_2$AB6W mutant indicates the proper filling of vesicle with glutamate and no postsynaptic receptor dysfunction (sytWT 23.9 ± 2.3 pA, n=25; sytC$_2$AB6W 23.4 ± 1.3 pA, n=21).

3.2.3.2 SytC$_2$A3W and sytC$_2$B3W rescue study indicates that the two C$_2$ domains cooperate in synaptic transmission

The next question to be clarified is whether this synaptic transmission enhancement is conducted by the two C$_2$ domains in a redundant or additive fashion. To address this question, similar experiments were done by rescuing sytKO neurons with the sytC$_2$A3W and the sytC$_2$B3W constructs. If the enhanced synaptic transmission is only relevant to one of the two C$_2$ domains, one of these constructs should behave as sytWT while another one as sytC$_2$AB6W. If both domains act in an additive, non redundant way, their phenotypes should lie in between the two extremes (sytWT and sytC$_2$AB6W).

As summarized in Fig. 3.14, all our data point to an additive gain of function phenotype as a function of the number of domains with tryptophan replacement. The EPSC amplitudes in the sytC$_2$A3W and sytC$_2$B3W mutants were again comparable to the sytWT and sytC$_2$AB6W (sytC$_2$A3W 1.8 ± 0.2 nA, n=62; sytC$_2$B3W 1.9 ± 0.1 nA, n=72, compared to Fig. 3.11 above, KW nonparametric test and Dunn's multiple comparison test show no difference between mutants and sytWT). The vesicular release probability (sytC$_2$A3W: 8.5 ± 0.7%, n=37;

sytC$_2$B3W 10.4 ± 1.3%, n=42; compared to Fig. 3.13 above), synaptic depression (Fig. 3.14 A), mEPSC rates (Fig.3.14 B) and apparent Ca^{2+} sensitivity (sytWT 1.79 ± 0.04 mM, sytC$_2$A3W 0.79 ± 0.04 mM, sytC$_2$B3W 1.09 ± 0.12 mM and sytC$_2$AB6W 0.59 ± 0.04 mM Fig. 3.14 C) were in between the phenotypes of sytWT rescue and sytC$_2$AB6W rescue. These data nicely demonstrates the non-redundant action of both C$_2$ domains, which strongly indicates that both C$_2$ domains participate almost equally to the regulation of Ca^{2+} sensitivity and release probability.

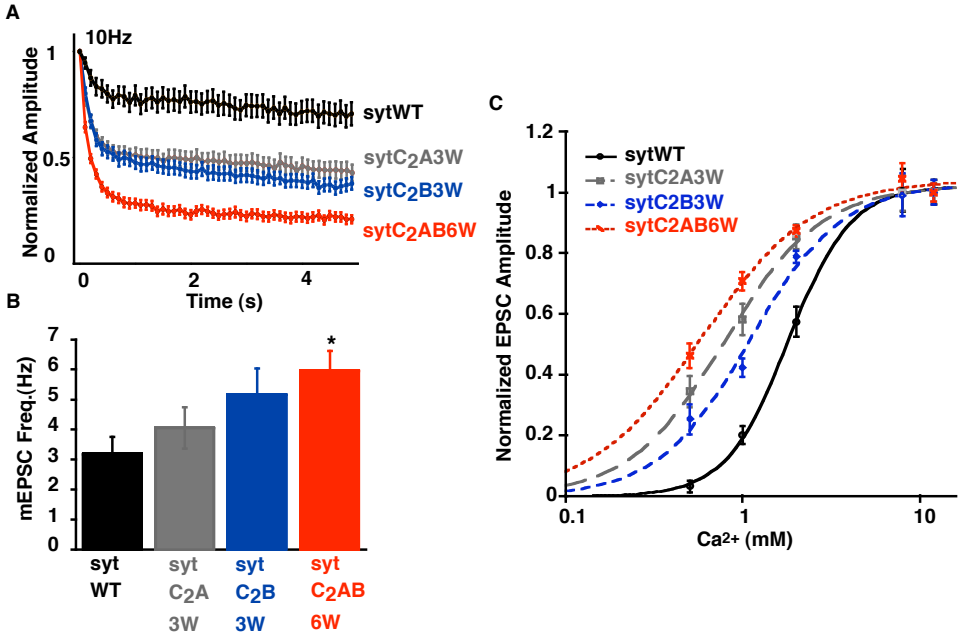

Figure 3.14 Additive effect of two C$_2$ domains in facilitating synaptic transmission. A, Short-term depression of syt tryptophan mutants and sytWT. B, mEPSC rate of neurons rescued by the four constructs rescued neurons (sytWT n=25, sytC$_2$A3W n=27, sytC$_2$B3W n=23 and sytC$_2$AB6W n=21. * indicates KW nonparametric test and Dunn's Multiple comparisons test, $p<0.05$, sytC$_2$AB6W compared to sytWT). C. External Ca^{2+} dependent EPSC amplitudes of four constructs rescued neurons (Ca^{2+} cooperativity of sytC$_2$A3W and sytC$_2$B3W are 1.6 ± 0.2 and 1.7 ± 0.3, between the value of sytWT (2.5 ± 0.1) and sytC$_2$AB6W (1.4 ±0.2). sytWT n=16, sytC$_2$A3W n=9, sytC$_2$B3W n=12 and sytC$_2$AB6W n=10).

3.2.4 Asymmetrical distribution of basic residues in the two C_2 domains regulating vesicular release probability

3.2.4.1 Neutralization of polybasic residues in the C_2B domain ($K_{326, 327}A$)

The polybasic region in the C_2B domain is important for interacting with multiple molecules (i. e. another copy of synaptotagmin, PIP_2 in plasma membrane, AP-2 and Ca^{2+} channels, etc. Chapman ER, et al., 1996; Sugita S, et al., 1996; Desai RC, et al., 2000; Fukuda M, et al., 1994; Sheng ZH, et al., 1997; Kim DK and Catterall WA, 1997). The syt $K_{326,327}A$ (syt2KA) mutant showed a 36% reduction of evoked release in the neuromuscular junctions of flies (Mackler JM and Reist NE, 2001). Syt2KA mutant rescued hippocampal neurons were compared side-by-side to the sytWT construct rescued neurons to evaluate the physiological role of the polybasic region in the C_2B domain of syt.

The efficiency of synaptic transmission is evaluated via the EPSC amplitudes. The mean EPSC amplitudes of the syt2KA mutant were significantly reduced to app. 50% of the wild type control (sytWT 1.05 ± 0.13 nA, n=40; syt2KA 0.46 ± 0.05 nA, n=40; Fig 3.15).

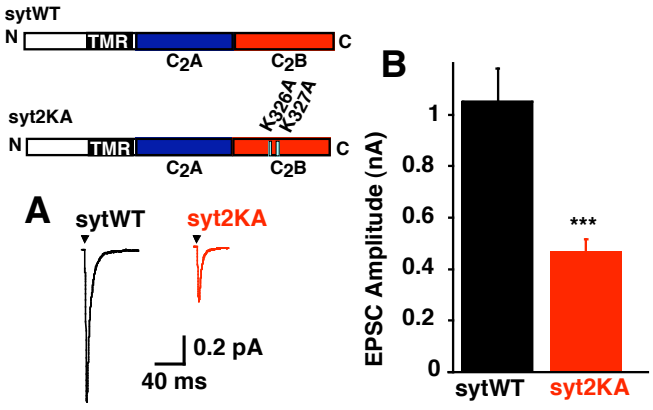

Figure 3.15 The EPSCs recorded from syt2KA and sytWT rescued sytKO neurons. A. typical synaptic responses from sytWT or syt2KA mutant. B. mean EPSC amplitudes of the two constructs (*** indicates t-test, p<0.001).

The EPSC time course of the syt2KA mutant was also compared to the sytWT rescue. EPSCs were integrated and fitted with a double exponential equation. No significant changes in the time constants of both the fast and slow components were detected (sytWT τ_{fast}= 8.0 ± 0.6 ms, τ_{slow}= 252 ± 27 ms n= 17; syt2KA τ_{fast}=

10.1 ± 1.0 ms, τ_{slow}= 236 ± 33 ms n= 12; Fig 3.16). The reduction in EPSC amplitude in the syt2KA mutant was exclusively due to a decrease in the amplitude of the fast component (sytWT Q_{fast}= 11.3 ± 1.4 pC, Q_{slow}= 2.7 ± 0.4 pC n= 17; syt2KA Q_{fast}= 6.2 ± 0.8 pC, Q_{slow}= 2.5 ± 0.5 pC n= 12; Fig 3.16). These results show that the main effect of the 2KA mutation is a selective reduction of the synchronous release.

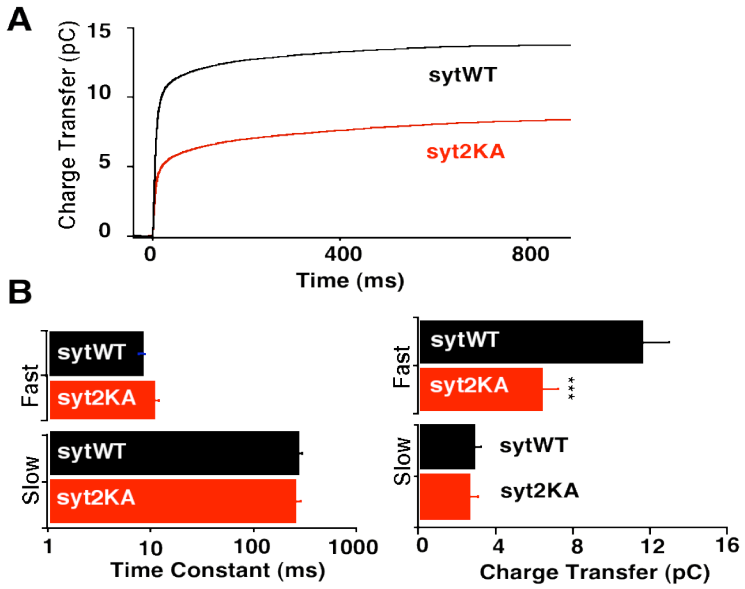

Figure 3.16 Time course of ESPC from sytWT and syt2KA mutants. A, exemplary cumulative EPSC charge responses from a sytWT and a syt2KA rescued neurons B, analysis of time constants and amplitudes with the double exponential fitting of the integrated responses (*** indicates t-test, p<0.001).

To define the RRP size, hypertonic sucrose solution (500 mM) was applied to the clamped neuron and the transient component of response was recorded. No significant differences in the RRP size between sytWT and syt2KA rescued neurons were observed (Fig 3.17 A). From these data, the vesicular release probability (Pvr) was calculated and the 2KA mutation showed a reduction in Pvr from 7.1 ± 0.6% (n=34, for sytWT) to 4.1 ± 0.6% (n=34, in syt2KA) (Fig 3.17 B). If considering that the 2KA mutation specifically reduced the synchronous release

component of EPSC, the actual reduction in this function was about 50% (Pvr_{fast} WT: 5.3 ± 0.2%, n=17; Syt2KA: 2.7 ± 0.1%, n=12).

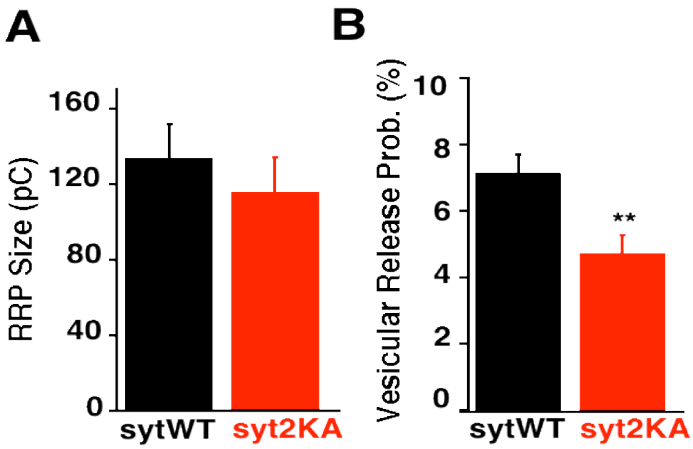

Figure 3.17 Readily releasable pool size and vesicular release probability of the syt2KA or sytWT recued neurons. A, similar readily releasable pool size of sytWT and syt2KA rescued neurons. B, mean vesicular release probability of wild type and 2KA mutant (sytWT n=34; syt2KA n=34, ** indicates t-test p<0.01).

It is worth noting that the mEPSCs amplitudes were not affected by neutralizing these two Lys to Ala residues (sytWT 21.0 ± 1.2 pA, n=16; syt2KA 19.9 ± 1.4 pA, n=12), indicating that the reduction of EPSC is not due to changes in neurotransmitter content in the vesicle or the sensitivity of the postsynaptic AMPA receptors. Consistent with the unchanged RRP size, the mEPSC frequency was not changed in the syt2KA mutant compared to the sytWT (sytWT 2.4 ± 0.4 Hz, n=16; syt2KA 1.9 ± 0.5 Hz, n=12).

3.2.4.2 Point mutation of Lys366 ($K_{366}Q$) in the C_2B domain

The similar characteristics of synaptic transmission between the neutralized polybasic stretch in the C_2B domain and the previously studied basic residue mutation $R_{233}Q$ in the C_2A domain (Fernandez-Chacon R, et al., 2001) leads to speculation of the roles of the basic residues in the C_2 domains. The

corresponding basic residue of R233 in the C_2B domain, Lys366 was also investigated. A mutation with neutralizing Lys366 in the C_2B domain (sytK$_{366}$Q) was compared to sytWT by rescuing in the sytKO neurons.

As to the initial test of evoked EPSC response, t-test shows no significant difference between sytK$_{366}$Q and sytWT constructs. The mean EPSC amplitude of sytK$_{366}$Q mutant is 2.06 ± 0.44 nA and for sytWT it is 2.00 ± 0.21 nA (sytK$_{366}$Q n=8, sytWT n=9; Fig. 3.18 B). Additionally, the RRP determined by 4 second application of 500 mM sucrose was unchanged in sytK$_{366}$Q mutant compared to sytWT rescues (sytK$_{366}$Q 220 ± 80 pC, n=6 and sytWT 195 ± 37 pC, n=7; Fig. 3.18 C).

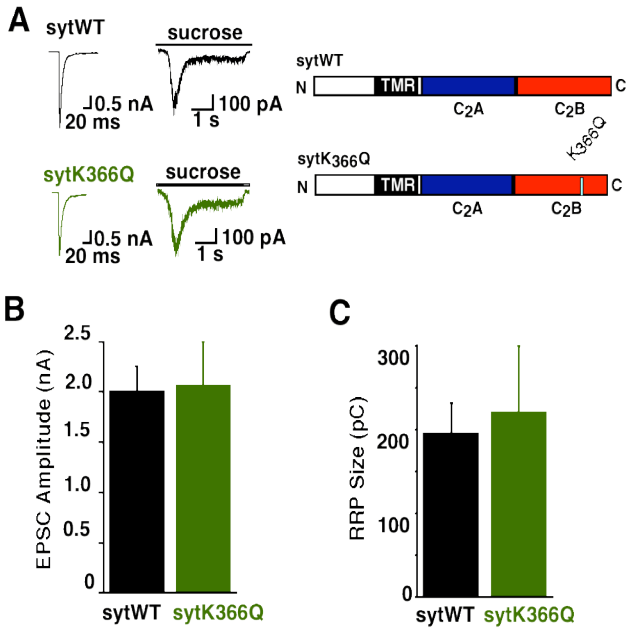

Figure 3.18 Synaptic properties of sytK$_{366}$Q and sytWT rescued neurons. A, typical evoked EPSC response and transient synaptic response induced by sucrose; Statistical comparison of EPSC amplitude (B) and RRP size (C) between sytK$_{366}$Q and sytWT.

3.2.4.3 Overview of the characteristics of three mutants (sytR$_{233}$Q, syt2KA and sytK$_{366}$Q) and sytWT rescued sytKO neurons

The vesicular release probability is correlated to short term plasticity with low release probability usually leading to short term facilitation and high release probability resulting in short term depression (as shown in sytC2AB6W study, Fig. 3.13). The 50% reduction of EPSC amplitude and Pvr in syt2KA mutant

compared to sytWT led to the investigation of short term plasticity of these two constructs. A 5 second 10Hz stimulation train was performed and as expected the low release probability mutant syt2KA showed short-term facilitation in contrast to the moderate synaptic depression in sytWT (Fig. 3.19 A).

The resemblance of the synaptic transmission phenotype between the syt2KA and the previously reported sytR$_{233}$Q is very interesting. To directly compare their similarity, a side-by-side experiment of syt2KA, sytR233Q and sytWT rescues was conducted. As shown in Fig. 3.19 B, the short-term plasticity of syt2KA and sytR$_{233}$Q was found to be nearly the same.

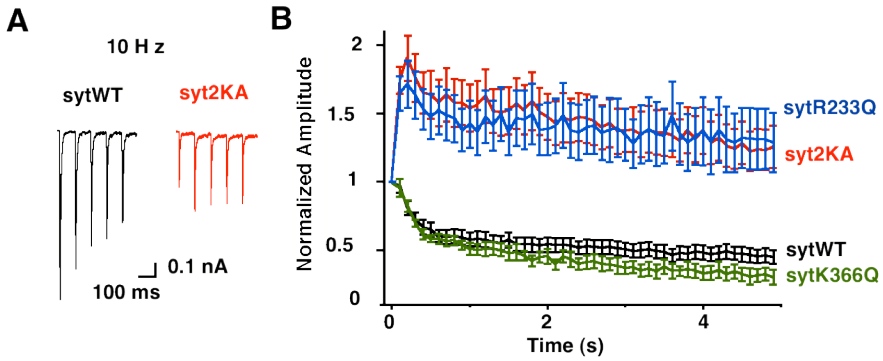

Figure 3.19 Short-term plasticity comparison of three mutants (syt$_{233}$Q, syt2KA and sytK$_{366}$Q) and sytWT. A, raw traces of the initial five consecutive EPSCs of sytWT and syt2KA mutant during a 10Hz action potential train; B, plot of normalized EPSC amplitudes (syt R$_{233}$Q n=35, syt2KA n=35, sytWT n=36 and sytK$_{366}$Q n=8).

Furthermore, to summarize all these characteristics in three mutants, the EPSC amplitude, RRP size and vesicular release probability were all normalized to the values of sytWT (Fig 3.20 A). By varying the Ca^{2+} concentrations in the external solution and later normalizing the EPSCs recorded in these conditions to the one in normal external solution, the Ca^{2+} dose response curve of these four constructs were plotted (Fig 3.20 B). The apparent Ca^{2+} sensitivity of sytR$_{233}$Q decreased about 1.7 fold compared to sytWT, so did syt2KA (sytR$_{233}$Q K_{Cad}= 2.8 ± 0.2 mM; syt2KA K_{Cad}= 2.9 ± 0.5 mM; sytK$_{366}$Q K_{Cad}= 1.7 ± 0.3 mM and sytK$_{366}$Q K_{Cad}= 1.8 ± 0.1 mM).

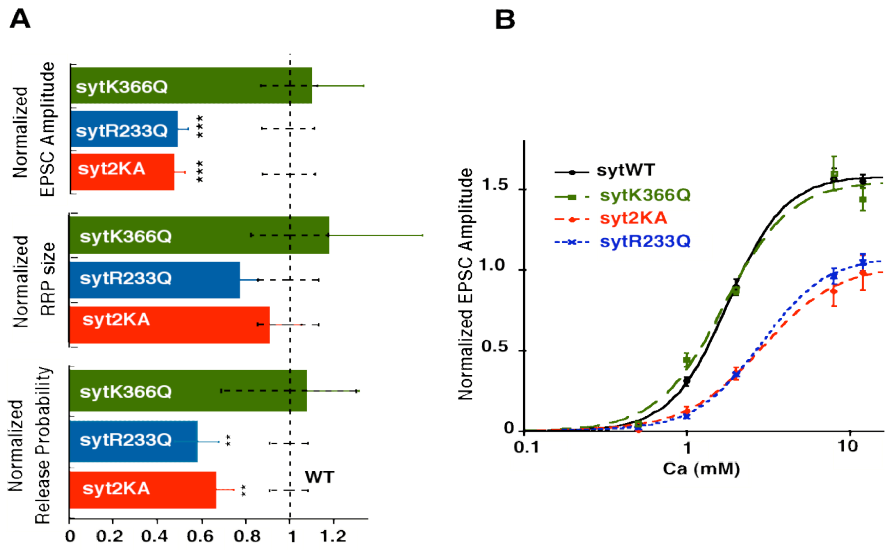

Figure 3.20 Overall comparison of synaptic properties of the three syt basic residue mutants (sytR$_{233}$Q, sytK$_{366}$Q and syt2KA) with sytWT rescue. A, EPSC amplitude, RRP size and Pvr of three mutants were normalized to sytWT (sytWT n=34, sytR$_{233}$Q n=33, syt2KA n= 34; sytWT n=9, sytK$_{366}$Q n=8; *** and ** indicate t-test, $p<0.001$ and $p<0.01$ respectively); Note that the comparison of sytWT vs. sytK$_{366}$Q and sytWT vs. sytR$_{233}$Q and syt2KA were done on separate sets of experiments. C. Synaptic response amplitude as a function of external Ca^{2+} concentration (sytWT n=9-15, sytR$_{233}$Q n=9, sytK$_{366}$Q n=8-12, syt2KA n=9-13).

In all the measured parameters, the four constructs can be divided into two groups according to their clearly distinct phenotypes: syt2KA and sytR$_{233}$Q, sytK$_{366}$Q and sytWT. The basic residues in the C2B domain that are the “function copy” of R233 exist in the polybasic region instead of the corresponding site of R233- K366, which indicates that the basic residues of syt regulating vesicular release probability distribute asymmetrically in the two C_2 domains.

3.2.5 Further analysis of the C_2B domain of syt1

The importance of the two C_2 domains of syt1 in triggering fast synaptic transmission has been shown in section 3.2.1. Both syt fragment mutants (sytΔC_2A and sytΔC_2B) cannot facilitate synchronous vesicular release (Fig. 3.7) by single action potential stimulation. However the analysis of synaptic

transmission during trains of action potential revealed partial rescue activity in sytΔC_2A transfected sztKO neurons.

3.2.2.1 Syt 1 with the deletion of the C_2A domain can partially rescue fast synaptic vesicular release

A train of 10Hz stimulation lasting 5 seconds was performed in sytΔC_2A rescued neurons, and compared to sytWT rescued neurons and sytKO neurons. Fig.3.21 shows the average EPSC traces of sytΔC_2A, sytWT rescues and sytKO during 10 Hz stimulation. There was a clear high-frequency stimulation dependent synchronous release activity in sytΔC_2A rescued neurons. As control, the EPSC time course of sytWT rescued neurons or sytKO neurons did not change prominently (Fig.3.21 B).

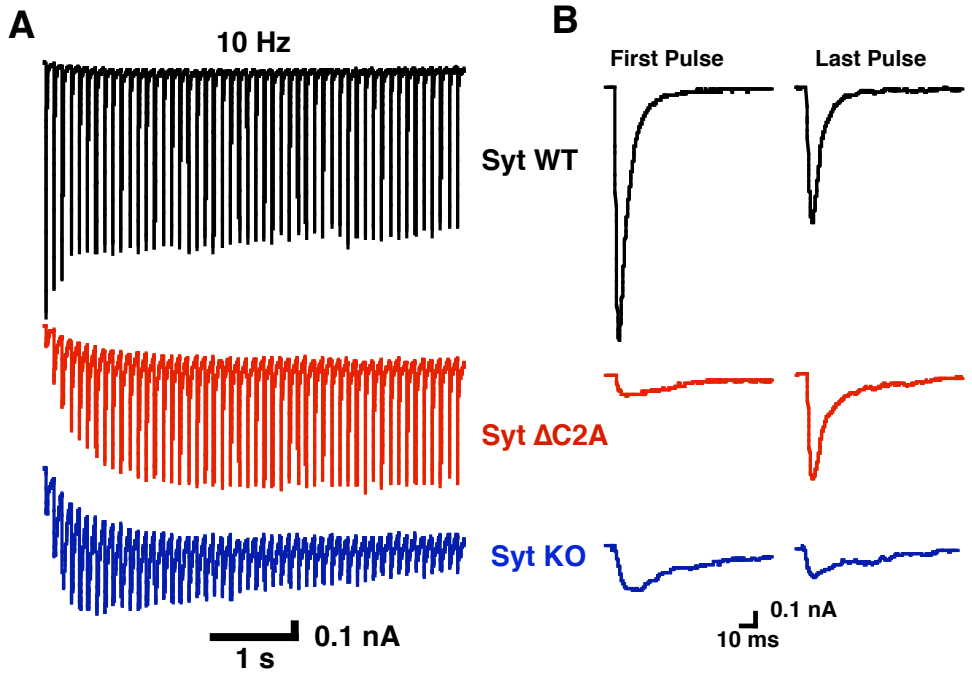

Figure 3.21 High frequency stimulation shifts asynchronous release to synchronous release in sytΔC_2A rescue. A, 50 consecutive EPSC traces of sytWT, sytΔC_2A rescued neurons or sytKO neurons in 10 Hz stimulation. B, The comparison of the first and last pulses evoked EPSC traces. (sytWT, n=11; sytΔC_2A, n=22; sytKO, n=15)

In order to quantify this shift of EPSC time course, a further analysis was performed. Since 10 Hz stimulation sets each EPSC trace in the 100ms range, I integrated the 100 ms EPSC traces and fitted them with single exponential equation. In case it gave unsatisfying results, a double exponential equation was performed. The time constants of each cumulative EPSC charge were plotted against time (Fig. 3.22) and were fitted with linear equation. Clearly, all the EPSC integrations of sytWT rescued neurons have two time constants (τ_{1st}= 5.9 ± 0.1 ms, τ_{2nd}=34.4 ± 2.0 ms). However in sytKO neurons, only one time constant of the cumulative EPSC charge was found (τ=36.2 ± 0.7 ms). For sytΔC_2A construct, EPSC integrations of the first three stimulations only can be fitted with a single exponential equation and all the rest have two components (τ_{1st}= 7.3 ± 0.1 ms, τ_{2nd}=36.3 ± 1.1 ms). Student's t-test shows a significant difference between the τ_{1st} of the sytWT and sytΔC_2A rescued neurons ($p<0.0001$), which indicates that sytΔC_2A can only partially rescue fast synaptic transmission in sytKO neurons compared to sytWT rescues.

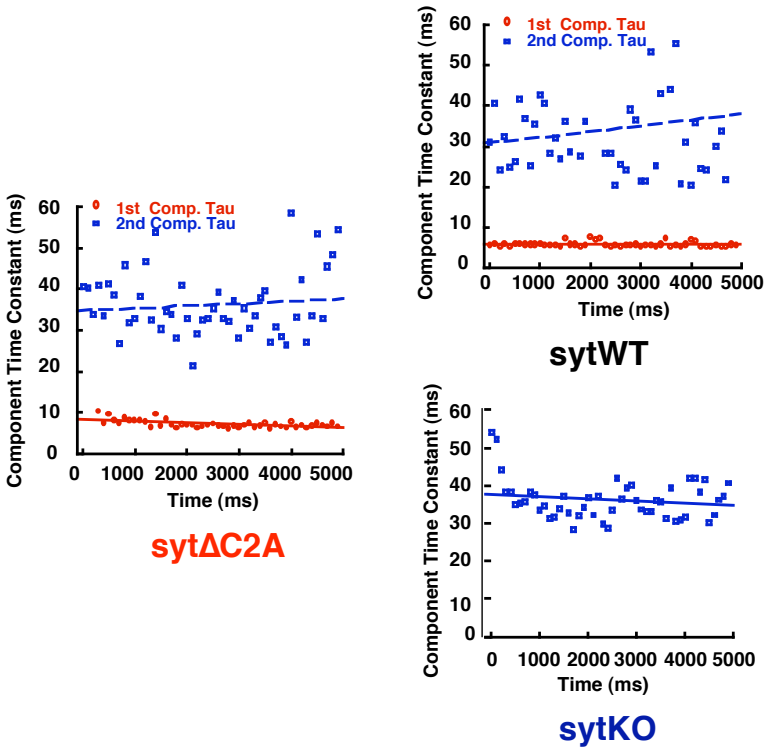

Figure 3.22 high frequency stimulation lead to partial rescue of fast release in sytΔC_2A rescue. The red dots represent τ of the fast component and the blue dots represent τ of the slow component of the 50 consecutive integrated EPSCs in a period of 100 ms.

3.2.2.2 Syt 1/7 chimerical constructs in the absence of syt1 C_2B domain cannot rescue fast synaptic transmission

The interesting finding of the partial rescue in sytΔC_2A mutant leads to a further investigation of the importance of each C_2 domain. Two critical questions arose from this finding: A) can the C_2B domain of syt1 be replaced with the C_2B domain from other synaptotagmin isoforms, for example the C_2B domain of syt7 and B) Is the C_2A domain of syt1 not essential in fast synaptic transmission?

For the first question, two syt1/7 constructs were designed (by Ok-Ho Shin) and tested, the syt1(syt7 C_2AB) (replacing the cytosolic part of syt1 with that from syt7) and syt1(syt7 C_2B) (replacing the C_2B domain of syt1 with that from syt7).

The evoked ESPC response from neither of the above constructs can mimic wild type rescued neurons (Fig. 3.23) and no EPSC shape shift was found during high frequency stimulation (Data not shown). Together with the finding that overexpression of syt7 in syt1 null neurons cannot rescue fast release (Jeong Seop Rhee, personal communication), the failure of these two constructs in triggering fast synaptic transmission indicates that the C_2B domain of syt1 is the sole molecule in syt1 regulating synchronous release and the C_2 domains of syt7 have distinct function comparing with those of syt1.

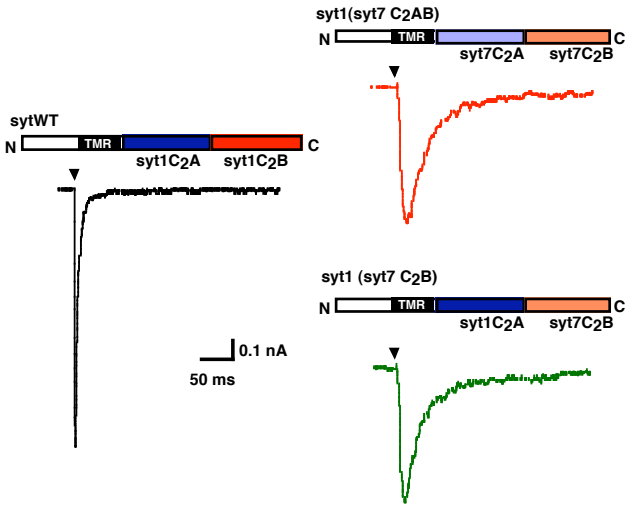

Figure 3.23 EPSC traces of different syt constructs (syt1WT, syt1(syt7 C_2AB) and syt1(syt7 C_2B)) rescued sytKO neurons.

3.2.2.3 Syt1/7 chimerical construct containing syt1 C_2B domain can partially rescue fast synaptic transmission

To answer the question of whether the C_2A domain of syt1 is essential in fast synaptic transmission, a new construct syt1(syt7 C_2A) (replacing syt1 C_2A domain with that from syt7) was designed (by Ok-Ho Shin) and tested in our system.

The initial test of evoked EPSC with the syt1(syt7 C_2A) construct showed synchronous release similar to sytWT rescues (Fig. 3.24 A). A side-by-side experiment of syt1(syt7 C_2A) and sytWT was performed to gain more detailed insight of this construct. The mean EPSC amplitude was reduced about 45% in syt1(syt7 C_2A) mutant compared to sytWT rescue (sytWT 2.52±0.33 nA; syt1(syt7 C_2A) 1.37±0.19 nA).

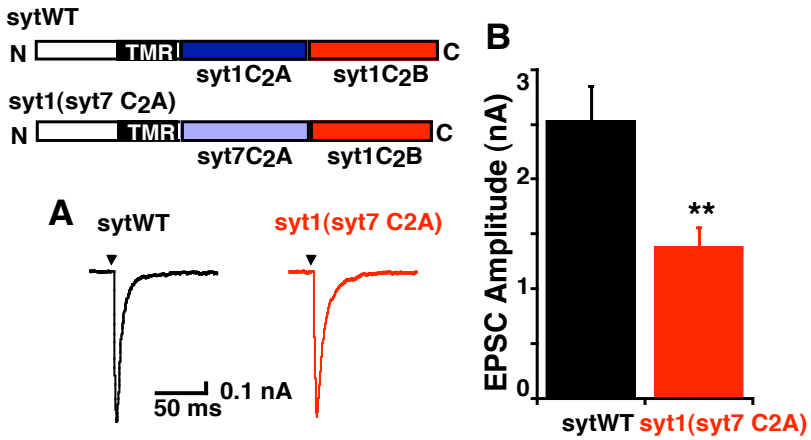

Figure 3.24 EPSC recorded from syt1(syt7 C_2A) or sytWT rescued sytKO neurons. A, a typical EPSC response from these constructs; B, Mean EPSC amplitude recorded from rescued neurons (sytWT, n=22; syt1(syt7 C_2A), n=24, ** indicates t-test $p<0.01$).

Further analysis of the EPSC cumulative charge was carried out and the characteristics of the two components from both syt1(syt7 C_2A) and sytWT rescued neurons were calculated.

The normalized cumulative EPSC charge of syt1(syt7 C_2A) mutant shows that the fast component increases slower than that of sytWT rescues but faster than that in sytKO neurons. This observation was confirmed in a further double exponential equation analysis. As shown in Fig. 3.25 B, the time constant of the fast component in syt1(syt7 C_2A) mutants was twice as the fast component in sytWT rescues (sytWT τ_{fast}= 8.3±0.7 ms, syt1(syt7 C_2A) τ_{fast} =16.9±1.5 ms), and the time constant of the slow component remained unaltered.

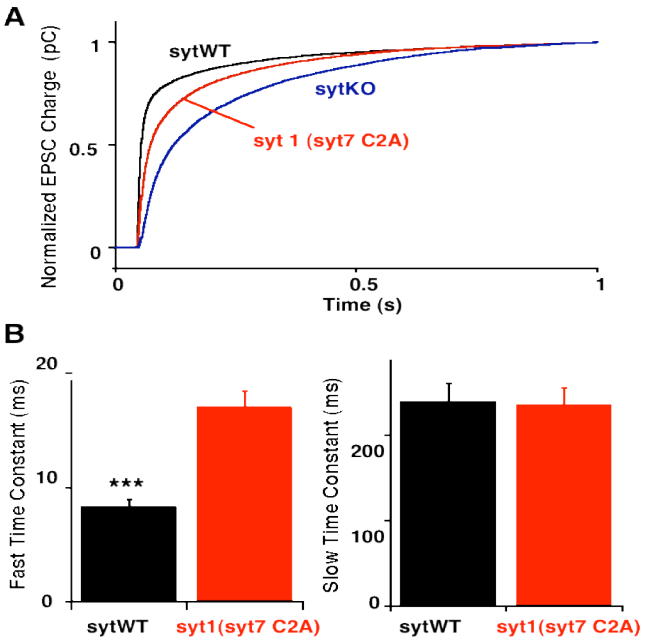

Figure 3.25 syt1(syt7 C_2A) mutant partial rescues synchronous release. A, normalized cumulative EPSC time course of syt1(syt7 C_2A), sytWT constructs rescued neurons and sytKO neurons. B, the time constants of two components given by double exponential curve fit (sytWT n=22, syt1(syt7 C_2A) n=23. *** indicates t-test $p<0.001$).

Besides the time constants, the amplitudes of the two components were also given by double exponential equation. The total charge in the chimerical mutant was about 50% larger than that of sytWT rescue (Fig. 3.26 A). This increase in the EPSC charge was contributed mainly from the slow component. As it is

shown in Fig. 3.26 B, no significant differences of the mean EPSC fast component charge were found between sytWT and syt1 (syt7 C_2A) construct (sytWT 19.8±2.1 pC, syt1 (syt7 C_2A) 23.1±2.8 pC); but the EPSC slow component in syt1 (syt7 C_2A) rescued neurons was almost three times as that of sytWT rescued neurons (sytWT 5.5±1.0 pC, syt1 (syt7 C_2A) 15.1±1.9 pC). The specific increase in asynchronous release without affecting the charge of synchronous component in syt1(syt7 C_2A) construct may be the function of the C2A domain of syt7, which has been implicated as the Ca^{2+} sensor for asynchronous vesicular release (Sugita S, et al., 2001; Sugita S, et al., 2002).

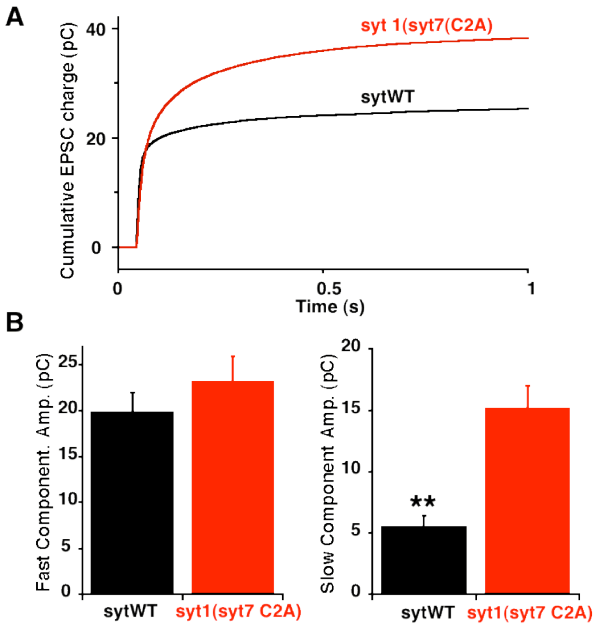

Figure 3.26 syt1(syt7 C_2A) enhances asynchronous release without affecting the amplitude of synchronous component. A, cumulative EPSC curve of syt1(syt7 C_2A) and sytWT constructs rescued neurons. B, the amplitude of two components given by double exponential curve fit (sytWT n=22, syt1(syt7 C_2A) n=23, ** indicates t-test $p<0.01$).

Although there is an increase of asynchronous release and therefore enhancement of the total vesicular release in the chimerical construct rescued neurons, the exact vesicular release probability cannot be quantified until the total number of primed synaptic vesicles is known.

Similar to the previous experiments, 500 mM sucrose was applied to the patched neurons for 4 seconds to record the transient response, which was quantified as RRP size. As shown in Fig. 3.27 A, the RRP size of the neurons rescued by sytWT is significantly smaller compared to sytKO neurons, while the RRP size in

syt1(syt7 C_2A) rescue is not significantly different from sytKO neurons. Consistent with previous data (Fig. 3.8), these results indicate that overexpression of the syt1 C_2A domain but not the syt7 C_2A domain will affect the homeostasis of RRP.

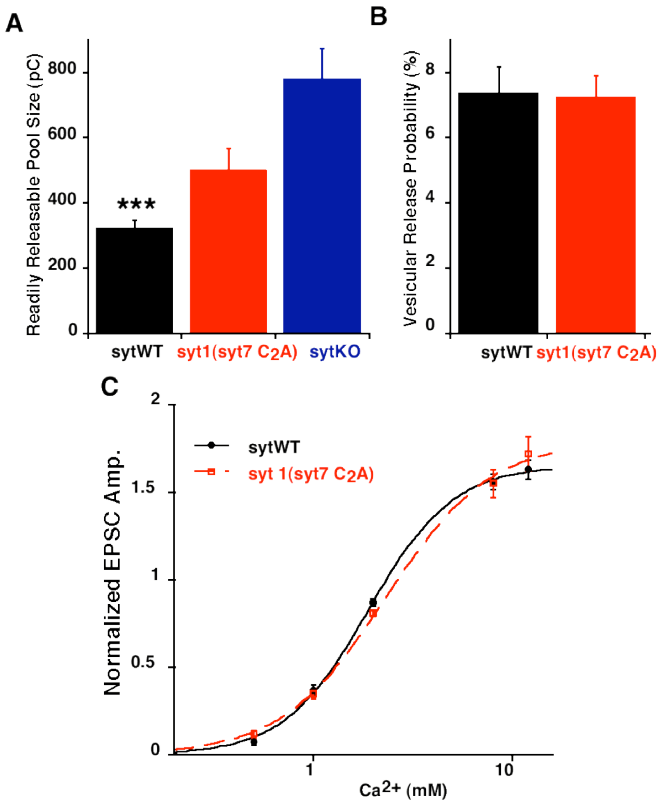

Figure3.27 neurons rescued by syt1(syt7 C_2A) has similar release probability as sytWT rescue. A, RRP size defined with hypertonic solution application. (*** indicates KW nonparametric test and Dunn's multiple comparisons test $p<0.001$, sytWT compared to sytKO: No significant difference was found between syt1(syt7 C_2A) and sytWT rescues); B, Vesicular release probability of sytWT and syt1(syt7 C_2A) mutant rescued neurons. sytWT n=22, syt1(syt7 C_2A) n=24 and sytKO n=18; C, External Ca^{2+} dependent EPSC responses.

The vesicular release probability was computed by normalizing the evoked response charge to RRP size. Stuendent's t-test showed no difference in release probability between sytWT and syt1(syt7 C_2A) rescued neurons. Additionally, the apparent Ca^{2+} sensitivity measurement shows no difference between sytWT and the chimerical construct either.

These data taken together indicate that modifying the syt1 C_2A domain by replacing it with the C_2A domain of a syt isoform syt7 did not change the overall efficacy of synaptic vesicle release, while it compromised the release toward slower kinetics. This leads to the conclusion that the C_2A domain participates in regulation of the fast vesicular release.

4. Discussion

4.1 Synchronous and asynchronous vesicular release

Syt has been implicated as the candidate of Ca^{2+} sensor for fast synaptic transmission in many previous reports. For instance, injection of synthetic peptides or antibodies that interfere with syt function greatly attenuates synaptic transmission *in vivo* (Bommert R et al., 1993; Fukuda M et al., 2000; Llinas RR et al., 2005). In addition, knocking out of the syt gene results in a reduction of synaptic response amplitude in various organisms including *C. elegans*, *Drosophila*, and mice (Nonet ML et al., 1993; Littleton JT et al., 1993; Geppert M et al., 1994). Although a crucial for syt in fast synaptic transmission has been well established, the specific function that syt plays in regulating synchronous and asynchronous release has not been investigated. The first part of my investigation serves to better resolve how syt regulates fast and slow release by analyzing the basal electrophysiological characteristics of sytKO hippocampal neurons.

Interestingly, I find that cumulative evoked EPSC charge is reduced in sytKO neurons (Fig. 3.2), which contradicts previous studies. In their studies, EPSC charge was found to be unaltered in sytKO neurons (Shin OH et al., 2003; Nishiki T and Augustine GJ, 2004a). Furthermore, the increase of τ_{fast} and τ_{slow} of 1s PSC integration in sytKO neurons compared to WT neurons (Table 3.1) suggests a role of syt beyond simply regulating fast synaptic transmission. Previous work (Nishiki T and Augustine GJ, 2004a) failed to uncover these differences likely because the EPSC was insufficiently integrated over 400 ms as opposed to 1 s resulting in incorrect estimation of the τ_{slow} by double exponential fit. Although the τ_{fast} in the sytKO neurons (~38 ms) is about as five times as that in the WT neurons (~7 ms), it is still much smaller than the τ_{slow} in the WT neurons (~170 ms), which indicates that the fast asynchronous release component in sytKO neurons is different from the asynchronous release in WT neurons. Alternatively

speaking, the loss of syt generates another form of asynchronous release. The delay of the slow component by knocking out syt may be due to two possibilities: a lost control of syt dependent inhibition of asynchronous release (Yoshihara M and Littleton JT, 2002) or regulation of slow component release by syt and its isoforms.

My results show that syt is not related to vesicle priming since RRP size defined by hypertonic solution application is unchanged (Fig. 3.3 A). However, the recovery of the EPSC after sucrose mediated RRP depletion is more rapid in sytKO neurons compared to WT neurons (Fig. 3.4). This observation suggests that either vesicle priming is accelerated or more likely that syt independent release (asynchronous release) recovers faster after RRP depletion. This is added evidence for a molecular heterogeneity within the pool of readily releasable vesicles (Murthy VN, et al., 1997; Rosenmund C, et al., 2002; Sakaba T and Neher E, 2001a-b).

According to the initial hypothesis (Goda Y and Stevens CF, 1994), two different Ca^{2+} sensors are responsible for synchronous and asynchronous release respectively. The sensor regulating asynchronous release has higher apparent Ca^{2+} affinity and is therefore capable of detecting the tail of presynaptic Ca^{2+} transient rise. Given this model, in the sytKO neurons the remaining asynchronous component should have higher Ca^{2+} sensitivity. However my results suggest that the apparent Ca^{2+} sensitivity is lower in sytKO neurons. This is also supported by the study that examined the apparent Ca^{2+} sensitivity of asynchronous release in the Complexin I and II knock out hippocampal neurons (Reim K, et al., 2001), where the apparent Ca^{2+} sensitivity of asynchronous release is lower than that of synchronous release. In any case, the change of the vesicle release by the removal of syt appears to be quite complex, as the triggered release become less steeply dependent on Ca^{2+} in sytKO neurons. For example, the vesicle release at low Ca^{2+} concentration (i. e. 0.5 mM) was more efficient in sytKO neurons than in WT neurons (Fig. 3.5).

Another important hypothesis explaining the existence of evoked synchronous and asynchronous release is the possible spatial distribution of the Ca^{2+} source (presynaptic Ca^{2+} channels) in relationship to its target (Ca^{2+} sensors) (Neher E, 1998; Meinrenken CJ, et al., 2002; Meinrenken CJ, et al., 2003). The EGTA pipette injection experiment partially supports this idea (Fig. 3.6). Since high concentration of Ca^{2+} buffer narrows the effective range of Ca^{2+} influx in triggering vesicular release, therefore in this condition, asynchronous release will be inhibited more severely than synchronous release. Additionally, syt may play an important role in associating with Ca^{2+} channels, as the polybasic region of syt has been shown to interact with Ca^{2+} channels (Sheng ZH, et al., 1997; Kim DK and Catterall WA, 1997). However, I found that the syt2KA mutant specifically reduce the fast release amplitude without affecting the time constants of the EPSC (Fig. 3.16), raising doubt as to whether the interaction between syt and Ca^{2+} channels is important for regulating synchronous release. Furthermore, the finding that vesicles can shift from asynchronous release to synchronous release with high frequency stimulation in sytΔC_2A mutant is hard to be explained by the spatial distribution of vesicles and Ca^{2+} channels hypothesis, because according to this hypothesis, the gradual elevation of Ca^{2+} concentration by high frequency stimulation inclines to trigger higher asynchronous release instead of higher synchronous release. This phenomenon can be explained in an alternative way: because the high EGTA concentration decreases the evoked Ca^{2+} transient amplitude, this leads to more inhibition of asynchronous released vesicles with lower Ca^{2+} sensitivity compared to synchronous released vesicles with higher Ca^{2+} sensitivity. Then one may argue that asynchronous released vesicles with lower Ca^{2+} sensitivity can not reconcile the above finding in sytΔC_2A mutant, since elevation of presynaptic Ca^{2+} concentration will lead to more asynchronous release instead of higher level of synchronous release. While the possible explanation of the phenotype of sytΔC_2A can be that synchronous release is determined by the syt C_2B domain-phospholipid interaction, and Ca^{2+} sensitivity of the vesicles is determined by full-length syt. For vesicles carrying sytΔC_2A

mutant, they can still undergo synchronous release, but the shortage of syt C_2A domain impaired their Ca^{2+} sensibility.

Overall, my results indicate that whether vesicles undergo synchronous or asynchronous release is more likely due to the distinct Ca^{2+} sensitivities of the vesicles instead of the spatial distribution of Ca^{2+} channels and vesicles. Clearly, the origin of synchronous and asynchronous release in evoked EPSC response is very complex and still remained to be determined.

4.2 The mechanism of action of syt in triggering vesicular release

Although many molecules interact with syt *in vitro*, including SNAP-25, syntaxin, phosopholipid, AP-2 and Ca^{2+} channels (Zhang X, et al., 2002; Tucker WC, et al., 2004; Shao X, et al., 1997; Fernandez-Chacon R, et al., 2001; Chapman ER, et al., 1998; Wu Y, et al., 2003), the *in vivo* partners of syt are not clear. Two main parts of my study clearly support the notion that the role of syt-phospholipid interaction is critical for synaptic vesicular release. Both the basic residue mutants (syt2KA, sytR$_{233}$Q), as well as the tryptophan replaced mutants (sytC$_2$A3W, sytC$_2$B3W and sytC$_2$AB6W) show parallel changes in biochemical Ca^{2+} dependent syt-phospholipid binding assays (performed by my collaborators, Ok-Ho Shin and Thomas C. Sudhof, discussed in the below) and Ca^{2+} triggered vesicle release. Additionally, the tryptophan replacement mainly altered the hydrophobic interaction properties of syt instead of changing the ionic protein-protein interaction, therefore the gain of function in these tryptophan mutants is due to enhancing the syt-phospholipid interaction rather than syt-protein binding.

Another major point in my study is related with the relative contribution of the two C_2 domains for evoked vesicle release. Neutralizing aspartates in the Ca^{2+} binding sites, consistent with prior studies (Robinson IM, et al., 2002; Nishiki T

and Augustine GJ, 2004b), revealed an essential role of the C_2B domain for synchronous release. In addition, although the Ca^{2+} binding sites in the C_2A domain have been suggested to be not essential for fast release (Stevens CF and Sullivan JM, 2003; Mackler JM, et al., 2002 and Fig. 3.9), I find that fast release is also defective in the sytΔC2A rescued neurons with low frequency stimulation (0.2Hz). This indicates that the C_2A domain may structurally accompany the C_2B domain for syt to fulfill its function. Furthermore the additive and non-redundant effect of the tryptophan replacement in the C_2A and C_2B domain (sytC_2A3W, sytC_2B3W compared to sytC_2AB6W) suggests that the C_2A domain-phospholipid interaction is similarly important as the phospholipid interaction mediated by the C_2B domain. The indispensable role of the C_2A also lies in that it can participate in regulating the homeostasis of readily releasable pool (Fig. 3.8A and Fig. 3.27A).

4.2.1 Neutralization of Asp in the Ca^{2+} binding pockets of syt C_2 domains suggests unequal contribution of the two C_2 domains in mediating the efficiency of vesicular release

Consistent with a previous study of the syt C_2A domain (Stevens CF and Sullivan JM, 2003), neutralization of the 2^{nd} to 4^{th} Asps in the C_2A domain leads to a reduction but not elimination of fast release (Fig. 3.9). This mutation in the C_2A domain is shown to greatly reduce Ca^{2+} dependent plasma membrane binding *in vitro* (Ok-Ho Shin, personal communication). These results suggest that Ca^{2+} dependent phospholipid binding of the C_2A domain is not essential for synchronizing vesicle release. Further support comes from previous report of $R_{233}Q$ mutant, where a reduction but not elimination of fast evoked response parallel with a decreased Ca^{2+} dependent syt-phospholipid binding was found (Fernandez-Chacon R, et al., 2001). Although the Ca^{2+} dependent syt-membrane interaction in the C_2A domain cannot determine fast release, it may regulate asynchronous release, since the sytC_2A3DA mutant shows a higher asynchronous release component but a similar vesicular release probability

compared to sytWT (section 3.2.2.1). The study of sytC$_2$B3DA and sytC$_2$AB6DA also support this idea. As shown in Fig.3.10 A, the sytC$_2$B3DA mutant reduced the EPSC charge, while sytC$_2$AB6DA had a comparable EPSC charge as sytWT rescued neurons, indicating the loss of control of the asynchronous release in sytC$_2$AB6DA mutant.

In contrast to the phenotype of sytC$_2$A3DA mutant, mutating the 2nd to 4th Asps in the C$_2$B domain eliminated synchronous release, which is consistent with a recent study (Nishiki T and Augustine GJ, 2004), showing that the 2nd and the 3rd Asps in the C$_2$B domain determine synchronous release. However, the time constants of the two components in the neurons rescued by sytC$_2$B3DA or sytC$_2$AB6DA is similar to that in the sytKO neurons (data not shown), in contrast to previous studies that the fast component is still detectable (Nishiki T and Augustine GJ, 2004). Additionally, neutralization of these Asps of the C$_2$B domain also greatly reduced Ca^{2+} dependent plasma membrane binding affinity *in vitro*, which suggests the importance of the C$_2$B-plasma membrane interaction in fast vesicular release.

In summary, the Ca^{2+} dependent syt-membrane interaction in the C$_2$ domains has distinct functions. The interaction in the C$_2$A domain can regulate but not determine synchronous release efficiency and inhibit asynchronous release, while the interaction in the C$_2$B domain determines synchronous release in all or none fashion.

4.2.2 Tryptophan replacement experiment reveals the importance of syt-membrane interaction in vesicular release efficiency and the cooperation of the two C$_2$ domains in fulfilling the functions of syt

There are three classes of interactions within syt, which have been found to determine/affect the functions of syt in vitro: A) the five aspartates in each C_2 domain functioning as the essential domains for Ca^{2+} mediated phospholipid binding; B) the basic residues distributed in the top loops or flanking side of syt that interacts with multiple molecules; C) the hydrophobic residues in the loop region, thought to undergo Ca^{2+} dependent insertion into the phospholipid membrane (Chapman ER and Davis AF, 1998; Bai J, et al., 2002). By replacing these hydrophobic residues with the most hydrophobic amino acid, tryptophan, ionic mediated protein-syt interaction in these regions should be unlikely affected, but the Ca^{2+} dependent phospholipid binding will be enhanced.

Previous analysis was performed by Ok-Ho Shin to determine the Ca^{2+} dependent syt-phospholipid binding of these tryptophan mutants *in vitro* (Fig. 4.1). As predicted by the design, a gradual increase of the Ca^{2+} dependent phospholipid binding was found in these three mutants. This suggests that the tryptophan mutation can drastically enhance the Ca^{2+} dependent phospholipid binding ability of syt. Consistent with the biochemical finding, my data showed enhanced synaptic release efficiency in all three tryptophan mutants. The nice correlation between biochemical and electrophysiological findings further reinforces the idea that syt-phospholipid interaction is crucial for syt to induce vesicular release.

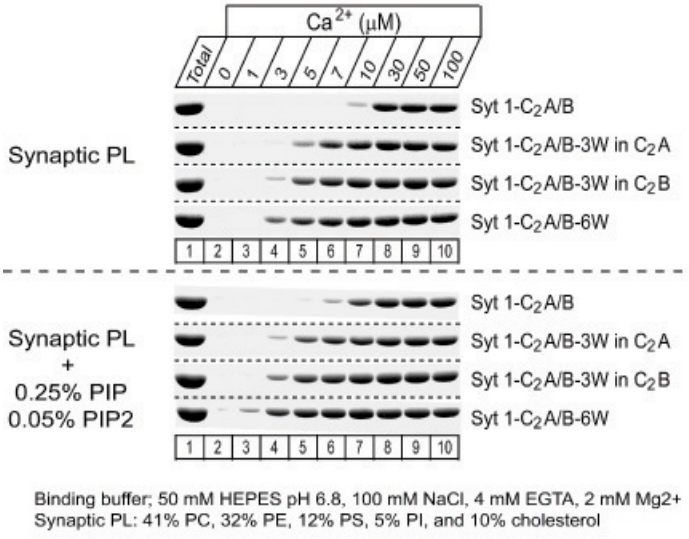

Figure 4.1. Ca^{2+} dependent phospholipid binding of different syt tryptophan mutants comparison with the sytWT (data provided by Ok-Ho Shin, for detailed methodological explanation, see Shin OH, et al., 2002.)

The three fold increase in the apparent Ca^{2+} sensitivity in sytC$_2$AB6W mutant leads to another interesting question: how is the EPSC time course of this mutant comparing to sytWT rescue? The idea behind the question is based on the previous model that evoked asynchronous release is regulated by another Ca^{2+} sensor with higher Ca^{2+} affinity (Goda Y and Stevens CF, 1994). If a higher affinity Ca^{2+} sensor for asynchronous release exists, we may expect a certain change (i. e. increase in asynchronous release) in the evoked release time course in the neurons rescued by "super syt" (sytC$_2$AB6W). The decovolution of evoked EPSC time course between the sytWT and the sytC$_2$AB6W rescued neurons overlaps. A more detailed analysis of the time constants of synchronous and asynchronous release and the contribution of each component to total release reveals no change between the sytWT and the sytC$_2$AB6W rescued neurons as well (Fig 4.2). These data suggest that the Ca^{2+} sensitivity of the asynchronous release Ca^{2+} sensor may be more than three-fold higher than that of syt. Alternatively, the explanation can be that syt solely plays a role in regulating synchronous vesicular release.

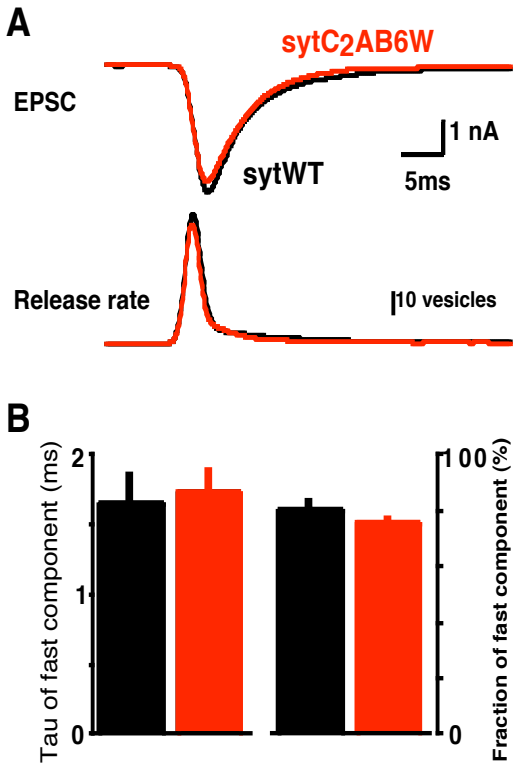

Figure 4.2 The high Ca^{2+} sensitivity mutant does not yield significant changes in the time course of neurotransmitter release. A. Top, exemplary EPSCs from SytWT (black) and SytC$_2$AB6W rescues (red); Below, EPSCs deconvolved with mean mEPSC time course to reveal the vesicular release rate. B. Release time course were fitted by two exponential equation. Bar plot of mean time constants (left) and relative amplitude of the fast component of release (right). Student's t-test shows no difference between sytWT (black) and sytC$_2$AB6W (red) (The slow component of release also did not reveal any change in its time course, not shown here).

The finding that the sytC$_2$A3W and the sytC$_2$B3W both display a similar behavior in the short term depression and an increase of apparent Ca^{2+} sensitivity indicates the important function of the C$_2$A domain in synaptic transmission. Previous studies of syt in *Drosophila* suggested that the C$_2$A domain is not important for synaptic function (Mackler JM, et al., 2002). However other studies implicated the Ca^{2+} binding region of the C$_2$A domain as part of the Ca^{2+} senor molecule (Stevens CF and Sullivan JM, 2003). Here, our study clearly shows that the C$_2$A domain is important for syt function and that both C$_2$A and C$_2$B domains contribute almost equally to regulate the Ca^{2+} sensitivity and probability of vesicle release.

Another finding is the gradual increase of mEPSC frequency in the order of sytWT< sytC$_2$A3W< sytC$_2$B3W< sytC$_2$AB6W. This observation can be correlated to the gradual increase of the apparent Ca^{2+} sensitivity in the three tryptophan mutants, since the elevation of the Ca^{2+} sensing ability of these mutants may let the vesicles start releasing in residue Ca^{2+} level. To test this hypothesis, the rescued neurons (with sytWT or sytC$_2$AB6W) were incubated in 50 μM EGTA-AM for 15 min (37 ºC) in order to accumulate a high concentration of EGTA in the presynaptic terminals, and then mEPSCs were recorded in presence of 300 nM TTX. To our surprise, Student's t-test indicated no change of spontaneous release rate either in the sytWT or in the sytC$_2$AB6W group after EGTA-AM application (The mEPSC frequency after EGTA-AM application was normalized to the mEPSC frequency before EGTA-AM application, sytWT 93.8± 12.5%, n=17; sytC$_2$AB6W 81.1± 16.2%, n=19). The unchanged mEPSC frequency suggests that the spontaneous release rate is Ca^{2+} independent. Another experiment recording mEPSC of sytC$_2$AB6W rescued neurons in the presence of 0 mM Ca^{2+} and 4 mM Ca^{2+} was performed by Dr. Rhee JS, to further test this idea. In this experiment, the spontaneous release rate was unchanged in either condition (data not shown), which also support the previous conclusion that the spontaneous release rate is Ca^{2+} independent in sytC$_2$AB6W. In summary, the increased mEPSC frequency in sytC$_2$AB6W mutant is not due to its three-fold

increase in the apparent Ca^{2+} sensitivity compared to sytWT. Possible explanation can be that the sytC_2AB6W mutant may enhance Ca^{2+} independent phospholipid interaction thus to increase spontaneous vesicle fusion rate.

4.2.3 Asymmetrical distribution of basic residues for regulation of release probability in the C_2A and C_2B domain suggests different orientation for the C_2 domains upon Ca^{2+} dependent membrane interaction

The effects of the syt2KA mutation in my study correlating with results previously obtained in the neuromuscular junctions in flies (Mackler JM, et al., 2001), generalize that perturbing the polybasic region leads to a significant decrease in vesicular release. In addition, the high resolution of the electrophysiological analyses of mammalian neuronal cultures allowed us to characterize in details a variety of synaptic parameters that led us to uncover the parallelism with the phenotype caused by the $R_{233}Q$ mutation. The observation that basic residues regulating vesicular release probability distribute asymmetrically in the two C_2 domains led to a further analysis of the origins of these phenotypes.

Ok-Ho Shin explored the Ca^{2+} dependence of phospholipid binding to a syt fragment containing both C_2-domains (C_2A/B fragment) at various Ca^{2+} concentrations in $R_{233}Q$ and 2KA mutants. In addition, he analyzed how increasing PIP and PIP_2 concentrations affect this Ca^{2+} dependence.

In the absence of PIP and PIP_2, phospholipid binding to the WT synaptotagmin 1 C_2A/B fragment required Ca^{2+} and the observed apparent Ca^{2+} affinity was significantly decreased by the $R_{233}Q$ mutation (Fig. 4.3 the left column), as described previously (Fernandez-Chacon et al, 2001). The 2KA mutation also decreased the apparent Ca^{2+} affinity, which suggests that the polybasic region is involved in Ca^{2+}-dependent phospholipid binding to syt. Addition of increasing amounts of PIP and PIP_2 increased the apparent Ca^{2+} affinity of all proteins, and

the higher PIP/PIP_2 concentrations induced some degree of Ca^{2+}-independent binding that was abolished by the 2KA mutation but not by the $R_{233}Q$ mutation (Fig. 4.3 the middle and right columns). Under all conditions tested in this series of experiments, both the $R_{233}Q$ and 2KA mutations decreased the apparent Ca^{2+} affinity of the C_2A/B fragment. The extent of this decrease was most similar at the intermediate PIP/PIP_2 concentrations (Fig. 4.3 the middle column). These results show that the similar decrease in the apparent Ca^{2+} sensitivity of release induced by these two mutations (Fig. 3.20 B) can be correlated with a similar alteration of Ca^{2+}-dependent phospholipid binding. On the other hand, the two mutations had clearly distinct effects on the Ca^{2+}-independent binding observed at the higher PIP/PIP2 concentrations, which hence do not correlate with the similarity of these two mutants in the examined electrophysiological parameters.

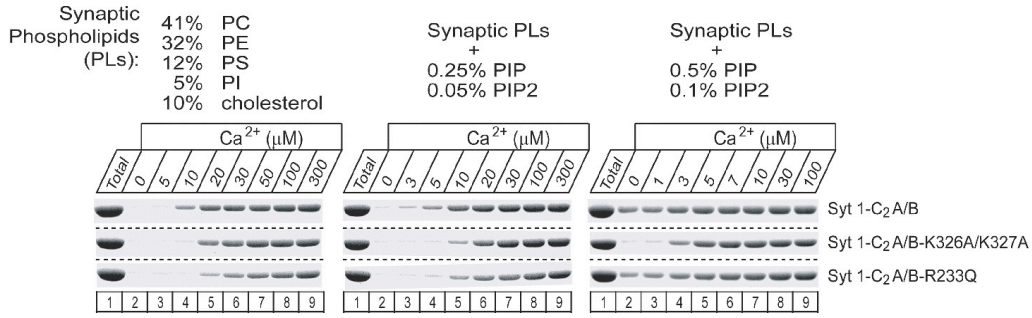

Figure 4.3 the Ca^{2+} dependent phospholipid binding of syt2KA and sytR$_{233}$Q mutants comparison with sytWT (data provided by Ok-Ho Shin).

Dr. Shin further studied the importance of electrostatic forces to the syt-phospholipid interaction by analyzing phospholipid binding in the absence and presence of Ca^{2+} as a function of the ionic strength, varying also the PIP/PIP_2 concentrations as in the previous set of experiments. At low ionic strength (50 mM NaCl) the phospholipid binding to the sytWT C_2A/B fragment in the absence of Ca^{2+} and PIP/PIP_2 was observed (Fig. 4.4 the left column). This result demonstrates that the ability of syt interacting with membrane in the absence of Ca^{2+} does not depend specifically on polyphosphoinositides. As expected, increasing the ionic strength decreased the binding observed in the absence and presence of Ca^{2+}, but both types of interactions became more resistant to NaCl

with increasing concentrations of PIP/PIP_2. These results show that binding of the synaptotagmin C_2A/B fragment to phospholipids in both the absence and presence of Ca^{2+} depends on a delicate energetic balance where electrostatic interactions play a critical role.

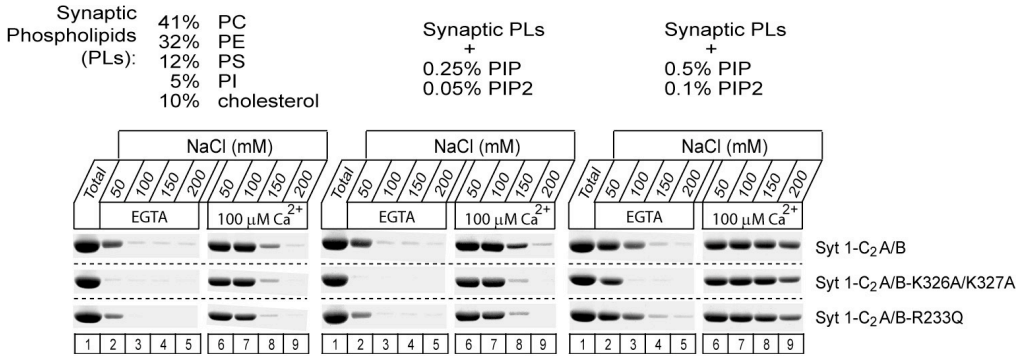

Figure 4.4 the Ionic strength dependent phospholipid interaction of syt2KA and $sytR_{233}Q$ comparison with sytWT (Data provided by Ok-Ho Shin .).

The study here implicates that Ca^{2+} dependent phospholipid binding of syt plays an important role for proper synaptic transmission. The observation that release is decreased instead of abolished by the 2KA mutation indicates that interactions are impaired but not completely abolished by this mutation. Indeed, these biochemical studies showed that Ca^{2+}-induced phospholipid binding fits this criterion, unlike many interactions showed to be abrogated by the 2KA mutation. The decrease in the observed Ca^{2+} affinity correlating with the decrease in the apparent Ca^{2+} sensitivity of release caused by the 2KA mutation further supports this idea. The fact that the phenotype induced by the 2KA mutation can be correlated with the effects on Ca^{2+}-induced phospholipid binding, indicates that any other interaction mediated by the polybasic region is less critical for the function of syt in release.

Initially, syt was believed to bind to lipids only in the presence of Ca^{2+}, but the observation of a Ca^{2+}-independent interaction with PIP_2-containing vesicles lead recently to the proposal that this interaction steers its membrane penetration activity and facilitates the rapid time scale of release (Bai J, et al., 2004b). The

data here show that PIP_2 is not strictly required for Ca^{2+}-independent binding of the C_2A/B fragment to phospholipids (Fig. 4.4, the left column), and that little binding occurs at physiological ionic strengths in the presence of amounts of phosphoinositides that are likely to be close to those present on synaptic membranes (but see McLaughlin et al., 2002). In addition, the effects of the $R_{233}Q$ and 2KA mutations on this interaction do not correlate with their *in vivo* phenotypes. Thus, it appears that the Ca^{2+}-independent lipid binding is not important for syt function, although we cannot rule out the possibility that such interaction occurs *in vivo* and the lack of a correlation with the electrophysiological data is due to a dominant effect of the Ca^{2+}-induced interaction. In any case, it seems unlikely that the Ca^{2+}-independent membrane binding facilitates the synchronous mode of release, since the 2KA mutation did not change the time course of fast release (Fig. 3.16 B).

Further more the study of basic residue Lys366 in the C_2B domain also indicates a correlation between biochemical and electrophysiological assays: the Ca^{2+} dependent phospholipid binding of the syt$K_{366}Q$ construct was similar to the sytWT results (Fig. 4.5). The observation that the polybasic region participates in Ca^{2+}-dependent phospholipid binding to the C_2A/B fragment, together with the different effects of the $R_{233}Q$ and $K_{366}Q$ mutations on binding, show that there are important differences in the mode of binding of the two C_2-domains to the lipids. The lack of an effect of the $K_{366}Q$ mutation on binding does not imply that the Ca^{2+}-binding loops are not involved in binding, since this observation just indicates that interactions between the Lys366 side chain and the lipids do not make a measurable energetic contribution to binding. However, this finding does reinforce the notion that the Ca^{2+} dependent phosopholipid binding of the basic residues of syt regulates vesicular release efficiency and the asymmetric distribution of these effective residues in the two C_2 domains suggest a different orientation of the two C_2 domains upon coming Ca^{2+} signal.

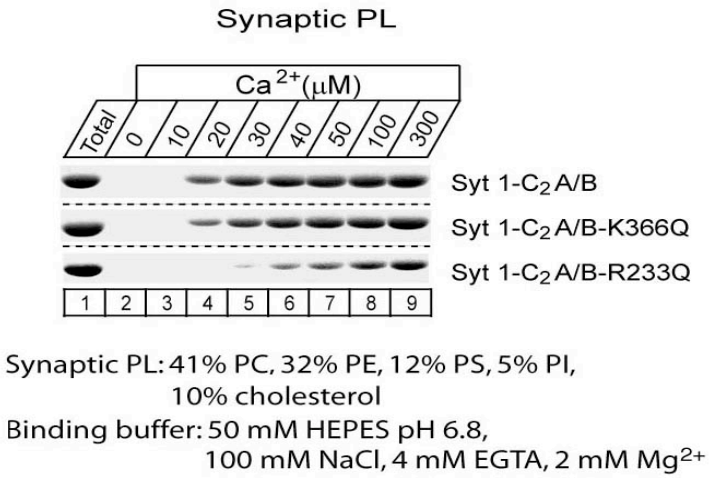

Figure 4.5 Ca^{2+} dependent phospholipid interaction of syt$K_{366}Q$ and syt$R_{233}Q$ in comparison with sytWT (Data provided by Ok-Ho Shin .).

Although all these mutations (Asps neutralization, basic residues neutralization, hydrophobic residues replacement with tryptophans) cannot fully reveal the mechanism of action of syt during vesicular release, the notion that syt facilitates vesicular fusion through its interaction with phospholipid in a Ca^{2+} mediated way was strongly supported. Phospholipids are not the sole molecules that interact with syt, but other protein(s) that have shown interaction with syt *in vitro* may more likely play a minor contribution to the mechanism of action of syt for vesicle release.

4.3 Discussion of syt1/7 chimera study

The first important finding in this syt1/7 chimera study is that syt1C_2B domain is essential for synchronous release. This notion has been proved in several studies, both in drosophila and murine preparations (Robinson IM, et al., 2002; Nishiki T and Augustine GJ, 2004b). Here I showed its importance using alternative methods. As shown in sytΔC_2A study, the high frequency stimulation of sytΔC_2A rescued neurons can shift EPSC time course from asynchronous release to synchronous release (Fig. 3.21), while there are still two defects of this mutant: A) The lower Ca^{2+} sensitivity in this mutant compared to sytWT rescue; B) Insufficient fast component rescue. One explanation of these defects may be originated from the structural shortage of the C_2A domain in sytΔC_2A. Another

mutant (syt1(syt7 C_2A)), by replacing syt1C_2A domain with syt7 C_2A domain had an insufficient fast component rescue without changing the apparent Ca^{2+} sensitivity (Fig. 3.25 and Fig. 3.27 C). This finding suggests the structural support of the C_2A domain for fast synaptic release, since slight difference between the structure of syt7 C_2A domain and syt1 C_2A domain leads to a significant effect on fast release time course. Furthermore the Ca^{2+} dependent syt-phospholipid assay showed a higher Ca^{2+} affinity of the syt7 C_2A domain compared to syt1 C_2A domain (Sugita S, et al., 2002; Shin OH, et al., 2002), while the similar apparent Ca^{2+} affinity of syt1 (syt7 C_2A) mutant and syt1 WT rescues raises doubts of the idea that syt1 C_2A domain is part of the Ca^{2+} sensor (Stevens CF and Sullivan JM, 2003).

Another finding that syt1 C_2A domain can regulate the RRP size (as shown in Fig 3.8 A) was supported in syt1 (syt7 C_2A) rescue experiment. The neurons with overexpression of syt1 C_2A domain (sytΔC_2B or sytWT rescue) have significantly reduced RRP size compared to sytKO neurons but the overexpression of syt7C_2A domain (syt1 (syt7 C_2A)) shows a comparable RRP size to sytKO neurons (Fig. 3.27 A). The observation of lack of inhibition of RRP size by overexpression of syt7 C_2A domain compared to syt1 C_2A domain suggests that the C_2A domains of syt1 and syt7 have distinct functions in regulating the homeostasis of RRP.

The last important finding is that asynchronous component was increased in syt1 (syt7 C_2A) mutant. Syt7 has been implicated as the Ca^{2+} sensor for asynchronous release because of its higher Ca^{2+} affinity for phospholipid binding (Sugita S, et al., 2002) and the finding here showed that syt7 C_2A domain may be responsible for it. The failure of rescuing fast synaptic response in both syt1 (syt7 C_2AB) and syt1 (syt7 C_2B) domain also suggested that syt7 C_2B domain has distinct function compared to syt1 C_2B domain. Whether syt7 C_2B domain also contributes to regulate asynchronous release, it is not clear.

5. Summary and conclusion

My thesis project explored the relationship between the structure and the physiological function of synaptotagmin 1 (syt), a putative Ca^{2+} sensor for vesicular release. The technique of conventional whole-cell voltage clamp and the cultured syt null (sytKO) mouse hippocampal neuron autapses transfected with Semliki forest virus carrying the mutated syt, were applied in this study.

The abundant information about syt gained from biochemical *in vitro* studies together with the controversial suggested mechanisms of action of syt in exocytosis deduced from these studies require a direct investigation of the physiological role of syt *in vivo*. In this study, three questions are mainly concerned: A) What are the possible functions of syt in vesicle recycle by studying sytKO neurons? B) Are the C_2 domains of syt redundant and what are their roles in synaptic transmission? C) What is the mechanism of action of syt in exocytosis?

The severely impaired synaptic transmission, especially the dramatic reduction of synchronous release component without altering the total fusion competent vesicles in sytKO neurons suggests the important role of syt for fast vesicle release. The faster recovery of asynchronous release in sytKO neurons compared to the recovery of synchronous release in WT neurons after the Ca^{2+} independent RRP depletion, indicates the heterogeneity of the fusion competent vesicle pool. The apparent Ca^{2+} sensitivity measurement and pipette injection of high concentration of EGTA in sytKO neurons reinforces the notion of distinct characteristics of synchronous and asynchronous release. These findings together suggest that synaptotagmin is the Ca^{2+} sensor for fast vesicle release and readily releasable vesicles with/without syt can display distinct properties in exocytosis.

The viral overexpression of exogenous mutated synaptotagmins in sytKO neurons clarified the non-redundant role of the two C_2 domains of syt in vesicle release. The C_2 domain truncation study showed the complete tertiary structure of synaptotagmin is important to keep efficient and fast vesicle release; The neutralization of Ca^{2+} binding sites in either C_2 domain study revealed the essential role of the C_2B domain for synchronizing vesicle release; Combining the above results and the syt1/7 chimera studies, the important function of the C_2A domain in controlling RRP size and regulating the asynchronous release component was clarified. The study of the basic residues in the C_2 domains supported the notion that the C_2 domains contribute unequally for syt fulfiling its function in vesicular release, which was supplemented by the study of tryptophan replaced mutants, showing that both C_2 domains can cooperatively contribute to synaptic transmission.

Through this study, together with the biochemical findings, the mechanism of action of synaptotagmin in vesicular release may be understood better. In general, the model that syt-phsopholipid interaction regulates the last step of vesicle fusion was supported, although the importance of the interaction between syt and the SNARE complex in this step cannot be ruled out. The basic residues study suggested that the R_{233} and $K_{326,327}$ residues in two C_2 domains bind equally to the plasma membrane in Ca^{2+} dependent way and this interaction was kept in a delicate balance state. Also in this study, the physiological consequence of the Ca^{2+} independent syt-PIP_2 interaction and the Ca^{2+} dependent syt oligomerization was shown to be unessential for fast synaptic transmission. The tryptophan replacement study showed a gain of function of syt in synaptic transmission and reinforced that the Ca^{2+} dependent syt-membrane insertion is critical for synaptic transmission.

6. Bibliography

Ashery U, Betz A, Xu T, Brose N, Rettig J. (1999). An efficient method for infection of adrenal chromaffin cells using the Semliki Forest virus gene expression system. *Eur J Cell Biol*. 78(8):525-32.

Bai J, Earles CA, Lewis JL, Chapman ER. (2000). Membrane-embedded synaptotagmin penetrates cis or trans target membranes and clusters via a novel mechanism. *J Biol Chem*. 275(33):25427-35.

Bai J, Wang P, Chapman ER. (2002). C_2A activates a cryptic Ca^{2+}-triggered membrane penetration activity within the C_2B domain of synaptotagmin I. *Proc Natl Acad Sci U S A*. 99(3):1665-70.

Bai J, Chapman ER. (2004). The C_2 domains of synaptotagmin--partners in exocytosis. *Trends Biochem Sci*. 29(3):143-51.

Bai J, Tucker WC, Chapman ER. (2004a). PIP_2 increases the speed of response of synaptotagmin and steers its membrane-penetration activity toward the plasma membrane. *Nat Struct Mol Biol*. 36-44.

Bai J, Wang CT, Richards DA, Jackson MB, Chapman ER. (2004b). Fusion pore dynamics are regulated by synaptotagmin*t-SNARE interactions. *Neuron*. 41(6):929-42.

Bekkers JM, Stevens CF. (1991). Excitatory and inhibitory autaptic currents in isolated hippocampal neurons maintained in cell culture. *Proc Natl Acad Sci U S A*. 88(17):7834-8.

Bollmann JH, Sakmann B, Borst JG. (2000). Calcium sensitivity of glutamate

release in a calyx-type terminal. *Science* 289(5481):953.

Bommert K, Charlton MP, DeBello WM, Chin GJ, Betz H, Augustine GJ. (1993). Inhibition of neurotransmitter release by C_2-domain peptides implicates synaptotagmin in exocytosis. *Nature* 363(6425):163-5.

Ceccarelli B, Hurlbut WP, Mauro A. (1973). Turnover of transmitter and synaptic vesicles at the frog neuromuscular junction. *J. Cell Biol.* 57:499-524.

Chapman ER, Hanson PI, An S, Jahn R. (1995). Ca^{2+} regulates the interaction between synaptotagmin and syntaxin 1. *J Biol Chem*. 270(40):23667-71.

Chapman ER, An S, Edwardson JM, Jahn R. (1996). A novel function for the second C_2 domain of synaptotagmin. Ca^{2+}-triggered dimerization. *J Biol Chem*. 271(10):5844-9.

Chapman ER, Davis AF. (1998). Direct interaction of a Ca^{2+}-binding loop of synaptotagmin with lipid bilayers. *J Biol Chem*. 273(22):13995-4001.

Chapman ER, Desai RC, Davis AF, Tornehl CK. (1998). Delineation of the oligomerization, AP-2 binding, and synprint binding region of the C_2B domain of synaptotagmin. *J Biol Chem*. 273(49):32966-72.

Chapman ER. (2002). Synaptotagmin: a Ca^{2+} sensor that triggers exocytosis? *Nat Rev Mol Cell Biol*. 3(7):498-508.

Chen X, Tomchick DR, Kovrigin E, Arac D, Machius M, Sudhof TC, Rizo J. (2002) Three-dimensional structure of the complexin/SNARE complex. *Neuron* 33(3):397-409.

Chen X, Tang J, Sudhof TC, Rizo J. (2005). Are neuronal SNARE proteins Ca^{2+}

sensors? *J Mol Biol*. 347(1):145-58.

Cheng Y, Sequeira SM, Malinina L, Tereshko V, Sollner TH, Patel DJ. (2004). Crystallographic identification of Ca^{2+} and Sr^{2+} coordination sites in synaptotagmin I C_2B domain. *Protein Sci*. 13(10):2665-72.

Collingridge GL, Isaac JT, Wang YT. (2004). Receptor trafficking and synaptic plasticity. *Nat Rev Neurosci*. 5(12):952-62.

Davletov B, Perisic O, Williams RL. (1998). Calcium-dependent membrane penetration is a hallmark of the C_2 domain of cytosolic phospholipase A2 whereas the C_2A domain of synaptotagmin binds membranes electrostatically. *J Biol Chem*. 273(30):19093-6.

Delaney KR, Tank DW. (1994). A quantitative measurement of the dependence of short-term synaptic enhancement on presynaptic residual calcium. *J Neurosci*. 14(10):5885-902.

Del Castillo J, Katz B. (1954a). Changes in end-plate activity produced by presynaptic polarization. *J Physiol*. 124(3):586-604.

Del Castillo J, Katz B. (1954b). Statistical factors involved in neuromuscular facilitation and depression. *J Physiol*. 124(3):574-85.

Del Castillo J, Katz B. (1954c). Quantal components of the end-plate potential. *J Physiol*. 124(3):560-73.

Del Castillo J, Katz B. (1954d). The effect of magnesium on the activity of motor nerve endings. *J Physiol*.124(3):553-9.

Desai RC, Vyas B, Earles CA, Littleton JT, Kowalchyck JA, Martin TF, Chapman

ER. (2000). The C_2B domain of synaptotagmin is a Ca^{2+}-sensing module essential for exocytosis. *J Cell Biol*. 150(5):1125-36.

Fasshauer D, Antonin W, Subramaniam V, Jahn R. (2002). SNARE assembly and disassembly exhibit a pronounced hysteresis. *Nat Struct Biol*. 9(2):144-51.

Fernandez I, Ubach J, Dulubova I, Zhang X, Sudhof TC, Rizo J. (1998). Three-dimensional structure of an evolutionarily conserved N-terminal domain of syntaxin 1A. *Cell* 94(6):841-9.

Fernandez-Chacon R, Konigstorfer A, Gerber SH, Garcia J, Matos MF, Stevens CF, Brose N, Rizo J, Rosenmund C, Sudhof TC. (2001). Synaptotagmin I functions as a calcium regulator of release probability. *Nature* 410(6824):41-9.

Fernandez-Chacon R, Shin OH, Konigstorfer A, Matos MF, Meyer AC, Garcia J, Gerber SH, Rizo J, Sudhof TC, Rosenmund C. (2002). Structure/function analysis of Ca^{2+} binding to the C_2A domain of synaptotagmin 1. *J Neurosci*. 22(19):8438-46.

Fukuda M, Moreira JE, Liu V, Sugimori M, Mikoshiba K, Llinas RR. (2000). Role of the conserved WHXL motif in the C terminus of synaptotagmin in synaptic vesicle docking. *Proc Natl Acad Sci U S A*. 97(26):14715-9.

Fukuda M, Aruga J, Niinobe M, Aimoto S, Mikoshiba K. (1994). Inositol-1,3,4,5-tetrakisphosphate binding to C_2B domain of IP4BP/ synaptotagmin II. *J Biol Chem.* 269(46):29206-11.

Fukuda M. (2003a). Molecular cloning, expression, and characterization of a novel class of synaptotagmin (Syt XIV) conserved from Drosophila to humans. *J Biochem (Tokyo).* 133(5):641-9.

Fukuda M. (2003b). Molecular cloning and characterization of human, rat, and mouse synaptotagmin XV. *Biochem Biophys Res Commun*. 306(1):64-71.

Gandhi SP, Stevens CF. (2003). Three modes of synaptic vesicular recycling revealed by single-vesicle imaging. *Nature* 423(6940):607-13.

Geppert M, Goda Y, Hammer RE, Li C, Rosahl TW, Stevens CF, Sudhof TC. (1994). Synaptotagmin I: a major Ca^{2+} sensor for transmitter release at a central synapse. *Cell* 79(4):717-27.

Gerber SH, Rizo J, Sudhof TC. (2001). The top loops of the C_2 domains from synaptotagmin and phospholipase A(2) control functional specificity. *J Biol Chem*. 276(34):32288-92.

Gerona RR, Larsen EC, Kowalchyk JA, Martin TF. (2000). The C terminus of SNAP25 is essential for Ca^{2+}-dependent binding of synaptotagmin to SNARE complexes. *J Biol Chem*. 275(9):6328-36.

Goda Y, Stevens CF. (1994). Two components of transmitter release at a central synapse. *Proc Natl Acad Sci U S A*. 91(26):12942-6.

Grass I, Thiel S, Honing S, Haucke V. (2004). Recognition of a basic AP-2 binding motif within the C_2B domain of synaptotagmin is dependent on multimerization. *J Biol Chem*. 279(52):54872-80.

Hamill OP, Marty A, Neher E, Sakmann B, Sigworth FJ. (1981). Improved patch-clamp techniques for high-resolution current recording from cells and cell-free membrane patches. *Pflugers Arch*. 391(2):85-100.

Han W, Rhee JS, Maximov A, Lao Y, Mashimo T, Rosenmund C, Sudhof TC. (2004). N-glycosylation is essential for vesicular targeting of synaptotagmin 1.

Neuron 41(1):85-99.

Heuser JE, Reese TS. (1973). Evidence for recycling of synaptic vesicle membrane during transmitter release at the frog neuromuscular junction. *J Cell Biol*. 57(2):315-44.

Hu K, Carroll J, Fedorovich S, Rickman C, Sukhodub A, Davletov B. (2002). Vesicular restriction of synaptobrevin suggests a role for calcium in membrane fusion. *Nature* 415(6872):646-50.

Hutt DM, Cardullo RA, Baltz JM, Ngsee JK.(2002). Synaptotagmin VIII is localized to the mouse sperm head and may function in acrosomal exocytosis. *Biol Reprod*. 66(1):50-6:

Jahn R, Lang T, Sudhof TC. (2003). Membrane fusion. *Cell* 112(4):519-33.

Jarousse N, Kelly RB. (2001). The AP2 binding site of synaptotagmin 1 is not an internalization signal but a regulator of endocytosis. *J Cell Biol*. 154(4):857-66.

Jarousse N, Wilson JD, Arac D, Rizo J, Kelly RB. (2003). Endocytosis of synaptotagmin 1 is mediated by a novel, tryptophan-containing motif. *Traffic* 4(7):468-78.

Jorgensen EM, Hartwieg E, Schuske K, Nonet ML, Jin Y, Horvitz HR. (1995). Defective recycling of synaptic vesicles in synaptotagmin mutants of Caenorhabditis elegans. *Nature* 378(6553):196-9.

Katz B, Miledi R. (1968). The role of calcium in neuromuscular facilitation. *J Physiol*. 195(2):481-92.

Kee Y, Scheller RH. (1996). Localization of synaptotagmin-binding domains on

syntaxin. *J Neurosci*. 16(6):1975-81.

Kim DK, Catterall WA. (1997). Ca^{2+}-dependent and -independent interactions of the isoforms of the alpha1A subunit of brain Ca^{2+} channels with presynaptic SNARE proteins. *Proc Natl Acad Sci U S A.* 94(26):14782-6.

Kishore BK, Wade JB, Schorr K, Inoue T, Mandon B, Knepper MA. (1998). Expression of synaptotagmin VIII in rat kidney. *Am J Physiol*. 275(1 Pt 2):F131-42.

Koh TW, Bellen HJ. (2003). Synaptotagmin I, a Ca^{2+} sensor for neurotransmitter release. *Trends Neurosci*. 26(8):413-22.

Li C, Ullrich B, Zhang JZ, Anderson RG, Brose N, Sudhof TC. (1995). Ca^{2+}-dependent and -independent activities of neural and non-neural synaptotagmins. *Nature* 375(6532):594-9.

Littleton JT, Stern M, Schulze K, Perin M, Bellen HJ. (1993). Mutational analysis of Drosophila synaptotagmin demonstrates its essential role in Ca^{2+}-activated neurotransmitter release. *Cell* 74(6):1125-34.

Littleton JT, Bai J, Vyas B, Desai R, Baltus AE, Garment MB, Carlson SD, Ganetzky B, Chapman ER. (2001). synaptotagmin mutants reveal essential functions for the C2B domain in Ca^{2+}-triggered fusion and recycling of synaptic vesicles in vivo. *J Neurosci.* 21(5):1421-33.

Llinas RR, Sugimori M, Moran KA, Moreira JE, Fukuda M. (2004). Vesicular reuptake inhibition by a synaptotagmin I C_2B domain antibody at the squid giant synapse. *Proc Natl Acad Sci U S A.* 101(51):17855-60.

McLaughlin S, Wang J, Gambhir A, Murray D. (2002). PIP_2 and proteins:

interactions, organization, and information flow. *Annu Rev Biophys Biomol Struct.* 31:151-75.

MacDermott AB, Role LW, Siegelbaum SA. (1999). Presynaptic ionotropic receptors and the control of transmitter release*. Annu Rev Neurosci*. 22:443-85.

Mackler JM, Reist NE. (2001). Mutations in the second C_2 domain of synaptotagmin disrupt synaptic transmission at Drosophila neuromuscular junctions*. J Comp Neurol*. 436(1):4-16.

Mackler JM, Drummond JA, Loewen CA, Robinson IM, Reist NE. (2002). The C_2B Ca^{2+}-binding motif of synaptotagmin is required for synaptic transmission in vivo. *Nature* 418(6895):340-4.

Mahal LK, Sequeira SM, Gureasko JM, Sollner TH. (2002). Calcium-independent stimulation of membrane fusion and SNAREpin formation by synaptotagmin I. *J Cell Biol*. 158(2):273-82.

Malenka RC. (2003). The long-term potential of LTP. *Nat Rev Neurosci*. 4(11):923-6.

Martinez I, Chakrabarti S, Hellevik T, Morehead J, Fowler K, Andrews NW. (2000). Synaptotagmin VII regulates Ca^{2+}-dependent exocytosis of lysosomes in fibroblasts. *J Cell Biol*. 148(6):1141-49.

Matthew WD, Tsavaler L, Reichardt LF. (1981). Identification of a synaptic vesicle-specific membrane protein with a wide distribution in neuronal and neurosecretory tissue. *J Cell Biol*. (1):257-69.

Meinrenken CJ, Borst JG, Sakmann B. (2002). Calcium secretion coupling at calyx of Held governed by nonuniform channel-vesicle topography. *J Neurosci*.

22(5): 1648-67.

Meinrenken CJ, Borst JG, Sakmann B. (2003). Local routes revisited: the space and time dependence of the Ca^{2+} signal for phasic transmitter release at the rat calyx of Held. *J Physiol*. 547(3): 665-89.

Miller RJ. (1998). Presynaptic receptors. *Annu Rev Pharmacol Toxicol*. 38:201-27.

Murthy VN, Sejnowski TJ, Stevens CF. (1997). Heterogeneous release properties of visualized individual hippocampal synapses. *Neuron* 18(4):599-612.

Neher E, Sakmann B. (1976). Single-channel currents recorded from membrane of denervated frog muscle fibres. *Nature* 260(5554):799-802.

Neher E. (1998). Vesicle pools and Ca^{2+} microdomains: new tools for understanding their roles in neurotransmitter release. *Neuron* 20(3):389-99.

Nicholson-Tomishima K, Ryan TA. (2004). Kinetic efficiency of endocytosis at mammalian CNS synapses requires synaptotagmin I. *Proc Natl Acad Sci U S A.* 101(47):16648-52.

Nishiki T, Augustine GJ. (2004a). Synaptotagmin I synchronizes transmitter release in mouse hippocampal neurons. *J Neurosci*. 24(27):6127-32.

Nishiki T, Augustine GJ. (2004b). Dual roles of the C_2B domain of synaptotagmin I in synchronizing Ca^{2+}-dependent neurotransmitter release. *J Neurosci*. 24(39):8542-50.

Nonet ML, Grundahl K, Meyer BJ, Rand JB. (1993). Synaptic function is

impaired but not eliminated in C. elegans mutants lacking synaptotagmin. *Cell* 73(7):1291-305.

Pabst S, Margittai M, Vainius D, Langen R, Jahn R, Fasshauer D. (2002). Rapid and selective binding to the synaptic SNARE complex suggests a modulatory role of complexins in neuroexocytosis. *J Biol Chem*. 277(10):7838-48.

Palay SL, Palade GE. (1955). The fine structure of neurons. *J Biophys Biochem* Cytol. 1(1):69-88.

Perin MS, Fried VA, Mignery GA, Jahn R, Sudhof TC. (1990). Phospholipid binding by a synaptic vesicle protein homologous to the regulatory region of protein kinase C. *Nature* 345(6272):260-3.

Poirier MA, Xiao W, Macosko JC, Chan C, Shin YK, Bennett MK. (1998). The synaptic SNARE complex is a parallel four-stranded helical bundle. *Nat Struct Biol*. 5(9):765-9.

Reim K, Mansour M, Varoqueaux F, McMahon HT, Sudhof TC, Brose N, Rosenmund C. (2001). Complexins regulate a late step in Ca^{2+}-dependent neurotransmitter release. *Cell* 104(1):71-81.

Regehr WG, Delaney KR, Tank DW. (1994). The role of presynaptic calcium in short-term enhancement at the hippocampal mossy fiber synapse. *J Neurosci*. 14(2):523-37.

Reist NE, Buchanan J, Li J, DiAntonio A, Buxton EM, Schwarz TL. (1998). Morphologically docked synaptic vesicles are reduced in synaptotagmin mutants of Drosophila. *J Neurosci*. 18(19):7662-73.

Rettig J, Neher E. (2002). Emerging roles of presynaptic proteins in Ca^{2+}-triggered exocytosis. *Science* 298(5594):781-5.

Rickman C, Davletov B. (2003). Mechanism of calcium-independent synaptotagmin binding to target SNAREs. *J Biol Chem*. 278(8):5501-4.

Rickman C, Archer DA, Meunier FA, Craxton M, Fukuda M, Burgoyne RD, Davletov B. (2004). Synaptotagmin interaction with the syntaxin/ SNAP-25 dimer is mediated by an evolutionarily conserved motif and is sensitive to inositol hexakisphosphate. *J Biol Chem*. 279(13):12574-9.

Rizo J, Sudhof TC. (2002). Snares and Munc18 in synaptic vesicle fusion. *Nat Rev Neurosci.* 3(8):641-53.

Rizzoli SO, Betz WJ. (2005). Synaptic vesicle pools. *Nat Rev Neurosci.* 6(1):57-69.

Robinson IM, Ranjan R, Schwarz TL. (2002). Synaptotagmins I and IV promote transmitter release independently of Ca^{2+} binding in the C_2A domain. *Nature* 418(6895):336-40.

Rosenmund C, Sigler A, Augustin I, Reim K, Brose N, Rhee JS. (2002). Differential control of vesicle priming and short-term plasticity by Munc13 isoforms. *Neuron* 33(3):411-24.

Rosenmund C, Stevens CF. (1996). Definition of the readily releasable pool of vesicles at hippocampal synapses. *Neuron* 16(6):1197-207.

Sakaba T, Neher E. (2001a). Calmodulin mediates rapid recruitment of fast-releasing synaptic vesicles at a calyx-type synapse. *Neuron* 32(6):1119-31.

Sakaba T, Neher E. (2001b). Preferential potentiation of fast-releasing synaptic vesicles by cAMP at the calyx of Held. *Proc Natl Acad Sci U S A*. 98(1):331-6.

Schiavo G, Gmachl MJ, Stenbeck G, Sollner TH, Rothman JE. (1995). A possible docking and fusion particle for synaptic transmission. *Nature* 378(6558):733-6.

Schneggenburger R, Neher E. (2000). Intracellular calcium dependence of transmitter release rates at a fast central synapse. *Nature* 406(6798):889-93.

Shao X, Li C, Fernandez I, Zhang X, Sudhof TC, Rizo J. (1997). Synaptotagmin-syntaxin interaction: the C_2 domain as a Ca^{2+}-dependent electrostatic switch. *Neuron* 18(1):133-42.

Sheng ZH, Yokoyama CT, Catterall WA. (1997). Interaction of the synprint site of N-type Ca^{2+} channels with the C_2B domain of synaptotagmin I. *Proc Natl Acad Sci U S A*. 94(10):5405-10.

Shin OH, Rizo J, Sudhof TC. (2002). Synaptotagmin function in dense core vesicle exocytosis studied in cracked PC12 cells. *Nat Neurosci*. 5(7):649-56.

Shin OH, Rhee JS, Tang J, Sugita S, Rosenmund C, Sudhof TC. (2003). Sr^{2+} binding to the Ca^{2+} binding site of the synaptotagmin 1 C_2B domain triggers fast exocytosis without stimulating SNARE interactions. *Neuron* 37(1):99-108

Stevens CF, Tsujimoto T. (1995). Estimates for the pool size of releasable quanta at a single central synapse and for the time required to refill the pool. *Proc Natl Acad Sci U S A*. 92(3):846-9.

Stevens CF, Williams JH. (2000) "Kiss and run" exocytosis at hippocampal synapses. *Proc Natl Acad Sci U S A*. 97(23):12828-33.

Stevens CF, Sullivan JM. (2003). The synaptotagmin C2A domain is part of the calcium sensor controlling fast synaptic transmission. *Neuron* 39(2):299-308.

Sorensen JB, Matti U, Wei SH, Nehring RB, Voets T, Ashery U, Binz T, Neher E, Rettig J. (2002). The SNARE protein SNAP-25 is linked to fast calcium triggering of exocytosis. *Proc Natl Acad Sci U S A*. 99(3):1627-32.

Sudhof TC. (1995). The synaptic vesicle cycle: a cascade of protein-protein interactions. *Nature* 375(6533):645-53.

Sudhof TC. (2002). Synaptotagmins: why so many? *J Biol Chem*. 277(10):7629-32.

Sudhof TC. (2004). The synaptic vesicle cycle. *Annu Rev Neurosci*. 27:509-47.

Sugita S, Hata Y, Sudhof TC. (1996). Distinct Ca^{2+}-dependent properties of the first and second C_2-domains of synaptotagmin I. *J Biol Chem.* 271(3):1262-5.

Sugita S, Han W, Butz S, Liu X, Fernandez-Chacon R, Lao Y, Sudhof TC. (2001). Synaptotagmin VII as a plasma membrane Ca^{2+} sensor in exocytosis. *Neuron* 30(2):459-73.

Sugita S, Shin OH, Han W, Lao Y, Sudhof TC. (2002). Synaptotagmins form a hierarchy of exocytotic Ca^{2+} sensors with distinct Ca^{2+} affinities. *EMBO J*. 21(3):270-80.

Sutton RB, Fasshauer D, Jahn R, Brunger AT. (1998). Crystal structure of a SNARE complex involved in synaptic exocytosis at 2.4 A resolution. *Nature* 395(6700):347-53.

Trommershauser J, Schneggenburger R, Zippelius A, Neher E. (2003). Heterogeneous presynaptic release probabilities: functional relevance for short-term plasticity. *Biophys J*. 84(3):1563-79.

Tucker WC, Chapman ER. (2002). Role of synaptotagmin in Ca^{2+}-triggered exocytosis. *Biochem J*. 366(Pt 1):1-13.

Tucker WC, Weber T, Chapman ER. (2004). Reconstitution of Ca^{2+}-regulated membrane fusion by synaptotagmin and SNAREs. Science 304(5669):435-8.

Ubach J, Zhang X, Shao X, Sudhof TC, Rizo J. (1998). Ca^{2+} binding to synaptotagmin: how many Ca^{2+} ions bind to the tip of a C2-domain? *EMBO J.* 17(14):3921-30.

Ullrich B, Li C, Zhang JZ, McMahon H, Anderson RG, Geppert M, Sudhof TC. (1994). Functional properties of multiple synaptotagmins in brain. *Neuron* 13(6):1281-91.

Wang CT, Lu JC, Bai J, Chang PY, Martin TF, Chapman ER, Jackson MB. (2003). Different domains of synaptotagmin control the choice between kiss-and-run and full fusion. *Nature* 424(6951):943-7.

Wang CT, Grishanin R, Earles CA, Chang PY, Martin TF, Chapman ER, Jackson MB. (2001). Synaptotagmin modulation of fusion pore kinetics in regulated exocytosis of dense-core vesicles. *Science* 294(5544):1111-5.

Weber T, Zemelman BV, McNew JA, Westermann B, Gmachl M, Parlati F, Sollner TH, Rothman JE. (1998). SNAREpins: minimal machinery for membrane fusion. *Cell* 92(6):759-72.

Wendland B, Scheller RH. (1994). Secretion in AtT-20 cells stably transfected

with soluble synaptotagmins. *Mol Endocrinol*. 8(8):1070-82.

Wu LG, Saggau P. (1997). Presynaptic inhibition of elicited neurotransmitter release. *Trends Neurosci*. 20(5):204-12.

Wu Y, He Y, Bai J, Ji SR, Tucker WC, Chapman ER, Sui SF. (2003). Visualization of synaptotagmin I oligomers assembled onto lipid monolayers. *Proc Natl Acad Sci U S A*. 100(4):2082-7.

Xu T, Bajjalieh SM. (2001). SV2 modulates the size of the readily releasable pool of secretory vesicles. *Nat Cell Biol*. 3(8):691-8.

Yoshihara M, Littleton JT. (2002). Synaptotagmin I functions as a calcium sensor to synchronize neurotransmitter release. *Neuron* 36(5):897-908.

Zhang X, Kim-Miller MJ, Fukuda M, Kowalchyk JA, Martin TF. (2002). Ca^{2+}-dependent synaptotagmin binding to SNAP-25 is essential for Ca^{2+}-triggered exocytosis. *Neuron* 34(4):599-611.

Zhang X, Rizo J, Sudhof TC. (1998). Mechanism of phospholipid binding by the C2A-domain of synaptotagmin I. *Biochemistry*. 37(36):12395-403.

Zhang JZ, Davletov BA, Sudhof TC, Anderson RG. (1994). Synaptotagmin I is a high affinity receptor for clathrin AP-2: implications for membrane recycling. *Cell* 78(5):751-60.

Zucker RS, Regehr WG. (2002). Short-term synaptic plasticity. *Annu Rev Physiol.* 64:355-405.

RESUME

Name: Liyi Li
Sex: Male
Marital Status: Single
Date of Birth: May 28, 1978
Place of Birth: JiangXi Province, P.R.China
Degree: B. S. PhD (in studying)

Education Background

Sept.18th, 2000- June 2005 In MS/PhD International Program of Molecular Biology, Goettingen University& International Max-Plank Research School, Goettingen, Germany

Sept. 1st, 1995- July 2nd, 1999 B.S. in Dept. of Biotechnology, Peking University, Beijing, China

Research Experience

April. 2004- April. 2005 Continuing PhD work in Prof. Christian Rosenmund's lab
Dept. of Molecular Human Genetics & Neuroscience Division, Baylor College of Medicine, Houston

Oct. 2001- April. 2004 PhD work in Prof. Erwin Neher 's Department, Dr. Christian Rosenmund's lab for "Functions of Synatotagmin-1 in Synaptic Transmission"
Dept. of Membrane Biophysics, Max-Plank Institute for Biophysics Chemistry, Goettingen

Dec., 2000- March, 2001 Lab rotation about "Pharmacological Study of AMPA Receptors in Cultured Hippocampual neurons "
Directed by Dr. Christian Rosenmund and Prof. Erwin Neher.

Dec., 1998 – July, 1999 Involved in the group studying "HIV-1 Maternal-Fetus Transmission".
Directed by Prof. Yunzhen Cao**.**
National Centre for AIDS Prevention & Control, Beijing

May, 1998 – Nov., 1998 Involved in the group studying "The Biochemical Activity of Trichosanthin (TCS) and its Transduction to Rice".
Directed by Prof. Zhangliang Chen.
National Laboratory for Protein Engineering & Plant Gene Engineering, Beijing

Honours

July , 1999 Best Thesis for B.Sc. degree ("HIV-1 Clinical Tests")

Sept., 2000 – Apr., 2005 Scholarship for MS/ Ph.D. study in Goettingen University and International Max-Plank Research School

Hobbies

Classical Music, Literature and History.